



City Research Online

City, University of London Institutional Repository

Citation: Villa Arango, S. (2020). Application of phononic crystals as liquid sensors for the development of novel point of care technologies. (Unpublished Doctoral thesis, City, University of London)

This is the accepted version of the paper.

This version of the publication may differ from the final published version.

Permanent repository link: <https://openaccess.city.ac.uk/id/eprint/24758/>

Link to published version:

Copyright and reuse: City Research Online aims to make research outputs of City, University of London available to a wider audience. Copyright and Moral Rights remain with the author(s) and/or copyright holders. URLs from City Research Online may be freely distributed and linked to.

City Research Online:

<http://openaccess.city.ac.uk/>

publications@city.ac.uk



Application of phononic crystals as liquid sensors
for the development of novel point of care
technologies

by
Simón Villa Arango

A thesis submitted in partial fulfillment for the
degree of Doctor of Philosophy

in the
Research Centre for Biomedical Engineering
School of Mathematics, Computer Science & Engineering
Northampton Square, London, EC1V 0HB

January 2020

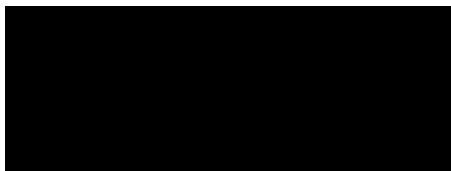
Declaration of Authorship

I, Simón Villa Arango, declare that this thesis titled, ‘Application of phononic crystals as liquid sensors for the development of novel point of care technologies’ and the work presented in it are my own. I hereby confirm that the work presented in this document was done wholly or mainly while in candidature for a research degree at City, University of London.

Any idea, result, or illustration originating from other researcher’s work has been appropriately acknowledged in the text by referencing to the original author.

This thesis has never been published or submitted elsewhere for obtaining an academic degree or professional qualification.

I grant powers of discretion to the City, University of London Librarian to allow this thesis to be copied in whole or in part without further reference to the author. The permission covers only single copies made for study purposes, subject to normal conditions of acknowledgement.



Simón Villa Arango

Acknowledgments

To my parents, Mauricio and Bibiana for always believing in me and pushing me to accomplish greatness.

To my brother, Tomás, who is always challenging me to go a step further with my projects.

To Ana, you are the love of my life, my true inspiration.

To my director, Panicos, for your patience, wisdom and expert guidance through this amazing journey in City, University of London.

To Robinson and the bioinstrumentation lab, you have my gratitude for your unfailing support and assistance

To City, University of London and to the EIA University in Colombia: I will always carry you with me, I become your ambassador and I thank you for giving me the opportunity to learn and to grow both academically and personally so much.

I am also grateful to my other family members and friends who have supported me along the way.

A special mention to the Royal Academy of Engineering for funding part of the activities performed in this PhD research.

Thanks for all your encouragement!

“Do not go where the path may lead, go instead where there is no path and leave a trail.”

Ralph Waldo Emerson

Abstract:

Currently, a rapid development of point of care technologies can be observed, mainly due to the alternative they offer to traditional complex laboratory equipment, not only saving costs, but also improving patients convenience, delivering quick and reliable measurement results, increasing the confidence in clinical decisions and most importantly, improving patient care. Phononic crystals were recently introduced, and their unique capabilities to control the transmission of waves has paved the way for the development of many applications, including the development of acoustic sensors. Phononic crystal sensors offer a fundamentally different measurement principle to the development of point of care technologies by enabling the measurement of the acoustic properties of small liquid samples. So far, various phononic crystal sensors have been proposed to be used as liquid sensors. However, they are still in very early stages of development and suffer several drawbacks like high analyte consumption, complex manufacturing procedures, highly dependent on ambient variables and no portability, making it impossible to implement them in point of care devices. The main objective of this study is to evaluate the potential implementation of multi-layered phononic crystals as liquid sensors for biomedical applications, especially for developing point of care technologies. Theoretical and experimental studies were performed in order to evaluate the behaviour of the designed structures. For computing the frequency response of phononic crystals, the transmission line model and the finite element method were used. Different liquid analytes were utilised during the experimental realisations to corroborate the results obtained during the theoretical studies. Variations in the acoustic properties of small liquid samples, resulted in measurable changes in the transmission coefficient of the phononic crystal, specifically shifting the frequency of relevant transmission peaks located inside bandgaps, which provide boundary conditions for eliminating noise and enhancing their quality factor. The introduction of multiple defect modes showed to be a feasible alternative to generate differential measurements in phononic crystals and compensate the effect of temperature. Furthermore, the use of biorecognition agents was also utilised and discussed to enhance the detection capabilities of this new sensors.

Table of Contents

Abstract:.....	5
List of Figures.....	6
List of Tables	18
List of Journal Articles.....	19
List of Congress Participations	20
Table of Contents.....	6
Chapter 1 - Introduction.....	21
1.1 Introduction	21
1.2 Aims and objectives.....	23
1.3 Contribution of the thesis.....	23
1.4 Chapter outline	24
Chapter 2 - Phononic Crystals: history and applications	27
2.1 Phononic crystals.....	27
2.2 History.....	30
2.3 Local resonances.....	36
2.4 Focalization	37
2.5 SAW phononic crystals and the use of higher frequencies.....	38
2.6 Defect modes on periodic structures.....	39
2.7 Tuning.....	40
2.8 Summary	42
Chapter 3 - The use of Phononic Crystals as sensors	43
3.1 Acoustic wave sensors	43
3.2 First approaches to Phononic crystal sensors	45
3.3 State of the art and limitations.....	56
3.4 Summary	58

Chapter 4 - Methods for simulating phononic crystals	59
4.1 Simulation Methods	59
4.2 Description of the transmission line model for simulating Phononic crystals	61
4.3 Summary	75
Chapter 5 - Theoretical study on the use of multi-layered phononic crystals as liquid sensors	76
5.1 Bandgap engineering	76
5.2 Theoretical study using the transmission line model for simulating phononic crystals	78
5.3 Theoretical study using the FEM software Comsol Multiphysics to evaluate the behaviour of multi-layered phononic crystal sensors in 2D.....	91
5.4 Conclusions on the theoretical study	97
5.5 Summary	98
Chapter 6 - Acoustic spectrometer: resonant sensing platform for measuring volumetric properties of liquid samples	99
6.1 Introduction:	99
6.2 Materials and Methods.....	101
6.3 Results and Discussion.....	106
6.4 Conclusions	107
6.5 Summary	108
Chapter 7 - Cavity Resonance Sensor with Disposable Analyte Container	110
7.1 Materials and Methods.....	110
7.2 Results and Discussion.....	117
7.3 Conclusions	121
7.4 Summary	121

Chapter 8 - Fully-disposable multi-layered phononic crystal liquid sensor with symmetry reduction and a resonant cavity	123
8.1 Materials and Methods.....	123
8.2 Results and Discussion.....	129
8.3 Conclusions	134
8.4 Summary	135
Chapter 9 - Differential Phononic Crystal Sensor: Towards a Temperature Compensation Mechanism for Field Applications Development.....	136
9.1 Materials and Methods.....	137
9.2 Results and Discussion.....	140
9.3 Conclusions	145
9.4 Summary	146
Chapter 10 - Phononic crystal biosensors: functionalization of resonant cavities to enhance selectivity in challenging applications	148
10.1 Materials and methods	149
10.2 Results and discussion	153
10.3 Conclusions	158
10.4 Summary	159
Chapter 11 - Use of Transient Time Response as a Measure to Characterize Phononic Crystal Sensors.....	160
11.1 Materials and Methods.....	160
11.2 Results and Discussion.....	165
11.3 Conclusions	168
11.4 Summary	169
12 Discussion.....	170

13 Conclusions.....	176
References.....	180

List of Figures

Figure 1 Schematic representation of a 1D Phononic crystal, grey discs on the sides represent ultrasonic transducers and the different colours of the thin layers represent different materials with high acoustic impedance mismatch. The graph on the right represents a typical bandgap of a phononic crystal.	28
Figure 2 Theoretical results obtained by Narayanamurti et al in a phononic crystal formed by a stack of 50 layers with a 0.95 and 0.90 impedance ratio. The graph shows the results for an ideal superlattice (a) and for a superlattice with a 10% random disorder in the layer thickness (b). The transmission spectra of all the structures display well defined bandgaps. Taken from [22].	32
Figure 3 Sculpture “El Organo” from Eusebio Sempere made by steel rods over a metallic platform. Taken and edited from [34].	34
Figure 4 Schematic representation of a surface acoustic wave device composed of 2 Interdigital transducers and a sensing film in which the analyte is deposited and it’s interrogated by the surface acoustic wave that travels from one interdigital transducer to the other. Taken from [90].	43
Figure 5 Photo of the experimental setup used by Lucklum et al. Taken from [17]..	47
Figure 6 . Photo of the optimised experimental setup used by Lucklum et al. taken from [95].	48
Figure 7 Photos and schematic representation of the elements used by Lucklum’s group to perform experimental realisations with their 2D phononic crystal sensor Taken from [105].	50
Figure 8 Experimental arrangement (a) and results (b) presented in the publication submitted by Lu et al. Taken from [109]	51
Figure 9 Phononic crystal sensor designed by the group of Salaman. Taken from [110].	52

Figure 10 Tubular Phononic crystal structure presented by Lucklum and Penneç. Taken from [112].	53
Figure 11 Effect of surface mass on the phononic crystal structures presented by Fygey's et al. Taken from [113].	54
Figure 12 Electrical transmission line representation	69
Figure 13 Simulation results of a structure composed of 7 consecutive layers with the analyte layer located in the middle of the structure. The simulation was performed using the transmission line model for simulating phononic crystals.	79
Figure 14 Simulation results of a structure composed of 7 consecutive layers with the analyte layer located in the middle of the structure. In red is the original structure, in black the effect of displacing the analyte resonance mode to frequencies nearer the border of the bandgap. The simulation was performed using the transmission line model for simulating phononic crystals.	80
Figure 15 Comparison of the simulation results of structures composed of 7 consecutive layers with an analyte layer located in the middle. In red is the original structure, in black the effect of replacing the solid layers by materials with lower acoustic impedance. The simulation was performed using the transmission line model for simulating phononic crystals.	81
Figure 16 Simulation results of a structure composed of 7 consecutive layers with an analyte layer located in the middle. This structure is composed of layers three times larger than the others investigated before. See Figures 13, 14 and 15. The simulation was performed using the transmission line model for simulating phononic crystals.	82
Figure 17 Behaviour of the bandwidth and sensitivity of the bandgap in a PnC structure whose layer thickness values were increased by a factor of 1, 3, 5 and 7.	83
Figure 18 Simulation results of increasing the layer thickness on PnC sensors. Larger values of layer thickness are represented by darker colours. The layer thickness values were increased by a factor of 1, 3, 5 and 7. The simulation was performed using the transmission line model for simulating phononic crystals.	84

- Figure 19 Simulation results of increasing the layer thickness on all the layers of the PnC sensor, except on the analyte layer. The simulation was performed using the transmission line model for simulating phononic crystals.....85
- Figure 20 Simulation results of increasing the layer thickness only to the analyte layer of the PnC sensor, leaving the other layers untouched. The simulation was performed using the transmission line model for simulating phononic crystals.....86
- Figure 21 Comparison of the simulation results of two PnC sensors, one with the central peak displaced to higher frequencies by reducing its layer thickness (black), and the other one using an overtone and multiplying the layer thickness by two. The simulation was performed using the transmission line model for simulating phononic crystals.87
- Figure 22 Comparison of the simulation results of two PnC sensors, one with 7 layers (black), and the other one with 11 layers (red). The simulation was performed using the transmission line model for simulating phononic crystals.88
- Figure 23 Comparison of the simulation results of two Phononic crystal sensors, one with 7 layers (black), and the other one with 11 layers (red). The high quality transmission peaks result from using 4 additional layers on the PnC structure. The simulation was performed using the transmission line model for simulating phononic crystals.89
- Figure 24 Simulation results of a phononic crystal structure with a symmetry reduction composed of a change on the dimensions of a liquid layer located on one side of the structure. The simulation was performed using the transmission line model for simulating phononic crystals.....90
- Figure 25 Effect of varying the speed of sound of the analyte layer on a phononic crystal structure composed of seven layers with an analyte layer located in the middle.91
- Figure 26 2D simulation results using the FEM software Comsol Multiphysics of a Phononic crystal sensor with an analyte layer on the middle structure composed of 5 consecutive layers (green) and 9. (blue).93

Figure 27 2D simulation results using the FEM software Comsol Multiphysics of a Phononic crystal sensor with an analyte layer on the middle structure composed of 5 consecutive layers (green) and 9. (blue). This time the analyte layer thickness was increased by a factor of 2.	94
Figure 28 2D simulation results using the FEM software Comsol Multiphysics of a Phononic crystal sensor with an analyte layer on the middle structure composed of 5 consecutive layers (green) and 9. (blue). This time the analyte layer thickness was increased by a factor of 3.	95
Figure 29 2D simulation results using the FEM software Comsol Multiphysics of a Phononic crystal sensor with an analyte layer on the middle structure composed of 5 consecutive layers (green) and 9. (blue). This time, the dimensions of all the PnC were increased by a factor of 3.	96
Figure 30 2D simulation results using the FEM software Comsol Multiphysics of a Phononic crystal sensor with an analyte layer on the middle structure composed of 5 consecutive layers (green) and 9. (blue). This time, the dimensions of all the liquid layers of the PnC were increased by a factor of 3.	97
Figure 31 Block diagram of the electronic characterization with a double sideband modulation. Source: [144].	101
Figure 32 Graphic representation of the acoustic spectrometer structure.	102
Figure 33 Block diagram of the electronic characterization system designed.	103
Figure 34 Acoustic spectrometer experimental arrangement.	105
Figure 35 Experimental results using different alcohols as analytes.	106
Figure 36 Theoretical results using different alcohols as analytes.	107
Figure 37 Representation of a glass cuvette filled with a liquid analyte and the acoustic wave path.	111
Figure 38 Fabricated Structure (a) with the glass cuvette in the middle and the ultrasonic transducers on each side and its respective graphic representation (b). ..	113

Figure 39 Electronic characterisation system for measuring frequency changes in phononic crystals.	114
Figure 40 Experimental (a) and simulative (b) results of the test using distilled water and n-propanol. The cavity is filled with an n-propanol solution in distilled water with a concentration of 5% by volumetric fraction (grey) and with distilled water (black).	118
Figure 41 Experimental (solid lines) and simulative (dotted lines) results of the test using n-propanol and ethanol solutions. The glass cuvette is filled with an n-propanol solution in water with a concentration of 5% by volumetric fraction (grey) and with an ethanol solution in water with a concentration of 5% by volumetric fraction (black). Dotted lines display 1D simulation and the solid lines the experimental results.	118
Figure 42 Comparison between the experimental transmission curves for water in the cavity (black) and the arrangement of 7 layers (grey).	119
Figure 43 Experimental results of the tests using commercial milk products. The glass cuvette is filled with whole milk (grey), lactose-free milk (black) and strawberry flavoured milk (light grey).	120
Figure 44 Schematic representation of the layer arrangement of the PnC structure.	124
Figure 45 First phononic crystal structure fabricated using the 3D printer and glass.	126
Figure 46 Second phononic crystal structure designed with a defect mode and fabricated using the 3D printer and glass. The central liquid layer has a different thickness than the other liquid layers in order to generate a transmission band inside the bandgap.	128
Figure 47 Experimental arrangement containing the designed structure, the transducers, and the electronic characterization system.	129
Figure 48 Simulation results of the first structure using distilled water (a) and ethanol (b) as analytes.	130

Figure 49 Simulation results of the second structure using distilled water as analyte.	131
Figure 50 Experimental results of the first structure using distilled water (a) and ethanol (b) as analytes.....	132
Figure 51 Experimental results of the second structure using ethanol solutions in water with a concentration of 0.02% (a) and 0.5% (b) in volume fraction.	133
Figure 52 Comparison of the experimental results of the second structure using ethanol solutions in water with a concentration of 0.02% (black) and a concentration of 0.5% (grey) in volume fraction.	134
Figure 53 Differential phononic crystal sensor designed with three defect modes..	138
Figure 54 Control phononic crystal sensor designed with only one defect mode....	139
Figure 55 Simulation results using the TLM of the control PnC sensor (a) and the differential PnC sensor (b). Distilled water was used as analyte.	141
Figure 56 Behaviour of the speed of sound of distilled water (a) and the frequency of the central peak of the control phononic crystal (b) when temperature is varied from 3 °C to 43 °C.	142
Figure 57 Effect of increasing 1 °C on simulations using the control PnC sensor. The black line shows the analyte at 23 °C, the grey line shows an increase of 1 m/s on the analyte and the dotted line shows the effect of adding 1 °C to the simulation.	143
Figure 58 (a) Influence of changes in the speed of sound of the analyte layer (a) and the temperature (b) on the relevant transmission peaks of the differential PnC sensor.	144
Figure 59 Relationship between the lateral peaks of the differential PnC sensor and the central peak of the control PnC sensor when the speed of sound of the analyte layer is varied.....	145

Figure 60 Close up of the experimental setup showing the phononic crystal biosensor, the wideband ultrasonic transducers and a 3D printed support structure used to hold to the setup in position.	150
Figure 61 Experimental setup showing the phononic crystal biosensor, the wideband ultrasonic transducers, the 3D printed support structure and the Rigol Spectrum Analyser.	151
Figure 62 Frequency response of the designed phononic crystal.....	154
Figure 63 Experimental results of the phononic crystal biosensor using different concentrations of BSA solutions in PBS buffer. The data was acquired 20 minutes after introducing the analyte in the resonant cavity.....	155
Figure 64 Frequency of maximum transmission of the phononic crystal biosensor using different concentrations of BSA solutions in PBS buffer. The data was acquired 20 minutes after introducing the analyte in the resonant cavity.....	156
Figure 65 Control measurement of the phononic crystal biosensor with a BSA solution in PBS with a concentration of 50ng/ml.	157
Figure 66 Frequency of maximum transmission of the phononic crystal biosensor using different concentrations of BSA solutions in PBS buffer. The data was acquired after washing the PnC biosensor and introducing PBS in the resonant cavity.	157
Figure 67 Phononic crystal structure representation.	161
Figure 68 Phononic crystal sensor used for the experimental realizations.....	162
Figure 69 Simulated frequency response of the phononic crystal sensor.....	163
Figure 70 Experimental results of the phononic crystal sensor using distilled water (solid line) and a lithium carbonate solution with a concentration of 0.01125 g/mL (dashed line).	165
Figure 71 Zoomed-in experimental results of the phononic crystal sensor using distilled water (black dashed and dotted line), and lithium carbonate solutions with a	

concentration of 0.01125 g/mL (grey solid line) and 0.0025 g/mL (grey dashed line).
..... 166

Figure 72 Transient time experimental results of the phononic crystal sensor using distilled water (dashed and dotted line), and lithium carbonate solutions with a concentration of 0.01125 g/mL (solid line) and 0.0025 g/mL (dashed line). 167

Figure 73 Relationship between the concentration of the lithium carbonate solution used as the analyte and the decay time obtained. 168

List of Tables

Table 1	Equivalences between the electrical and acoustic parameters.....	73
Table 2	Designed Structure Properties	78
Table 3	Analytes used for the preliminary tests	105
Table 4	Designed structure properties	113
Table 5	Properties of the Analytes used	115
Table 6	Simulation Configuration Values	116
Table 7	Properties of the Materials used for the simulations.....	129
Table 8	Material properties of the PnC sensors used.	137
Table 9	Properties of the materials and layers	151
Table 10	Properties of the layers.....	161
Table 11	Lithium carbonate solutions.	164
Table 12	Decay time at different concentration values.	167

List of Journal Articles

Villa-Arango, S., Torres Villa, R., Kyriacou, P., Lucklum, R., **2016.** *Cavity Resonance Sensor with Disposable Analyte Container for Point of Care Testing.* IEEE Sensors J. 16, 6727-6732. doi:10.1109/jsen.2016.2584240.

Villa-Arango, S., Torres Villa, R., Kyriacou, P.A., Lucklum, R., **2017.** *Fully-disposable multi-layered phononic crystal liquid sensor with symmetry reduction and a resonant cavity.* Meas. J. Int. Meas. Confed. 102, doi:10.1016/j.measurement.2017.01.051.

Villa-Arango, S., Betancur-Sánchez, D., Torres, R., Kyriacou, P.A., Lucklum, R., **2017.** *Differential Phononic Crystal Sensor: Towards a Temperature Compensation Mechanism for Field Applications Development.* Sensors. 17(9), 1960. doi:10.3390/s17091960.

Villa-Arango, S., Betancur-Sánchez, D., Torres, R., Kyriacou, P.A., **2018.** *Use of Transient Time Response as a Measure to Characterize Phononic Crystal Sensors.* Sensors. 18(11), 3618; <https://doi.org/10.3390/s18113618>.

List of Congress Participations

Villa-Arango, S., Torres Villa, R., Kyriacou, P.A., Lucklum, R., **2016.** *Acoustic spectrometer: resonant sensing platform for measuring volumetric properties of liquid samples.* CLAIB2016 VII Latin-American congress on biomedical engineering, Bucaramanga, Colombia. [Conference]

Villa-Arango, S., Betancur-Sánchez, D., Torres, R., Kyriacou, P.A., Lucklum, R., **2018.** *Using the symmetry reduction technique to cancel the effect of temperature on phononic crystal sensors.* 3rd international conference in nanophotonics and nanophononics - ENPPC#3. Beni Suef University, Egypt. [Conference - Keynote]

Villa-Arango, S., Uribe, S., Montagut, Y., Ocampo, S., Betancur, J. E., Torres, R., Kyriacou, P.A., **2018.** *Phononic crystal biosensors: using antigen-antibody reactions to detect specific proteins.* 3rd international conference in nanophotonics and nanophononics - ENPPC#3. Beni Suef University, Egypt. [Conference - Keynote]

Villa-Arango, S., Betancur-Sánchez, D., Torres, R., Kyriacou, P.A., Lucklum, R., **2018.** *Dual-cavity phononic crystal: sensing platform for performing multi-analyte measurements.* BCS2017 Baltic Conference Series. Stockholm, Sweden. [Conference]

Chapter 1 - Introduction

1.1 Introduction

Humanity has seen a fast and growing technological development in the last decades bringing medicine to new levels; from the discovery of the electrocardiograph by Willem Einthoven and the use of x-rays in the early 1900s, to modern healthcare centres with nuclear medicine equipment, organ transplantation, biotechnology and tissue engineering. However, a troubling fact for the technological advancement in medicine is that novel technology is often more expensive than its predecessor, making the cost of access to health care services to constantly increase with each new technology that is brought into the market. This situation is becoming more and more difficult for local governments that can't sustain stable health care systems. According to the World Health Organization, WHO, the progress towards the Millennium Development Goals was slowed down by the lack of low-cost diagnostic systems and point of care tests, PoCT, and countries with lower economic power, including developing countries, have great difficulties in accessing rising technological advances that carry increasingly higher costs [1].

The development of novel alternative diagnostic systems in the form of point of care tests is one of the most important issues today, not only because there is a need for novel alternatives for measuring different very complex analytes and diagnosing complicated diseases, but because PoCT technologies enable a shift in the health care system towards preventive medicine. The point of care concept is not new, in fact, scientists have been working on PoCT for over 30 years now, and a clear example of that is the wide use of PoCT for measuring analytes like lactate and glucose through test strips all over the globe [2].

Devices designed for PoCT aim to provide low cost, fast and reliable tests for patients, either at home or in a medical facility, thus avoiding the need for sending samples to specialised laboratories and enabling physicians to make relevant diagnostic decisions at the time of the test, therefore, dramatically improving patient care [3].

Recent advances in biofluid sensing technologies have brought a series of new sensors and devices that could become reliable and inexpensive solutions for PoCT. These advances might bring significant progress to the practice of medicine and the healthcare technology industry. According to some authors, some of the most promising technologies to accomplish this goal are acoustic technologies, among others [4].

There is an increasing interest of the scientific community on the development of new acoustic resonant sensors and their wide applicability. Among these are phononic crystal sensors, which have only been recently introduced, and their unique capabilities to selectively control the transmission of waves through solid and liquids has opened the possibility to develop numerous sensing applications, especially for measuring the properties of liquid samples [5].

The recently introduced phononic crystal sensors have shown to be useful for measuring volumetric properties of small liquid samples, which is a prerequisite for developing PoCT devices, since the availability of an analyte is very limited especially when referring to blood, urine, saliva or any other biofluid samples. Furthermore, their unique capability to selectively control the propagation of sound, the great variety of designs, the possibility of having various experimental arrangements, and the scalability of the structures depending on the requirements of the applications, have made phononic crystals very attractive for the development of biomedical sensors, specially, point of care testing devices [6].

The popularity of phononic crystals and their application as sensors has increased in the last decade and has driven research groups to develop multiple applications to measure the properties of liquids. However, there are still many issues that limit their performance and prevent them from entering in the select group of technologies that are used in point of care testing devices. Four main issues have been identified; the first one regarding the materials used for their manufacture and their need to be compatible with biomedical applications and waste disposal good practices. The second one related with the required volume of analyte (fluid) and the need to reduce it to less than 50 uL of biofluid sample. The third issue with current technologies is that the measurements are very susceptible to fluctuations in temperature and other

ambient variables, impeding the realization of exact measurements. Finally, the fourth issue is the lack of means to differentiate the origin of the variations in the speed of sound of complex mixtures being this a major obstacle to determine small changes in specific analytes.

1.2 Aims and objectives

In an effort to address the limitations of current phononic crystal sensors, the primary aim of this thesis is to evaluate the potential implementation of phononic crystals as liquid sensors for biomedical applications, especially for developing point of care technologies, by developing theoretical and experimental studies on multiple phononic crystal structures. This work presents a literature review on phononic crystals, the current state of the development of phononic crystal sensors, a theoretical study evaluating multi-layered phononic crystal sensors to develop point of care applications and also experimental realisations corroborating the computational results and presenting novel PnC sensor structures that overcome some of the limitations of current technology. Finally, the report outlines the conclusions and will describe future work needed to provide a point of care device based on phononic crystal sensors.

1.3 Contribution of the thesis

Phononic crystal sensors are a very interesting alternative to develop point of care sensors. Their unprecedented control of the transmission of waves through periodic media allows them to generate transmission features that can be used to determine the properties of liquids by tracking the frequency of defect modes isolated in bandgaps that serve as filters.

One of the most attractive features of using phononic crystals as sensors is that the measurement principle is fundamentally different from current trending technologies, e.g. electrochemical and optical. They measure the speed of sound of the sample, thus, acquiring information that could complement or replace current technologies.

This research aims to push forward the current limitations of phononic crystal sensors, which nowadays are predominantly theoretical and without a clear path towards the

development of real applications due to multiple barriers impeding their translation to practical testing in the field.

The study of the effect that geometrical and material parameters has on bandgap engineering and on the introduction of defect modes to measure the properties of liquid samples could prove useful to obtain essential insights for the design of phononic crystal sensors and how to overcome current limitations of the technology.

Furthermore, the development of a temperature compensation mechanism would contribute on enabling their use in different conditions and measurement locations.

Examining the behaviour of multiple phononic crystal structures via experimental realizations is complementary to the primary aim of this thesis, as well as directly contributing to the existing body of knowledge on the use of phononic crystals as sensors. The comparison of the experimental behaviour of different phononic crystal structures would provide a unique setting to improve the current state of the art of the technology.

Whereas some phononic crystal sensors have been investigated before by different authors, a similar study exploring the potential of the use of defect modes both to determine the properties of liquid samples via multiple measurement characteristics as well as to develop differential measurements has not been previously performed and it can contribute to the current knowledge on phononic crystals.

In addition, the use of biorecognition agents to enhance the selectivity of the sensor system could provide a useful technique to develop applications where the measurement of complex mixtures is needed and current phononic crystals are unable to be applied.

1.4 Chapter outline

To begin with, the following chapter will provide a literature review of phononic crystals, starting with their introduction in 1992 by Sigalas et al and outlining the most important work made in the area so far. The chapter then goes to describe some

common applications of phononic crystals and how the introduction of defect modes on otherwise periodical structures has boosted their development.

Next, chapter three will describe the use of phononic crystals as liquid sensors and how the control of the propagation of acoustic and elastic waves can be used to obtain relevant information about small liquid samples. This chapter presents a brief review of the first approaches performed by other research groups on the area and the various strategies that they have previously employed to develop sensors using these novel resonant structures. Chapter three will also discuss some of the drawbacks associated with the current methods and present a description of the approach selected to develop a point of care PnC sensor, pointing out the reasons for selecting it as the appropriate technique for later experimental and theoretical works.

Since the design and evaluation of the new phononic crystal sensor will be carried out both using theoretical and experimental realisations, chapter four will first give an introduction to the different methods that have been developed for simulating the frequency behaviour of phononic crystals, and then will describe the principle and theory behind the simulation method selected for performing the theoretical studies, the transmission line model for simulating multi-layered structures. When describing the TLM for simulating phononic crystals, particular attention is paid to the analogy made between the electrical transmission line and the acoustic transmission line as this analogy is fundamental for understanding the transmission of waves through thin layers in periodic structures.

The fifth chapter of this report is based on a theoretical study on the use of phononic crystals as liquid sensors carried out to determine the potential that multi-layered PnC have to be used in the development of biomedical sensors, especially for point of care applications, whilst chapter six through eight, will cover a series of experimental realisations performed using different analytes to corroborate the theoretical findings. Chapter six will begin by briefly explaining the methodology used, and will then highlight the materials that were required to perform each test and the procedure carried out. After presenting the materials and methods, results and discussions will be presented, especially showing the influence of small variations in the acoustic

properties of the different analytes on characteristic transmission features obtained during the theoretical and experimental realisations.

Chapters 6 through 11 will introduce phononic crystal designs that aim to overcome the limitations of current technologies. First, chapter 6 will present a phononic crystal sensor that has a removable element that serves as a containment unit for hazardous samples. Then, chapter 7 introduces the replacement of coupling media for additional phononic crystal layers that are included in bandgap engineering.

Chapter 8 presents a fully disposable multi-layered phononic crystal liquid sensor with symmetry reduction and a resonant cavity. Experimental realisations and their comparison with theoretical simulations are also presented and discussed.

Chapter 9 presents a phononic crystal sensor that, by introducing additional defect modes into a phononic crystal sensor structure, can carry out differential measurements as a temperature compensation mechanism. Theoretical studies using the transmission line model and analytes at various temperatures are also studied and discussed.

Chapter 10 introduces a new phononic crystal biosensor. Experimental and theoretical realizations to study the properties and behaviour of the PnC biosensor by using an antigen antibody reaction are presented and discussed.

Chapter 11 illustrates results from a study exploring the feasibility of using the transient response as a measure to acquire additional information about the analyte.

Finally, Chapter 12 and Chapter 13 will conclude the thesis by discussing the main findings from the studies. Chapter 13 will also lay out limitations, and suggestions for future work to improve the results obtained in this thesis towards the implementation of point of care phononic crystal sensors in the biomedical industry.

Chapter 2 - Phononic Crystals: history and applications

2.1 Phononic crystals

Over the past few decades, the control and manipulation of elastic and acoustic waves has attracted abundant attention to the scientific community. The study of periodic composite materials with wave scattering properties like metamaterials and phononic crystals (PnC), has brought numerous developments and applications that would otherwise be very challenging to realise. Telecommunication technologies is one of the areas where research groups have been more actively working on the fundamental problem and developing applications with these novel composite structures. Waveguiding, confinement and filtering phenomena at wavelength scale have been extensively studied. Phononic crystals have also been used for signal processing, sound isolation and imaging applications among other interesting applications [5].

Phononic crystals are composite materials that are artificially manufactured to have a spatial periodic modulation of their acoustic and elastic properties. The periodicity allows them to exhibit a special control over a selective transmission of mechanical elastic waves in solids, and acoustic waves in fluids. PnC are designed to control, direct, and manipulate waves, and one of their most interesting properties is the ability to reflect waves at desired frequency ranges, whatever their polarisation or wavevector. The periodicity and difference in elastic properties of the constituent materials of phononic crystals can lead to Bragg scattering and/or local resonance effects, making the phononic crystal to behave like a mirror in certain ranges of frequencies and neglecting the propagation of waves through the structure. These ranges are called bandgaps and the process for designing them is commonly called bandgap engineering [5, 8 - 10].

Like their optical counterparts, the photonic crystals, phononic crystals enable the configuration of their band structure and dispersion curves by fine-tuning the geometry, dimensions, and materials of their structure. All these characteristics

strongly modify the frequency response of the system and are exploited in the different applications where phononic crystals have successfully been implemented [5, 8 - 10].

Phononic crystals can be formed by stacking a series of consecutive thin homogeneous layers with large acoustic impedance mismatch and with lateral dimensions much larger than their thickness. The impedance mismatch facilitates the reflection of waves, therefore, strengthening the effect of the bandgaps. This type of phononic crystals are known as phononic superlattices or multi-layered phononic crystals due to the geometry of the structure and layers. This configuration is used in order to approximate their behaviour to a one-dimensional system. The layers are arranged periodically and, therefore, create a spatial modulation of the acoustic properties throughout the structure, facilitating the selective reflection of acoustic and elastic waves and the generation of bandgaps. A schematic representation of a 1D phononic crystal with its respective frequency response can be observed in Figure 1 [11].

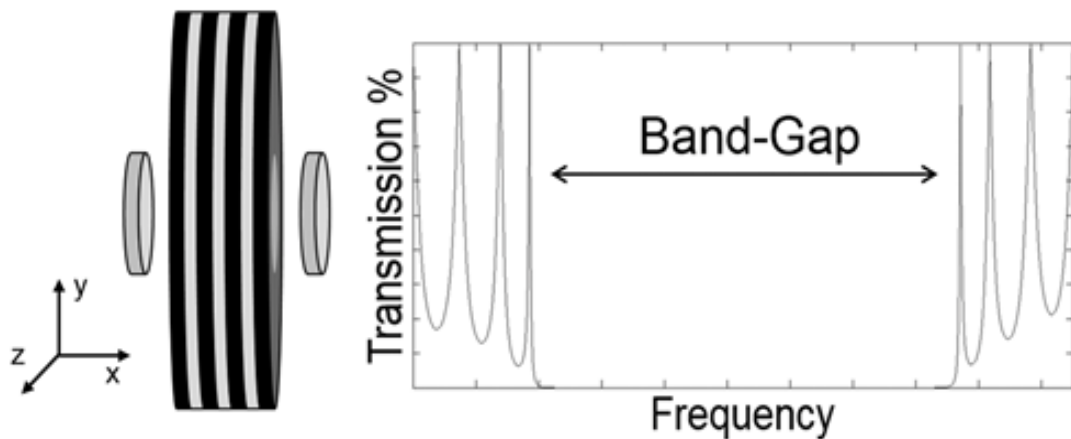


Figure 1 Schematic representation of a 1D Phononic crystal, grey discs on the sides represent ultrasonic transducers and the different colours of the thin layers represent different materials with high acoustic impedance mismatch. The graph on the right represents a typical bandgap of a phononic crystal.

Similarly to any periodic structure, the propagation of acoustic waves in a phononic crystal is governed by the Bloch or Floquet theorem, from which one can derive the band structure in the corresponding Brillouin zone. The periodicity of the structures, that defines the Brillouin zone, may be in one (1D), two (2D), or three dimensions (3D) [12] [13].

The most relevant acoustic properties of the materials composing the phononic crystal structure are mass density, the modulus of elasticity and the longitudinal and transverse wave velocities of the constituent materials. Conventional 2D phononic crystals are composed of a homogeneous matrix and a periodic repetition of scattering centres with different acoustic impedance to the matrix in order to facilitate the dispersion of waves and thus generate frequency bands in which the structure reflects waves in all vectors of incidence. 3D phononic crystals are usually formed by a uniform lattice of high-density scatterers placed within a low-density host matrix. The 3D structures are more complex to analyse and there is less literature presenting complete bandgaps and applications that have been experimentally confirmed using this type of structures. Phononic crystals can be designed using solid–solid, liquid–liquid or solid-liquid structures. Gases can also be used as constituent materials of phononic crystals [5] [8] [14].

The topology of phononic crystals plays a very important role on the bandgap engineering. PnC designs can be classified by their topology in two categories: cermet topology crystals or network topology crystals. Crystals with a cermet topology are also called acoustic phononic crystals and are composed of a liquid matrix and embedded solid scatterers with high density, while crystals with a network topology, or elastic phononic crystals, have a solid matrix and low-density scattering units [15] [16].

While the acoustic properties of the materials that form a PnC are important for the design of bandgaps, the geometry and dimensions of the structure are the ones that finally enable the generation of these bands. Applying Bragg's dispersion theory, the unique interactions that are generated inside the PnC and that allow the formation of bandgaps, arise essentially due to the periodicity present in the crystal, and are manifested when the lattice constant is comparable to the wavelength of the propagating wave, which means, that the working frequency of the PnC is inversely proportional to its dimensions. Some researchers also apply Mie dispersion theory to design bandgaps, which is a localized dispersion and can be usually found in the scattering units of the PnC [11].

The design of bandgaps in 1D phononic crystal structures or phononic superlattices is performed by selecting adequate materials with large enough acoustic impedance mismatch between the layers that form the crystal and by calculating the thickness of each layer so that the maximum reflection generated by each individual layer is located in the same frequency range. The bandwidth and depth of the generated bandgap will depend on the ratio of acoustic impedances between consecutive layers, the larger it is, the larger the scattering effect of the structure, generating a wider frequency range with large acoustic rejection over which phonons are not transmitted [17].

2.2 History

Phononic crystals are periodic composite structures that, through spatial modulation of their elastic/acoustic properties, can selectively control the transmission of waves. Their study is a recent topic, in which the majority of publications have been made in the last two decades. The major interest of the scientific community on investigating the properties and potential applications of phononic crystals began after Sigalas and Economou demonstrated theoretically for the first time the appearance of forbidden frequency bands in periodic structures [5].

Even though the work of Sigalas and Economou first described phononic crystals and is considered the basis for the development of further studies in the area, it is important to highlight the involvement and contribution of other researchers to the understanding of the physics and the behaviour of elastic waves in periodic structures that precede these publications [5].

The first quantitative study in which the propagation of waves in periodic media is studied was introduced by Newton in the 17th century. Newton's model is a discrete system used to obtain the speed of sound in air and consisted of a series of identical masses connected with springs having the same properties [18].

Newton's model and its extensions were studied extensively by numerous researchers for decades, leading to various theories describing wave propagation in periodic systems. Within the great contributions made by these works is the birth of solid state physics when Bloch applied the Floquet theorem to the movement of electrons in

crystalline solids and brought new concepts such as the transmission and forbidden bands in wave transmission in solids. Another important researcher worth mentioning for his great contribution to the development of the theory of propagation of elastic waves in periodic media is Brillouin and the introduction of the Brillouin zone [12] [13] [19].

Levine presented in 1966 a publication that studies the reflection of harmonic waves in periodic layered structures, then, in 1974, Rorres discussed the problem of reflection and transmission of waves in a finite crystal dimension. However, the first experimental evidence of a phononic crystal was not presented until 1979, when Narayanamurti et al investigated the propagation of high frequency phonons through a superlattice of GaAs / AlGaAs, which can be classified as a 1D or multi-layered phononic crystal. In their research, they found a selective transmission that was generated by the superlattice when the wavelength of the phonons was equal to twice the period of the lattice, therefore, fulfilling the condition for Bragg scattering, which states that waves with wavelengths comparable to the lattice constant of a crystal are not transmitted. The authors called their discovery a dielectric phonon filter due to its similarity to the optical dielectric filters. They also showed that a 10% random disorder in the layer thickness made no significant variations on superlattices with large amount of layers. Figure 2 shows the theoretical results presented by Narayanamurti et al in their publication [20] [21] [22] [23].

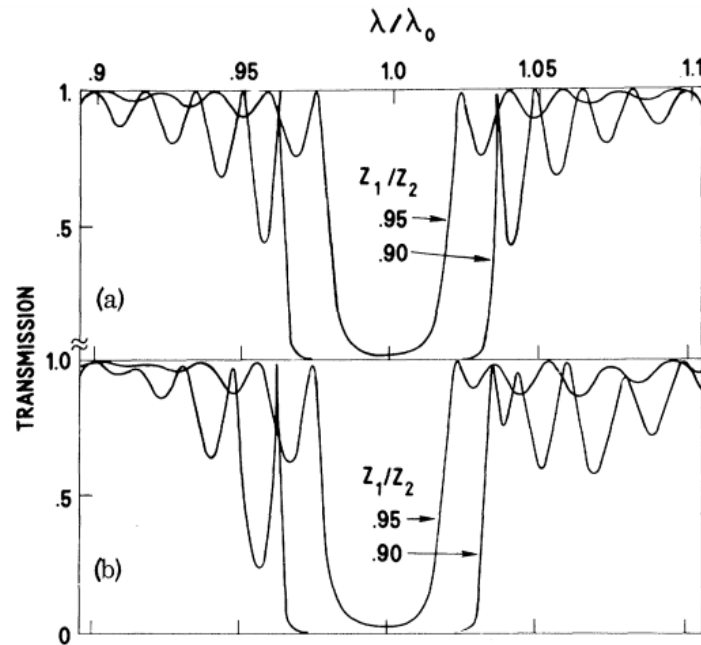


Figure 2 Theoretical results obtained by Narayanamurti et al in a phononic crystal formed by a stack of 50 layers with a 0.95 and 0.90 impedance ratio. The graph shows the results for an ideal superlattice (a) and for a superlattice with a 10% random disorder in the layer thickness (b). The transmission spectra of all the structures display well defined bandgaps. Taken from [22].

Achenbach et al published in the late eighties a theoretical study in which they predicted the absence of propagation modes in a structure formed by a series of solid layers with spherical inclusions, being this one of the first theoretical evidences of a stopband in a complex periodic structure [24].

That same year, the group of Yablonovitch and the group of Sajeev presented almost simultaneously the appearance of photonic crystals, defined as periodic structures having a spatial modulation of the dielectric constant and presenting frequency bands in which no electromagnetic wave propagation is permitted. The existence of these rejected bands attracted great attention from the scientific community, not only because of their rich physics, but also for their broad band of applications, therefore, increasing the growth in the very active field of photonics [25] [26].

The development of periodic structures with forbidden frequency bands or bandgaps was already evident in the publications of Achenbach and Narayanamurti, but it was thanks to the contribution generated by Yablonovitch that a new interest in structures that could selectively control the transmission of waves grew. Phononic crystals are

the acoustic analogue to photonic crystals, but instead of generating bandgaps for electromagnetic waves, PnC generate bandgaps for elastic and acoustic waves, which are even theoretically more complex to realize because of a number of additional parameters that enter the problem of propagation of waves, like the propagation of shear waves, the density and the Lamé coefficients [22] [24] [25].

Some authors have explored the possibility of designing mixed crystals, which integrate phononic crystals and photonic crystals. These structures are called phoxonic crystals and they are used to study the simultaneous control of the propagation and interaction of phonons and photons. The design of these crystals is done mainly using a periodic spatial modulation of the elastic properties and the dielectric constant of the materials on a similar wavelength scale [27] [28].

After Sigalas and Economou presented their first work referring to phononic crystals, and introduced the topic to the scientific community with a studio in a periodic arrangement of high density spheres embedded in a low density host matrix, Kushwaha et al quickly began to work in this growing area and published the first complete full band structure simulation for periodic elastic materials [5] [8].

The efforts and resources of the first research groups who ventured to work on phononic crystals focused at first on understanding and simulating the different necessary conditions for obtaining complete bandgaps with the highest possible bandwidth and depth. The initial application envisioned by the different groups working on phononic crystals was to use these new structures as elastic filters. A complete bandgap is a frequency band in which the propagation of waves is forbidden for all directions of propagation [29] [30] [31] [32] [33].

One of the first publications in which experimental evidence of bandgaps is presented in the audible range using phononic crystals appears a few years after the introduction of the term phononic crystal and was presented by Martinez-Sala et al in 1995. In this publication, the attenuation of sound waves caused by a statue of Eusebio Sempere in Madrid made of metal bars periodically arranged was studied, Figure 3. This sculpture and its acoustic properties attracted the attention of more research groups like the one of Sigalas and Economou in 1996, Kushwaha and Djafari-Rouhani in 1997 and 1998

and also the group of Robertson et al in 1998, who, through their research, determined that the bandgap found in the structure was a pseudo-band as it was only present in a limited number of directions of propagation [29] [30] [31] [32] [33].



Figure 3 Sculpture “El Organo” from Eusebio Sempere made by steel rods over a metallic platform. Taken and edited from [34].

In 1998, the group of Montero de Espinosa experimentally observed the first complete ultrasonic bandgap in two dimensions using a mixed crystal formed by aluminium (Al) films with a periodic array of cylindrical inclusions that were filled with mercury (Hg). The bandgap observed in the experimental studies was located at a frequency around 1 MHz. The idea was to use inclusions with a low propagation velocity, composed of mercury, but with a higher density than the homogeneous host, composed of aluminium. The experimental setup included broadband ultrasonic transducers of 20 mm of diameter, a signal generator, an oscilloscope, and a phase amplitude analyser for obtaining the frequency response. Later that year, two additional groups reported complete 2 dimensional bandgaps, Vasseur et al conducted experiments in duralumin cylindrical inclusions in a homogeneous matrix host of epoxy, and, Sanchez-Perez et al, performed their experimental setup with rigid cylinders in an air matrix. It is important to notice that the publication made by Vasseur et al has great added value, since they used an analytical model, developed by Kushwaha et al, to corroborate the

experimental findings, highlighting the importance of theoretical prediction models and realising previous bandgap engineering to facilitate the acquisition of good results [14] [35] [36] [37] [38].

In the constant quest to optimize the designs of the phononic crystals and to find the various features that allow researchers to obtain complete bandgaps with higher bandwidth and depth, Kushwaha et al presented a structure composed of 3 groups of metal bars of different radii in a consecutive arrangement which can be considered as the first study that proposed adding the properties of three phononic crystals with different geometries with the objective of enhancing the frequency response of the cascade design structure. Using this consecutive arrangement and the properties of the three different phononic crystals, Kushwaha et al managed to get a bandgap with an amplified bandwidth between 2 and 11 kHz [39].

The group led by Rubio managed to experimentally observe in 1999 that bandgaps with frequencies in the audible range that were obtained using periodically arranged solid pillars in air were equal to the bandgaps obtained using hollow pillars, showing that the formation of bandgaps is independent from the material of the scatterer if the host matrix is air and the scatterers are composed of rigid materials. In these cases, the geometry of the structures plays the most important role in the design of bandgaps [40].

Multiple experiments were conducted by Goffaux et al with phononic crystals composed of pillars with different geometries that were rotated systematically on their own axis. The pillars, which in this case are the scattering centres of the phononic crystal structure, were embedded in a host matrix of air. The researchers found that the width of the resulting bandgap strongly depended on the angle at which the pillars were positioned. With these results, the authors proposed the possibility of designing phononic crystals with tuneable bandgaps [41].

In the last two decades numerous studies have been conducted to study the different factors that affect the formation of the phononic crystal bandgaps. These studies have concluded that the density contrast between adjacent materials composing the phononic crystals is one of the most important factors for the formation of complete

bandgaps. Crystals composed of solid materials allow the generation of bandgaps more easily if the scattering units have a high density and are embedded in a host matrix of low density. It is interesting how for phononic crystals containing liquids it's the other way around, since in this type of structures, it is easier to obtain bandgaps with low density scatterers embedded in a high-density host matrix. It has also been found that a high contrast in sound velocities of the materials is another important factor for the formation of these forbidden gaps. As for the other factors that affect the formation of bandgaps, structures with a cubic face-centred form seem to favour its formation in 3D phononic crystals [30] [37] [38] [40] [42] [43] [44] [45] [46].

Kuang et al conducted theoretical studies which found that the use of circular bars is not the most optimal choice when designing phononic crystals with wide bandgaps, while the use of hexagonal, square and triangular bars appears to be best option, although its manufacturing presents greater difficulties if the structures are in the range of a few millimetres [47].

2.3 Local resonances

A major breakthrough in understanding how to design and comprehend the formation of bandgaps in 3D phononic crystals occurred when Liu et al presented their work in locally resonant structures. On this study, they showed that bandgaps are created not only due to Bragg scattering, but also due to locally resonant units. On their publication in the year 2000, they present a phononic crystal in the audible range that consists of lead spheres of one centimetre in diameter coated with silicone rubber that are embedded in a rigid homogeneous epoxy matrix. By carefully separating the rigid spheres from the rigid matrix with an elastic material that serves as an interface, the generation of low frequency resonances that occur due to the movement of the spheres with respect to the surrounding matrix becomes feasible. This effect can be taken advantage of for creating bandgaps, as was shown by the researchers with a bandgap around 400 Hz, which is a very interesting result because the wavelength of waves travelling through epoxy at that frequency is of several meters and is two orders of magnitude above the lattice constant of crystal [48].

Continuing with their research, Liu et al, managed to demonstrate after many calculations that, at frequencies above the resonance frequency, the real part of the effective mass density becomes negative, which means that the core of the spheres oscillates in opposite phase than the applied wave field. This effect generates an exponential attenuation of the waves propagating through the structure, similar to the absorption of electromagnetic waves by the atoms when the frequency of the incident radiation is close to the natural resonant frequency of the atom. The contribution of Liu et al is very important because the generation of bandgaps in structures with locally resonant units does not depend on the periodicity in which the scatterers are organised but on their density reaching a threshold. This conclusion was experimentally demonstrated by Liu with an experimental study with a 3D structure formed by a monolayer of locally resonant units, randomly organized, where the minimum of transmission was located almost in the same position as in the case of an organized 3D phononic crystal. These features make phononic crystals formed by locally resonant units ideal for the development of applications that require sound attenuation and show that PnC are incredibly rich in ways for controlling the transmission of waves [49].

2.4 Focalization

One of the main motivations for many research groups to start studying phononic crystals was the possibility of observing negative refraction of acoustic waves in a similar way as in photonic crystals. The first experimental evidence of focusing ultrasonic waves with a 3D phononic crystal due to negative refraction was reported by Yang et al in 2004. Numerous groups have worked on understanding how to control the focusing of acoustic and elastic waves through phononic crystals, both theoretically and experimentally, in order to obtain high-resolution far-field images [50] [51] [52] [53] [54].

Li et al worked also on focusing acoustic waves using the equi-frequency contours of the corners of the first Brillouin zone with phononic crystals with locally resonant elements. Despite obtaining good quality images, the focal point was very close to the diffraction limit and therefore it is incorrect to catalogue it as a super resolution [55].

Hakansson et al group worked on the problem of focusing in a different way. In their publications they present an acoustic lens that allows the focusing of incident 2D plane waves, unlike the aforementioned publications in which the approach was to focus sound waves coming from point sources. Hakansson et al used an algorithm combining the MST method and a genetic algorithm to design the acoustic lens, which consisted of rigid cylinders in air that generated sound amplification via constructive interference. It is important to note that this structure does not use negative refraction for focusing the sound waves. In their experimental studies it was possible to observe an amplification of 6 dB at the focal point [56].

2.5 SAW phononic crystals and the use of higher frequencies

Both Surface Acoustic Waves (SAW), and Bulk Acoustic Waves (BAW), have been studied in the development of phononic crystals. Designs using SAW resonators have working frequencies typically on the order of GHz and their lattice constant is in the order of nanometres, while designs using BAW resonators are typically in the range of MHz and their lattice constant is in the order of micrometres and even millimetres, which facilitates their fabrication and enables the implementation of microfluidic systems in the designs, thus, generating solid/liquid structures [57].

The majority of previously reported phononic crystal devices have been constructed by hand, assembling scattering inclusions in a viscoelastic medium, predominantly air, water or epoxy, resulting in large structures limited to frequencies below 1 MHz. Recently, phononic crystals and devices have been scaled to higher frequency ranges (30–300 MHz) and by utilizing microfabrication and micromachining technologies. Micro-phononic crystal devices realized in low-loss solid materials are emphasized along with their potential application in radio frequency communications and acoustic imaging for medical ultrasound and non-destructive testing [57].

Many groups have discussed the issue of bringing the use of phononic crystals to higher frequencies, of the order of GHz, using the scalability in frequency by modifying the size of crystal. Taking Braggs dispersion theory into account, the lattice constant of a crystal is inversely proportional to the wavelength of a propagating wave and, therefore, in order to work at higher frequencies one should just use a scaling

factor to shrink the dimensions of the structure until the desired frequency range is achieved. The group of Ramprasad studied the scalability of phononic crystals reaching even the atomic level. This research wanted to evaluate the validity of the assumptions of continuum mechanics and suggests that at dimensions smaller than 1 nanometer these assumptions become invalid, meaning that phononic crystals remaining in the GHz range would have no problems. These results were experimentally verified in subsequent publications made by other authors [57] [58] [59] [60] [61].

2.6 Defect modes on periodic structures

One of the recently introduced features in the study of phononic crystals is the use of point and line defects. Torres et al studied the localization phenomena present when reducing the symmetry of the crystals using point and line defects, and Sigalas et al present theoretical studies of point and line defects in 2D and plane defects in 3D [62] [63] [64].

The study of Caballero et al in 1999 found that by introducing an additional scattering unit in the centre of each unit cell of a crystal a broadening of the bandgap could be achieved [65].

James et al conducted experimental studies in 1D phononic crystals and found that when reducing the symmetry of the crystal by removing one of the layers a transmission band appeared within the frequency range of the bandgap [66].

Munday et al performed a series of experimental studies in a one dimensional phononic crystal with a waveguide formed by alternating segments of cylindrical pipes of different diameters and found out narrow transmission bands within the frequency of the bandgaps [67].

Psarobas et al worked in a theoretical study on a 3D phononic crystal made of planes with spherical scatterers. A defect was added to the structure by changing the dimensions of the spheres in one of the planes. In their study, they found out a vibration mode that generated a very narrow transmission band within the bandgap if the plane with the defect was located in the centre of the structure, whereas when the plane began

to be moved towards the surface of the structure, the transmission band tended to disappear [68] [69].

Khelif's group studied experimentally the possibility of introducing a defect state in an otherwise regular 2D phononic crystal composed of metal rods arranged in a square lattice. The defect was introduced by removing a rod from the crystal. In this publication they showed how the inclusion of this defect generated a transmission peak within the bandgap. They also studied theoretically the possibility of finding similar results by changing the removal of the rod with the inclusion of hollow cylinders filled with water and that the central frequency of these transmission bags could be tuned by changing the internal radius of the cylinders. Motivated by the results of previous studies, Khelif et al used the same structure, but instead of removing a single cylinder, they removed a whole line of cylinders and created a waveguide with a line defect. The results of this experimental study were not very satisfactory because even though a transmission band was generated within the bandgap, its bandwidth was almost equal to the one presented by the bandgap [70] [71] [72].

Pennec et al conducted simulations to show that one of their previous phononic crystal structures, which could be tuned by changing the inner ratios of the cylinders of a phononic crystal, could also be tuned by changing the properties of the contained liquid, thus speeding up the tuning process. Pennec's group also explored the possibilities of using the phononic crystals for multiplexing and demultiplexing sound waves by using a waveguide with a bifurcation capable of transmitting two waves with different frequencies. Theoretical results using FDTD technique found that alternating hollow cylinders having different internal radii or filled with different liquids could achieve the transmission and subsequent separation of two waves of different frequencies through the proposed structure [73].

2.7 Tuning

The first tuneable phononic crystal using electric fields was proposed by Yeh in 2007. In its publication, Yeh presents a design of a 2D phononic crystal consisting of an array of cylinders embedded in a host matrix of an electrorheological material whose properties could be varied by applying an electric field to the crystal. Although it is

evident in their study that the variation of the bandgap was very small, their study was very valuable because the possibility of tuning phononic crystals with electric fields opened the door to the development of various applications where selectivity is required in variable frequency ranges [10].

Bertoldi's group, where also interested in the development of tuneable phononic crystals, and presented a design using an elastomeric solid, which, upon application of a force, changed its physical properties substantially, thus, shifting the frequency of the bandgap [74].

In 2008, Chen and Yang used a structure in which the frequency of some of the transmission bands in their phononic crystal could be modified by changing the inner radius of the pillars constituting the scattering centres of the structure. In their study, they used cylindrical actuators composed of a dielectric elastomeric material in order to control the position of these transmission bands by applying electric fields that modified the properties of the cylinders. The theoretical studies presented by the authors also show the feasibility of using this type of tuneable phononic crystal structures in applications such as acoustic switches and tuneable acoustic lenses [75] [76].

A year later, 2009, the group of Robillard used magnetoelastic materials to perform the tuning of the bandgaps in a phononic crystal by applying a magnetic field to these materials. The problem with this design was that the applied magnetic field had to be very strong in order to observe any changes [9].

The advances regarding the introduction of defect states to the phononic crystals and the possibility of tuning them in various ways having a selective control of the propagation of acoustic and elastic waves make it possible to visualize many applications in the area of elastic filters, mirrors, lenses, multiplexers or demultiplexers, as many groups have already demonstrated with both experimental and theoretical studies [64] [71] [77] [78] [79] [80] [81] [82] [83] [84] [85] [86] [87] [88] [89].

2.8 Summary

This chapter presented an overview of the history and applications of phononic crystals. The most relevant acoustic properties of the materials composing the phononic crystal along with the importance of the topology, geometry and dimensions of the structure were described and discussed. The effect of Bandgaps in phononic crystals was introduced and how they are created using Braggs dispersion theory and local resonances. Other properties of phononic crystals like focusing, point and line defects, tunability and their use at higher frequencies were also presented.

The next chapter will describe the application of phononic crystals in sensing applications by using defect modes as well as the main contributions in this topic.

Chapter 3 - The use of Phononic Crystals as sensors

3.1 Acoustic wave sensors

Acoustic waves are currently used in a large variety of application fields. One of the most challenging applications of acoustic waves is their use in sensing technologies, for example, in chemical/biochemical analysis or in process monitoring and control.

The general concept of an acoustic wave sensor relies in the interrogation of a medium of interest by introducing an acoustic wave into it and then probing its acoustic properties.

Figure 4 shows a schematic representation of an acoustic wave sensor

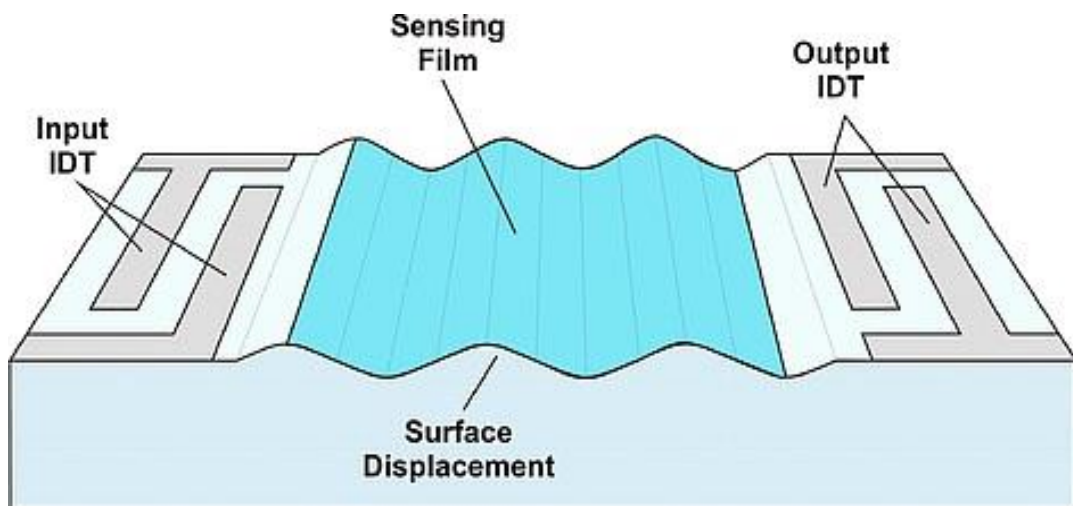


Figure 4 Schematic representation of a surface acoustic wave device composed of 2 Interdigital transducers and a sensing film in which the analyte is deposited and it's interrogated by the surface acoustic wave that travels from one interdigital transducer to the other. Taken from [90].

When the acoustic wave travels through the medium or along its surface, it is influenced by the different material intrinsic properties and geometric parameters of the host medium. Amongst the intrinsic material parameters of interest on acoustic wave devices are mass density, elastic moduli, longitudinal and transverse speed of sound and viscosity. Some of the important geometric parameters that affect the transmission of waves on these devices are the layer thickness and the acoustic path length. Any variations in the characteristics of the medium directly affect the

transmission of waves, generating important changes on the frequency response of the medium. Using adequate acoustic wave transducers, the characteristics of the resulting wave are translated into a voltage signal that can be processed and analysed. Changes in the analysed samples can be monitored by measuring the frequency or phase characteristics of the frequency response of the acoustic wave sensor [91].

Acoustic wave sensors can be classified according to the nature of the acoustic waves and vibration modes involved in the interrogation of the properties of the analytes. They are usually named after the type of acoustic wave dominant in the device and one can distinguish two basic acoustic wave sensor types: ultrasonic sensors and acoustic wave microsensors [91].

Ultrasonic sensors are formed by two ultrasonic transducers that are constantly emitting and receiving ultrasonic waves travelling through a medium. The transducers are usually manufactured using piezoelectric materials which enable the conversion of electrical signals into acoustic waves and vice versa with good efficiency and over a wide range of frequencies. Ultrasonic sensors rely on the measurement of time of flight of an impulse through a medium. The time of flight is determined both by the separation of the transducers and the velocity of propagation of the acoustic waves through the medium. The measurement of the speed of sound in liquid samples is very useful in many applications but in order for ultrasonic sensors to be sufficiently accurate and sensitive they require a large separation between the transducers and, therefore, a large volume of analyte, which is in many cases rather difficult to accomplish [91].

Acoustic microsensors rely not on the measurement of the time of flight of a travelling wave but on the analysis of the frequency response of the system. The frequency of relevant transmission features generated by different resonances inside the system is related to the velocity of the travelling wave and the dimensions of the structure. These sensors are resonant sensors and changes on the acoustic properties of the surface of the resonator, generate variations on the resonant frequency of the system [91].

The most important task of acoustic wave sensors is to deliver the valuable information of different parameters of interest of an analyte. This information is carried by the

ultrasonic wave and it can be related to the liquid level in a tank, the mass density, viscosity or speed of sound of a liquid, or the concentration of a toxic compound in a biofluid, among others.

3.2 First approaches to Phononic crystal sensors

The selective control of elastic and acoustic waves using phononic crystals has attracted the attention of the scientific community and has made numerous groups around the world to concentrate their efforts on using these novel resonant structures in diverse applications. Recently, the disruption of the symmetry in otherwise regular periodic structures has been used to create defect states in the frequency response of phononic crystals. These are localised modes that allow the phononic crystal to have narrow transmission bands located in frequencies inside the bandgap. This distinctive characteristic paves the way for the creation of high-quality frequency filters, waveguides, multiplexers and demultiplexers among others. The properties of the transmission bands that are generated inside the bandgap in phononic crystals with symmetry reduction depend on the defect state which enabled their appearance, therefore, any variation in the elastic or acoustic properties of the material composing the defect could generate changes in the frequency response of these transmission bands [6] [92].

With frequencies in the range of MHz, phononic crystal structures can be assembled in macroscopic dimensions, making the use of liquids as constituent materials feasible, and opening the possibility to the fabrication of solid-liquid phononic crystals. Using liquids as part of the design of phononic crystals has been fundamental for facilitating the development of sensing applications, especially in the development of liquid sensors. The concept of these sensors is based on the introduction of defect modes that appear as relevant transmission features inside bandgaps and that are visible in the transmission spectrum of the phononic crystal. These resonant modes can be formed by point, line or plane defects that are introduced in an otherwise regular periodic structure. It is important to notice that the liquid samples that are going to be analysed, or analytes, become also part of the structure of the crystal, and, therefore, any variation in their acoustic properties causes changes in the frequency response of the defect modes that they generate. Phononic crystal liquid sensors measure variations in

the longitudinal component of the sound velocity of small liquid samples, however, these changes are given by molar mass, molar volume and adiabatic compressibility, which are directly related to the intermolecular interactions of complex mixtures, therefore, phononic crystals could be classified as chemical sensors [6].

The measures of interest in phononic crystal sensors are similar to those on micro-acoustic sensors: the frequency of maximum transmission, the peak amplitude and the peak bandwidth, taken as full span at half peak value.

This section will cover some of the most relevant publications from different research groups around the world that present phononic crystal structures and their use as sensors, especially for liquid sensing applications.

3.2.1 Lucklum et al

Lucklum's group was the first research group that started working on the use of phononic crystals as liquid sensors. The Institute for micro and sensor systems at the Otto-von-Guericke University in Magdeburg has been working on resonant sensors for the past few decades. They first started working on thickness shear mode resonators and quartz crystal microbalances and, in 2008, they moved to the study of phononic crystals and their use as liquid sensors. Taking advantage of the technique of symmetry reduction, which consists of modifying one of the layers of the crystal in order to introduce defect modes, Lucklum's group managed to design phononic crystals whose frequency response had distinctive transmission features that were linked to the acoustic properties of a liquid sample [93].

In its publication in 2008, Lucklum's group used a 1D transmission line model to simulate a 1D phononic crystal composed of steel and water layers. The layers were periodically arranged, and the analyte was positioned in the middle layer. In total, there were 8 layers of steel, 6 layers of water and the analyte layer. Simulation results using the transmission line model, TLM, showed that a transmission peak appeared within the bandgap. This transmission band was clearly sensitive to changes in the acoustic properties of analyte layer: the longitudinal component of the speed of sound and the density. The publication however presented experimental results using a simpler structure composed of five consecutive layers: two aluminium layers with a layer

thickness of 3 mm, two water layers with a layer thickness of 12 cm, and a central analyte layer with a layer thickness of 0.9 mm. For the realisation of the experimental tests two ceramic ultrasonic transducers with a central frequency of 1 MHz and an impedance analyser were used, Figure 5. The impedance analyser acquired the transducer admittance response. The experimental results obtained were not in accordance with the simulations, this largely due to the significant limitation of a 1D simulation when calculating the response of structures with layers with large layer thickness dimensions [17] [93] [94].

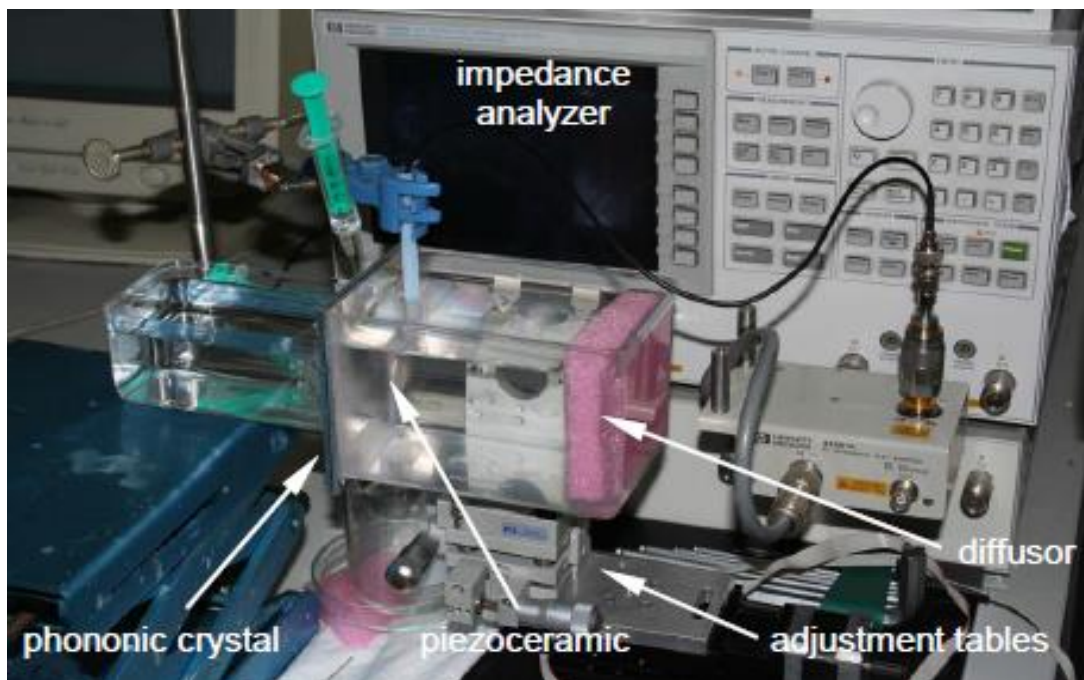


Figure 5 Photo of the experimental setup used by Lucklum et al. Taken from [17]

Continuing with his studies of phononic crystals and their use as sensors, Lucklum presented in 2009, in collaboration with Li, a theoretical and experimental study of a phononic crystal similar to the one presented in the previous study but this time with the experimental evaluation of a structure consisting of 7 consecutive layers with an optimized experimental setup obtaining more satisfactory results, Figure 6 [95].

The large layer thickness of the water layers was reduced in order to improve the response of the system. Changes on the frequency of relevant transmission peaks were distinguishable when varying the properties of the analyte layer. Distilled water and propanol were used as analytes on the experimental realisations.

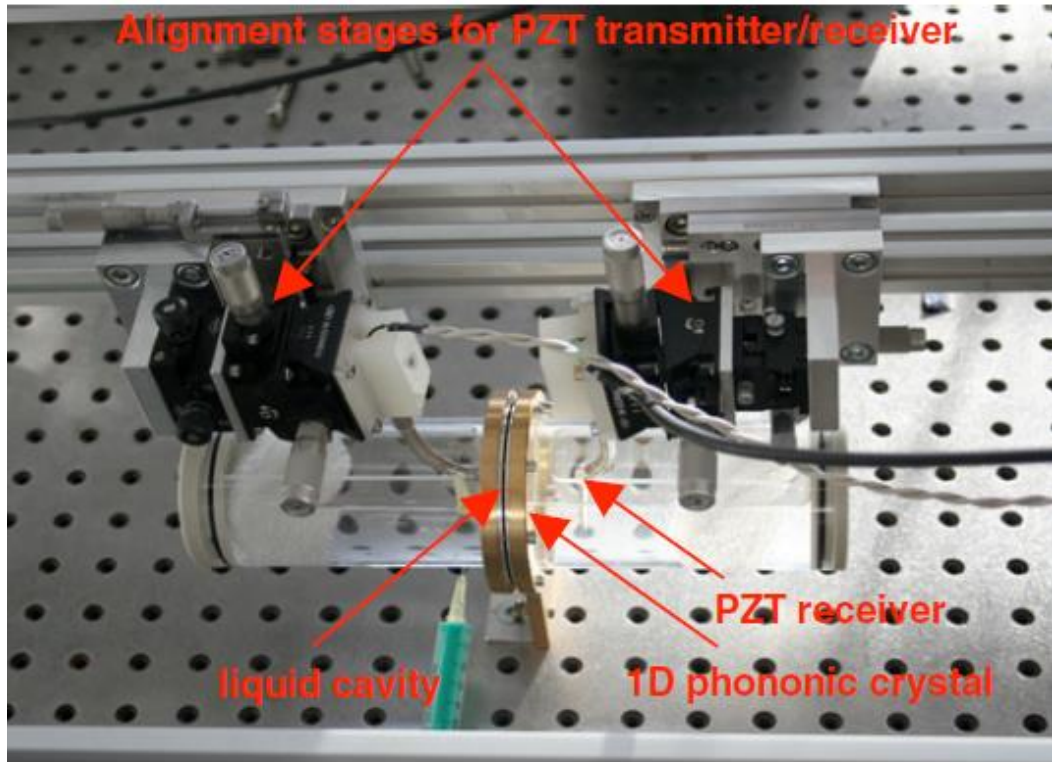


Figure 6 . Photo of the optimised experimental setup used by Lucklum et al. taken from [95]

The authors also performed a theoretical study using the Multiple Scattering Method (MST), in which they analysed a host matrix of aluminium with a series of cylindrical inclusions that could also be used as a liquid sensor, however, the sensitivity of this structure did not improve the one from the 1D structure studied before.

In later studies on 1D and 2D phononic crystal structures, Lucklum further evaluated the geometrical properties of phononic crystals that could be used to optimise the design of phononic crystals and their use as sensors [6] [95] [96] [97] [98] [99].

In 2011, Lucklum's group presented a new study on phononic crystal liquid sensors. In this theoretical and experimental study, a totally different phononic crystal was used. This time a phononic crystal with normal incidence of ultrasonic waves was presented. The structure consisted of an aluminium plate of 0.5 mm thickness with a series of cylindrical inclusions with a diameter of 0.5 mm and arranged periodically with a 1.5 mm lattice constant. The frequency of the ultrasonic waves used in their studies was around 1MHz. The plate was immersed in different liquid mixtures and the frequency spectrum was obtained using broadband submersible transducers and an

impedance analyser. Additional data about the mechanical behaviour in frequency of the structure was obtained using a laser vibrometer. The experimental results obtained during these tests were very promising but significant improvements must be done to the system in order to prevent the use of large amounts of analyte in order to find an application in the industry, especially where low analyte consumption is required like in biomedical applications and point of care testing technologies [92] [100] [101] [102] [103] [104] [105].

In 2012, Lucklum's group returned to the concept of designing a 2D phononic crystal having a parallel incidence of the ultrasonic waves. This time they used a line defect to induce a transmission band inside the bandgap. The structure studied in their publication was a steel bar acting as the host matrix with periodically arranged cylindrical inclusions and a slit in between. The slit acted as a cavity resonator and contained the analyte. The structure used for the experimental realisations can be observed in Figure 7.

The theoretical results of the simulations using the Finite Difference Time Domain (FDTD), method and the experimental results with binary mixtures of alcohol and distilled water showed changes in the frequency response that are very promising for using this structure as a liquid sensor, therefore, they ventured to test it in a real application with gasoline blends to assess the alcohol content of gasoline. The results of these tests showed changes in the transmission peaks present in the rejected band. The authors comment however that there is still much to be done to optimize the structure as it is difficult to differentiate some of the transmission peaks that have a very low signal to noise ratio. Another problem present on the produced PnC sensor is that there is a need for using a coupling medium between the transducers and the PnC structure, and minimal changes in the thickness or acoustic properties of the coupling can affect the frequency response of the structure. The coupling used was glycerol and its evaporation could cause rapid changes that would negatively affect the sensing system [104] [105] [106] [107] [108].

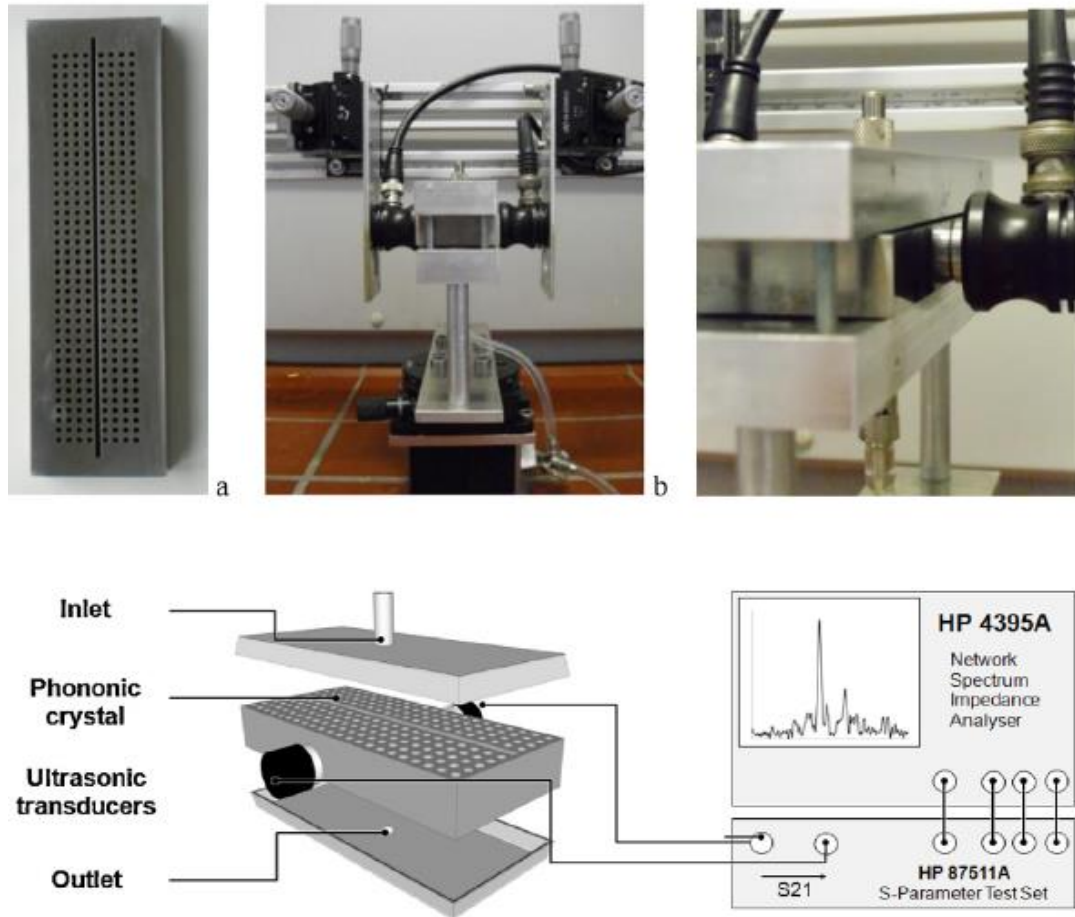


Figure 7 Photos and schematic representation of the elements used by Lucklum's group to perform experimental realisations with their 2D phononic crystal sensor Taken from [105].

3.2.2 Lu et al

The research group led by Lu conducted both theoretical and experimental investigations on a phononic crystal structure composed of a 1D array of Helmholtz resonators made of aluminium in order to determine the properties of the solutions in which it was immersed. The investigations were performed using n-propanol solutions with different concentration values as analytes. Although the experimental results differ from the simulations showing minimums of transmission that are located in different frequencies, these results show that changes in the solution in which the 1D phononic crystal is immersed can induce changes, no matter how small, in the frequency spectrum, thus allowing the use of this structure as a liquid sensor. Apart from the little sensitivity and the different results between the simulations and the experimental realisations, one big drawback of this structure is the need to use around

20 ml of analyte to perform the measurement. This volume is not very large considering common applications, but in the case of biomedical applications where analyte consumption is critical, these large volumes make it impossible to implement this PnC sensor in real applications. The experimental arrangement (a) and results (b) presented by Lu et al on their publication can be observed in Figure 8 [109].

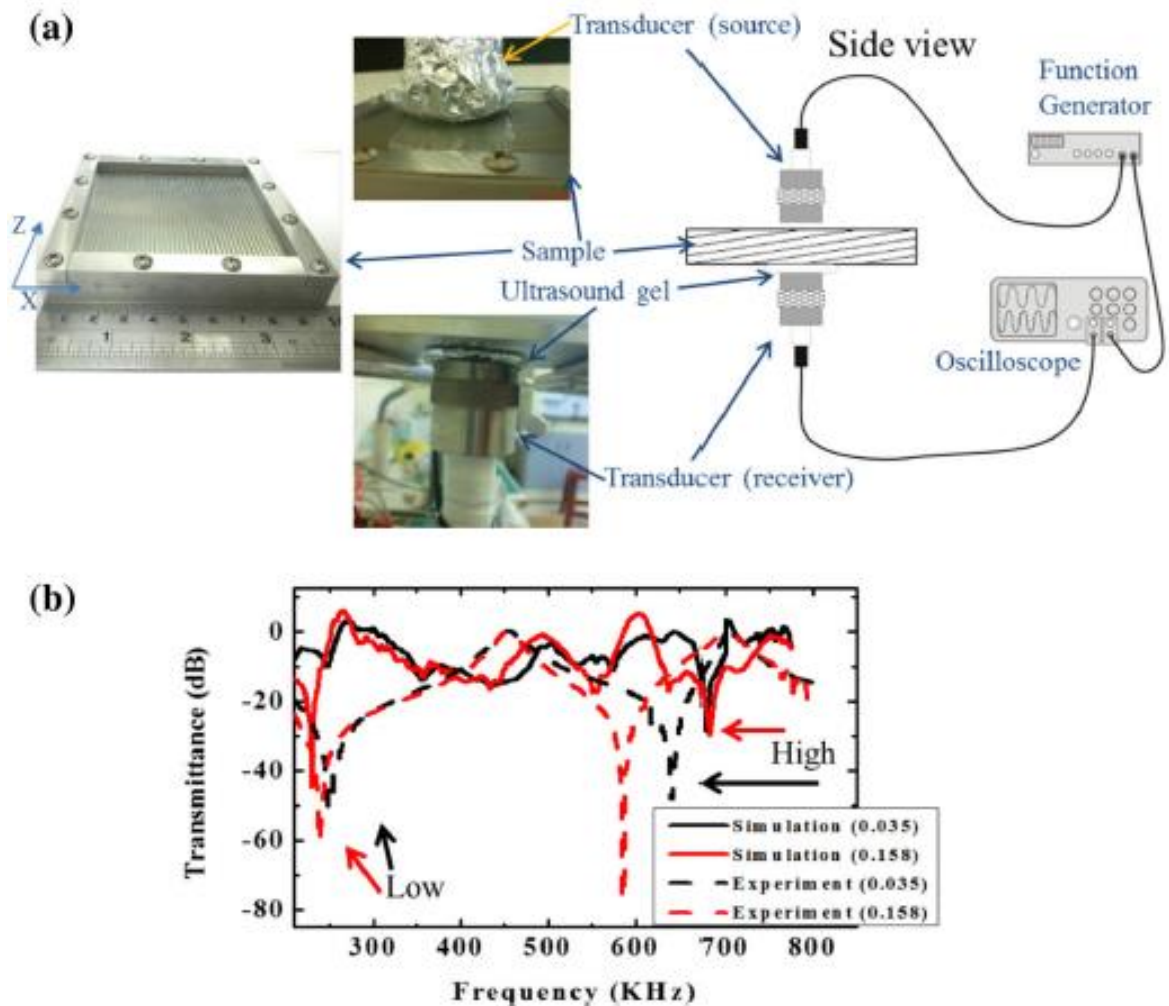


Figure 8 Experimental arrangement (a) and results (b) presented in the publication submitted by Lu et al. Taken from [109]

3.2.3 Salaman et al

Another research group working on the use of phononic crystals as liquid sensors is the group led by Salaman in Turkey. Salaman et al presented in 2014 a liquid sensor based on phononic crystal structures similar to the one designed by Lucklum et al in the sense that they also used a line defect, a waveguide, in a 2D phononic crystal, Figure 9. In this study, simulations were performed with the Finite Element Method

(FEM), to numerically investigate the behaviour of a phononic crystal composed of a series of water-filled cylindrical inclusions in a mercury host matrix. This structure had also a number of point defects that formed a waveguide in the centre of the crystal, these defects are a series of smaller inclusions which were located in the middle of the structure. Different concentrations of ethanol in distilled water were used in order to observe the behaviour of the structure. Theoretical results showed that this phononic crystal structure varies its frequency spectrum when the analyte contained in the cylindrical inclusions is modified, thus making it possible to use this structure as a fluid sensor. However, having a host matrix composed of mercury makes it inconvenient to manufacture it and difficulties its use in the industry [110].

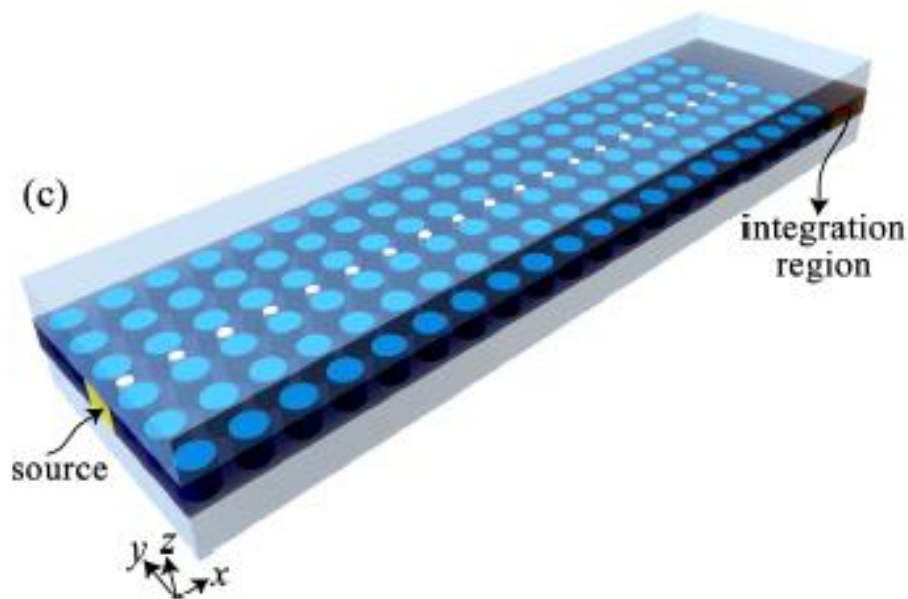


Figure 9 Phononic crystal sensor designed by the group of Salaman. Taken from [110].

3.2.4 Lucklum and Pennec

The group led by Lucklum started a collaboration on 2015 with a group in France led by Pennec and they presented a joint paper in which they propose the first sensor based on a tubular phononic crystal structure to facilitate on-line monitoring of fluids in pipes. The proposed structure has a series of cylindrical inclusions in two directions: along the tube and around its circumference. Preliminary theoretical studies show that this type of structures have characteristics that classify them as potential liquid sensors. The proposed sensing system is interesting although very difficult to realize in actual applications given the necessity to evaluate the displacement field on the tubular

structure with a continuous flow. No experimental results have been presented on this kind of phononic crystals [111] [112].



Figure 10 Tubular Phononic crystal structure presented by Lucklum and Pennec. Taken from [112].

3.2.5 Figeys et al

Figeys et al worked on the development of a phononic crystal structure composed of quasi-fractal perforations to increase the sensitivity of their system in biosensing applications. Such perforations are implemented in BAW resonators to increase their surface area versus volume ratio. The design presented by Figeys's group on a recent publication shows local resonances with scattering effects of acoustic waves that could be used in biosensing applications by adhering a mass on the surface of the resonator inducing a change in the resonance frequency, Figure 11. In a theoretical study, the authors present evidence supporting the hypothesis that the wave vectors undergo a change in frequency due to the adhesion of mass to the surface of the sensor. This structure has a similar working principle to the Quartz Crystal Microbalance (QCM) since it relies on surface mass changes to evaluate an analyte. The authors didn't perform experimental studies with the designed PnC structures [113].

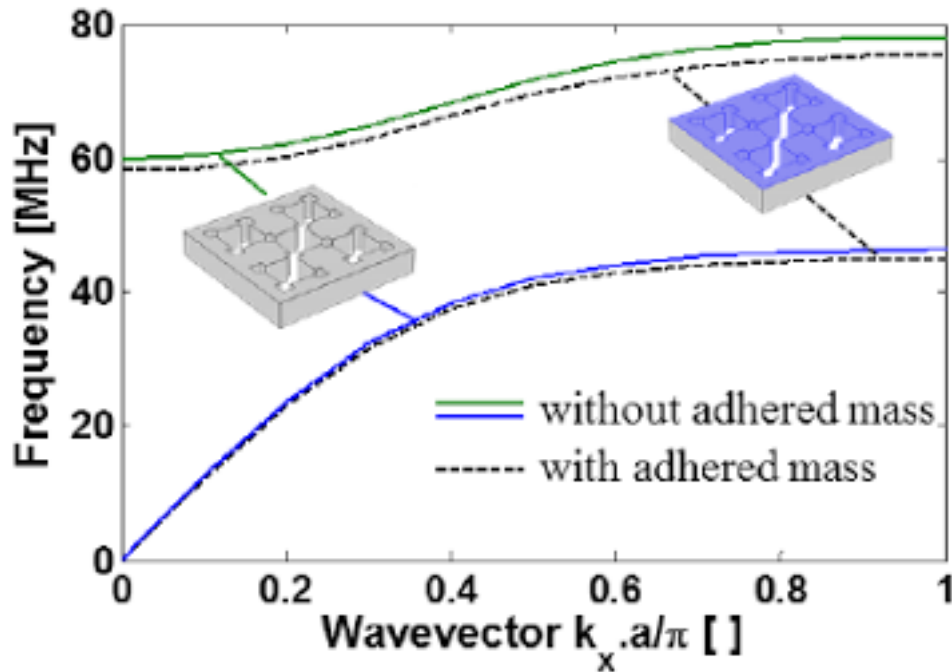


Figure 11 Effect of surface mass on the phononic crystal structures presented by Fygey's et al. Taken from [113].

3.2.6 Aly et al

The group of Aly et al presented a theoretical study in 1D in which they analyse the effects of some physical parameters in the transmission spectrum of the phononic crystals using a 1D Transmission Line Model (TLM). Within the parameters that are commonly studied, temperature is constantly left aside in this type of studies, but their group paid special attention to it. As a result, it was found that the temperature had a direct effect on the behaviour in frequency of phononic crystals and that it affected the morphology of both transmission and stop bands. It is important to notice that in this study an increase of hundreds of degrees Celsius was needed to significantly notice changes in the bandgap and therefore an optimization process becomes necessary in order to be able to use them as temperature sensors. It is clear how the real implementation of phononic crystals as sensors is more on the field of liquid sensors than on measuring temperature or other physical parameters. The investigation of Fygey's group was important in the way that it evaluated the potential effect of temperature in phononic crystal liquid sensors [114].

3.2.7 Xu et al

That same year, 2013, the group of Xu et al, studied the effects of using a phononic crystals with a ferroelectric ceramic material, BST, with rectangular inclusions on its surface and at different temperatures. In theoretical results it was found that changes of only 10 degrees Celsius generate substantial changes in the frequency response of the crystal, this due to the high thermal sensitivity of BST. Although the authors did not visualized their structure as a sensor but as a Lamb wave tuneable filter, this theoretical evidence supports the hypothesis that temperature can affect the performance of phononic crystal sensors if the constituent materials are sensitive to temperature changes, like in the case of liquids, whose sound velocity is strongly affected by these type of changes [115].

3.2.8 Deng et al

Deng et al performed theoretical investigations in phononic crystals with a central slit designed to present transmission peaks of high quality that could be used in the development of applications as biochemical sensors. The simulated crystals consisted of two silicon wafers separated by a slit and with a periodicity of square inclusions in the upper and lower surfaces of the structure. The plate thickness was 0.17 mm, the central slit 0.05 mm and the square groove 0.13 mm. The entire structure was immersed in different liquid mixtures to test their properties and the theoretical results proved that such structures had a high-quality factor and a good sensitivity to measure changes in speed of sound and density of the liquid. The problem using this type of structures is that their manufacture and experimental verification is still very challenging to realize despite the recent advances in microfabrication technologies [116].

3.2.9 Surface acoustic wave phononic crystal sensors

The different studies regarding the use of phononic crystal sensors as liquid sensors presented so far show theoretical and experimental evidence of structures that work using bulk acoustic waves to interrogate them. There are some research groups that have also conducted theoretical studies in phononic crystal sensors using surface acoustic waves to interrogate them at higher frequencies. Most of the computational

results presented by these groups are obtained performing simulations using a finite element method software like Comsol Multiphysics. These theoretical studies have shown feasible to develop SAW phononic crystal sensors at high frequencies, going from hundreds of MHz to a few GHz. The higher probing frequencies enable the resonant sensors to increase the sensitivity of the system, however, the use of higher frequencies also brings more difficulties to the manufacture of the structures. Another problem of using these structures is that they become very sensitive to environmental changes, like slight temperature or pressure variations [117] [118] [119] [120] [121] [122].

3.2.10 Phoxonic crystal sensors

The group led by Lucklum and the one led by of Amoudache published papers together in which they presented both theoretical and experimental evidence of the benefit of measuring the speed of light and sound in fluids simultaneously using structures that combine the characteristics of photonic crystals and phononic crystals to develop a new platform for biochemical sensing. The authors call such structures phoxonic crystals [27] [123].

3.3 State of the art and limitations

Phononic crystal sensors rely on the measurement of the resonance frequency of a discontinuity in the bandgap, if the frequency of this characteristic transmission feature is located in the range of MHz, the dimensions of the defect that enabled its appearance is macroscopic enabling the use of fluids as constituents materials and adequate for characterising liquid samples. Phononic crystals merge the properties of ultrasonic sensors and acoustic microsensors by using the propagation of ultrasonic waves through the medium and measuring the resonance frequency of characteristic transmission features [94] [124].

Although phononic crystals have been successfully implemented in proof of concept investigations as liquid sensors, they have some important limitations that are worth mentioning.

- **Few experimental evidence:** Even though there is a lot of theoretical work on this topic, there are very few groups who have ventured into developing experimental work using phononic crystals as liquid sensors.

It is important to notice that from the phononic crystals designed as liquid sensors using BAW, only the ones presented by the groups of Lucklum et al, from the Otto von Guericke University of Magdeburg, and the one presented by the group of Lu et al, from the National Central University in Taiwan, have been manufactured and experimentally verified. Lu's group conducted one experiment on a 2D phononic crystal and Lucklum's group conducted two experiments on 1D phononic crystals and 2 experiments on 2D phononic crystals.

Moreover, most of the experimental tests have been performed using alcohol solutions on distilled water and only one publication shows experimental testing on a different analyte, gasoline. The manuscript shows the potential implementation of PnC sensors in octane number determination. The experimental results of these two groups are promising but still far from ready for their implementation on challenging applications like biomedical applications, especially for their implementation in point of care testing technologies.

- **Material compatibility:** Biomedical applications such as point of care testing requires a careful handling of the materials that enter in contact with the biofluid sample. The materials need to be compatible with this type of application and the sensor cartridge needs to be either disposable or sterilizable.
- **Complex acoustic coupling:** One of the key challenges when introducing phononic crystals into sensing applications is a reliable acoustic coupling between the analyte container or sensor chip and the measurement instrument. The sensors presented so far use mostly an alcohol-based coupling that can rapidly change its characteristics due to evaporation.
- **Bulky sensor structures:** The phononic crystal sensors explored by the multiple groups working on this topic are very bulky. All the experimental realisations were performed with phononic crystals having very large dimensions and therefore not very suitable for developing challenging applications.

- **High analyte consumption:** Biomedical applications, especially the development of Point-of-care technologies, is one of the most interesting application fields for phononic crystal sensors. The rapidly increasing interest in these technologies is mainly due to the possibility to deliver quick measurement results of a wide variety of analytes in small sample volumes. Phononic crystal sensors still have a large analyte consumption which difficulties their use in such applications.
- **High dependence on controlled environments:** Since the measurement of the properties of the liquids using phononic crystal sensors is mostly related to the speed of sound of the samples, temperature plays a very important role in order to keep the measurements stable. Small variations in temperature can cause measurement errors by changing the speed of sound of the liquids under probe.
- **Complex mixtures:** The measurement of the speed of sound of the liquid sample is a good way to characterize binary mixtures, however, when a complex mixture is used as analyte, the speed of sound is insufficient to provide reliable information about a specific component of the sample.

3.4 Summary

In summary, this chapter described the principles of acoustic wave sensors. Intrinsic material and geometrical parameters of interest on acoustic wave devices were discussed. Some of the most relevant publications from different research groups around the world that present phononic crystal structures and their use as sensors, especially for liquid sensing applications have also been reviewed, along with some of the limitations and open challenges of acoustic wave devices and phononic crystal sensors.

The next chapter will present an overview of the methods used to simulate the frequency response of phononic crystals.

Chapter 4 - Methods for simulating phononic crystals

4.1 Simulation Methods

There are numerous methods for simulating the frequency response of phononic crystals including the one-dimensional transmission line model (TLM), the eigenmodes matching theory (EMMT), the multiple scattering theory (MST), the plane wave expansion method (PWE), the finite element method (FEM) and the finite difference time domain (FDTD) [6] [17] [94] [125] [126] [127].

Among the methods used to simulate the behaviour of phononic crystals and predict the band structure in theoretical studies, the plane wave expansion method, PWE, based on the expansion coefficients in the periodic wave equation as Fourier sums seems to be most popular and has been used in studies of 2D and 3D crystals. Using this methodology, the importance of factors such as the speed and density contrast between host matrix and scattering centres, the crystal lattice type, the volume fraction of the components and the shape of the scattering centres has been verified. The PWE method, despite being very useful to simulate different structures efficiently, showed convergence problems when calculating crystals with liquid components due to the fading of the shear modulus in liquids which causes finite Fourier transform of the Lamé coefficient not converge. This problem has been traditionally solved by using an imaginary value of this coefficient which causes the appearance of unrealistic effects [30] [35] [42] [128].

The multiple scattering theory, MST, was developed by three groups independently. This technique provides more accurate results for systems with spherical scattering centres and calculates the reflection and transmission coefficients allowing a direct comparison with experimental results [69] [129] [130].

Another analytical method for computing the band structure of 2D phononic crystals is the variational method, VM, introduced by Sanchez-Perez. This method shows improvements in convergence time when comparing it to the plane wave expansion

method. Various studies have determined that it has a good convergence at high frequencies for 2D periodic structures but, as the PWE method, it has some problems when used in mixed structures with liquids [36] [131] [132].

Another simulation technique that is widely used for the simulation of phononic crystal structures is the Finite Difference Time Domain (FDTD). This method has been recently adapted for performing calculations of the transmission of elastic waves in phononic crystal structures. This technique discretizes the wave equation in the time domain as well as in space using appropriate boundary conditions, thus having the advantage of observing the time evolution of the elastic displacement throughout the phononic crystal structure. The FDTD is able to calculate any kind of structure, including finite crystals with good results, but has the disadvantage of consuming large amounts of memory and computation time [128] [133] [134].

The group of Vasseur et al conducted a thorough theoretical study of the PWE and FDTD methods and performed experimental studies with solid and hollow cylinders made of copper, Cu, with a homogeneous host matrix of air and water separately. These studies showed that when performing simulations in air, both methods have very similar outcomes below 10 KHz, but when the frequency is increased, only the FDTD method had results that were consistent with the results obtained in the experimental essays. When using water instead of air as the host matrix, the FDTD matched up only until 40 KHz, when there was still a dependence based on the wall thickness of the cylinders [135].

The finite element method, another common method for simulating the response of complex phononic crystal structures, was used by the group of Jensen et al in order to perform the optimisation of 2D phononic crystals. In their study, they used an epoxy matrix with periodically arranged inclusions made of aluminium. They were able to show that the FEM method could be successfully used to simulate the frequency response of phononic crystal structures in optimisation processes [136].

Sigalas and Garcia used the FDTD method in their studies on 3D phononic crystals composed of spheres of mercury, Hg, embedded in a homogeneous host matrix made of aluminium, Al. Their studies were performed to determine the importance of the

transverse components in solid structures, concluding that when these components are ignored, different results were obtained. Similar studies have been developed by other researchers in pursuit of a better understanding of the effect of these transverse components with similar results. [137] [138]

The group led by Lucklum in the Otto-von-Guericke Universität in Magdeburg has been using the Transmission Line Method for simulating phononic crystals composed of thin layers obtaining good results using less computational power and time than other methods. The transmission line model uses an analogy between the acoustic impedance and the electrical impedance to calculate the transmission and reflexion coefficients of 1D structures. The theoretical and experimental realisations conducted by Lucklum's group consisted of solid/liquid multi-layered phononic crystals [95] [97] [99].

4.2 Description of the transmission line model for simulating Phononic crystals

Some basic concepts of mechanical waves and acoustics are presented in the next section prior to the introduction of the transmission line theory and the transmission line method for simulating phononic crystals.

4.2.1 Mechanical waves

Mechanical waves are perturbations of matter that travel through a medium, whose particles undergo displacements due to the travelling wave. Waves transfer energy through the propagating medium, not matter, and while they can cover great distances, the displacements induced in the medium's particles are very limited and, when all the energy of the mechanical work that caused the oscillation is transferred, the particles go back to their initial equilibrium position.

4.2.2 Periodic Transverse Waves

Transverse waves are waves that oscillate perpendicular to the energy transfer, which means that if the propagating direction is along the x-axis, then, the particles in the medium undergo periodical displacements along the y-z plane. It is very important to

point out that the motion of the transverse waves through a medium is different from the motion of a particle of the medium.

Periodic waves travel through a medium following a propagation vector with a constant velocity, while the motion of the particles in the medium is perpendicular to the propagating vector and follow a simple harmonic motion.

Periodic transverse waves formed by simple harmonic motion are also called sinusoidal waves, and the interesting thing about this kind of waves, is that any other periodic wave can be represented as a combination of sinusoidal waves, making them particularly interesting to analyse.

A periodic transverse wave propagating through a string would create a repeating pattern of crests and troughs, the length of one complete wave sequence is called wavelength, λ , and it's the distance between one crest to the next one. The periodic transverse wave has a constant travel speed, c , and the time needed for the wave to travel the distance of one wavelength is called the period, T , therefore, the speed of propagation of the wave equals to the wavelength multiplied by the frequency. See equations (1), (2) and (3).

$$c = \frac{\lambda}{T} \quad (1)$$

$$f = \frac{1}{T} \quad (2)$$

$$c = \lambda f \quad (3)$$

The wave speed of mechanical waves is independent of the frequency and relies only on the mechanical properties of the propagating medium. For that reason, when the frequency increases, the wavelength decreases so that their product stays the same. Equation 3.

4.2.3 Periodic longitudinal waves

Longitudinal waves are waves that oscillate in parallel to the energy transfer, which means that the particles in the medium undergo displacements in the same direction

as, and the opposite direction to, the propagating vector. While the wave pulse travels, it creates compression and rarefaction regions, compression regions are the regions of increased density while rarefaction regions are the regions of reduced density. Due to the parallel movement of the waves and the compression and rarefaction regions created when the wave pulses travel through the medium, mechanical longitudinal waves are also called compression waves and one common type of these waves are sound waves.

The wavelength of mechanical longitudinal waves is calculated by measuring the distance between one rarefaction region to the next or one compression region to the next, the pattern that is created moves along the direction of propagation with a constant wave speed, while each particle on the medium oscillates following a simple harmonic motion parallel to the energy transfer. The wave speed fundamental equation, equation (3) holds for all types of periodic waves, but the actual value of the wave speed might be different for each wave type at the same frequency.

4.2.4 Wave function

All the particles in a sinusoidal wave oscillate with simple harmonic motion with the same amplitude and frequency, however, each particle oscillates with a different phase depending on their spatial position. The displacement of a particle in a sinusoidal wave travelling through a string can be described with a wave function that depends on the time, t , and the propagation coordinate, x . equation (4).

$$y(x, t) = A \cos\left[\omega\left(t - \frac{x}{c}\right)\right] \quad (4)$$

The wave function can be rewritten in terms of the wavelength and the period as:

$$y(x, t) = A \cos\left[2\pi\left(\frac{t}{T} - \frac{x}{\lambda}\right)\right] \quad (5)$$

The wave number, k , is another important quantity that describes the number of oscillations or cycles per unit distance, analogue to the frequency that describes the number of oscillations or cycles per unit time.

$$k = \frac{2\pi}{\lambda} \quad (6)$$

Another important quantity that has not been included yet into the wave equation is a phase offset, φ_0 , which relates to the initial angle of the sinusoidal function. Including the phase offset into the wave function and rewriting it in terms of the wave number we get:

$$y(x, t) = A \cos[\omega t - kx + \varphi_0] \quad (7)$$

It is important to notice that the expression $[\omega t - kx]$ is the phase of the wave, φ , and it must not be confused with the phase offset φ_0 .

4.2.5 Particle velocity and acceleration

The transverse velocity, v , of a particle in a transverse wave can be obtained by deriving the wave function with respect to the time, t . x is left as a constant because we are looking at a particular spatial point. See equation (8)

$$v(x, t) = \frac{\partial y(x, t)}{\partial t} = -\omega A \sin[\omega t - kx + \varphi_0] \quad (8)$$

It is clear in equation (8) that the particle velocity varies with time acquiring a maximum speed of ωA . The acceleration, a , of a particle in a transverse wave can be obtained by deriving equation (8) with respect to the time, t . x is left as a constant because we are looking at a particular spatial point. See equation (9)

$$a(x, t) = \frac{\partial v(x, t)}{\partial t} = -\omega^2 A \cos[\omega t - kx + \varphi_0] = -\omega^2 y(x, t) \quad (9)$$

Calculating the second partial derivative of the wave function with respect to x leaving t as a constant gives us:

$$\frac{\partial^2 y(x, t)}{\partial x^2} = -k^2 A \cos[\omega t - kx + \varphi_0] = -k^2 y(x, t) \quad (10)$$

Knowing that $\omega/k=c$, the following equation can be obtained from equations (9) and (10).

$$\frac{\partial^2 y(x,t)/\partial t^2}{\partial^2 y(x,t)/\partial x^2} = \frac{-\omega^2 y(x,t)}{-k^2 y(x,t)} = c^2 \quad (11)$$

Finally giving the wave equation in one space dimension, see equation (12). The wave equation can also be derived from other physical settings and describes the propagation of waves with a fixed wave speed in one direction.

$$\frac{\partial^2 y(x,t)}{\partial t^2} = c^2 \frac{\partial^2 y(x,t)}{\partial x^2} \quad (12)$$

4.2.6 Acoustic impedance

The acoustic impedance is a measure of the opposition that a medium exerts to a propagating wave. It characterises the existing relationship between the particle velocity and the sound pressure generating it. It is the ratio of acoustic pressure applied to a system, P , to the resulting acoustic flow, U . There is a close analogy between the acoustic impedance and the electrical impedance, which is the ratio of the voltage to the resulting current flow. The acoustic impedance is very useful in the determination of acoustic power, intensity and the reflection and transmission coefficients when waves travel from one medium to another.

The specific acoustic impedance is the ratio of the acoustic pressure, P , to the acoustic flow velocity, u , which is the same as the flow per unit area. Equation (13)

$$Z = P/U \quad (13)$$

$$z = P/u \quad (14)$$

The specific acoustic impedance, z , is an intrinsic property of the medium in which acoustic waves propagate, while the acoustic impedance, Z , depends both on the geometry and the properties of the medium, and varies strongly when the frequency of the propagating wave changes. The acoustic impedance is an indicator of how much sound pressure is generated by a certain acoustic flow at a specific frequency. Equation (14)

The characteristic acoustic impedance of a medium for plane sound waves is equal to the density multiplied by the velocity of the acoustic waves along the direction of

propagation, therefore, increasing with an increase in the speed of sound of the medium as well as in its mass density. Equation (15)

$$z = \rho c \quad (15)$$

4.2.8 Standing waves

Standing waves or stationary waves are waves in which each point on the axis of the propagation medium has a fixed amplitude value. This phenomenon can occur due to a parallel displacement of the medium with the same velocity and opposite direction as the propagating wave, or, in a stationary medium, due to the interference of two waves travelling in opposite directions. The interference can also occur due to the effect of resonance, in which waves are reflected back and forth inside a medium, sometimes called resonator, generating interference. The points located along the axis of propagation that never move are called nodes, while the points located exactly in the middle between nodes are called antinodes. The amplitude of the wave is at its maximum in the antinodes.

This special type of waves are called standing waves, or stationary waves, because the wave pattern stays at the same spatial position at all times, unlike travelling waves.

In order to understand standing waves, it is important to use the principle of superposition of waves which states that the resultant amplitude at each point is the vector sum of the amplitudes of the original waves. The resulting wave can have a larger amplitude, constructive interference, the same amplitude or a lower amplitude, destructive interference, than the individual waves.

The resulting wave function for the displacement at any point of the standing wave, S_3 , formed by the interference of two individual waves, S_1 and S_2 , travelling through a string with a finite length, can be written as the sum of the two wave functions. Equation (16).

$$S_3(x, t) = S_1(x, t) + S_2(x, t) = A_1 e^{i(\omega t - kx)} + A_2 e^{i(\omega t + kx)} \quad (16)$$

In order for a standing wave to appear in a medium that is of finite length and that is fixed on both ends, the length of the medium, L , needs to be equal to an integer number

of the wavelengths divided by two, so that there is a node positioned on each end of the medium. See equation (17)

$$L = \frac{n\lambda}{2} \quad (n = 1,2,3,4, \dots) \quad (17)$$

It is important to notice that waves can still exist if the medium's length does not satisfy equation (17), only that they will not have a stationary wave pattern with static nodes at the ends of the medium.

The fundamental frequency of a standing wave is the wave that satisfies equation (17) with n equal to one, and will be the one corresponding to the largest wavelength since the frequencies tend to increase with each consecutive value of n . The other frequencies are called harmonics or overtones.

4.2.9 Reflection and transmission of waves at a boundary

When waves travel from a medium to another there is a sudden change of the impedance that affects the propagation of the waves generating reflection and transmission effects.

An incident wave travelling from a medium with density, ρ_1 , and wave velocity c_1 , to a different medium with density, ρ_2 , and wave velocity c_2 , will meet a discontinuity in impedance at $x = 0$. At this point, the impedance changes from $z_1 = \rho_1 c_1$ to $z_2 = \rho_2 c_2$.

The displacement of the incident wave has the form of the wave function expressed as an exponential function, equation (18). The wave is traveling in the positive x -direction and after it meets the discontinuity where the impedance of the medium changes, two waves are generated, a reflected wave, equation (19), traveling in the opposite direction as the original wave, and a transmitted wave, equation (20), traveling in the same direction as the transmitted wave. The transmitted wave will have a different wave velocity, c_2 , since it is now travelling through a different medium.

$$y(x, t) = A e^{i(\omega t - kx)} \quad (18)$$

$$y_R(x, t) = A_R e^{i(\omega t + k_R x)} \quad (19)$$

$$y_T(x, t) = A_T e^{i(\omega t - k_T x)} \quad (20)$$

The reflection, R, and transmission, T, coefficients are the relative values of the amplitude of the reflected and transmitted waves with respect to the original wave. In order to calculate the coefficient, boundary conditions must be established. The first one is that there is **no discontinuity on the displacement** and the second one is that there is a **continuity of the transverse force**, N (dy/dx), giving as a result a continuous slope. At $x = 0$, the first boundary condition results in equation (21).

$$A e^{i(\omega t - kx)} + A_R e^{i(\omega t + k_R x)} = A_T e^{i(\omega t - k_T x)} \quad \therefore \quad A + A_R = A_T \quad (21)$$

The second boundary condition at $x = 0$ gives equation (22)

$$N \frac{\partial y(x, t)}{\partial x} + N \frac{\partial y_R(x, t)}{\partial x} = N \frac{\partial y_T(x, t)}{\partial x} \quad \therefore \quad -NkA + NkA_R = -NkA_T \quad (22)$$

And expressing it in terms of the wave speed results in equation (23)

$$-N \frac{\omega}{c_1} A + N \frac{\omega}{c_1} A_R = -N \frac{\omega}{c_2} A_T \quad (23)$$

Taking into account that the wave speed in a string is equal to the square root of the mechanical tension divided by the density, equation (23) can be rewritten in terms of the impedance, equation (24).

$$Z_1 A - Z_1 A_R = Z_2 A_T \quad (24)$$

The reflection and coefficient amplitudes can be derived from equation (23) and using the relation from equation (21). See equations (25) and (26).

$$\text{Reflection coefficient} \quad \frac{A_R}{A} = \frac{Z_2 - Z_1}{Z_1 + Z_2} \quad (25)$$

$$\text{Transmission coefficient} \quad \frac{A_T}{A} = \frac{2Z_1}{Z_1 + Z_2} \quad (26)$$

4.2.10 Transmission line theory

The transmission line theory was developed in the 1800s for modelling circuits working at high frequencies. When designing circuits at high frequencies, the finite speed of the propagating signal cannot be neglected, as it is done in conventional circuit design tools and equations as Kirchhoff's laws, failing to account for the time delay or phase shift induced when the finite velocity of the propagating wave is large enough.

When current flows inside a transmission line, a coaxial cable for example, electrons move down one conductor of the cable and return on the other. This flow of current induces a series inductance associated with the magnetic field created. Given the imperfect insulation of the conductors, some energy will be stored instantaneously in the electric field, inducing a shunt capacitance. If we consider a model with losses, a series resistor and a shunt conductance should be added as well given the imperfections on the conductors and the leakages between them. The equivalent circuit of the described transmission can be observed in Figure 12.

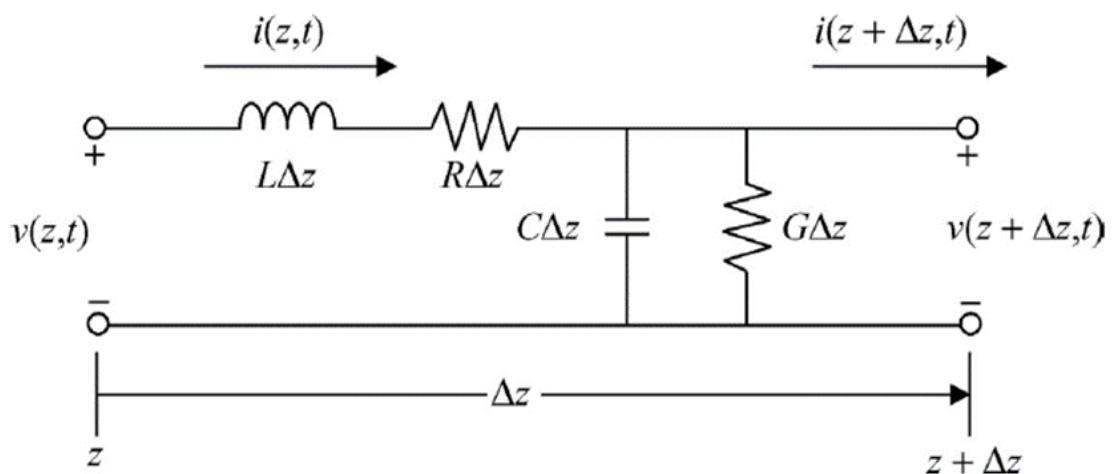


Figure 12 Electrical transmission line representation

The depicted model of a transmission line considers a very short section of length Δz . Since it is a lumped circuit model of a transmission line, we can now use the Kirchhoff's laws to find an equation for the voltage and one for the current behaviour of this circuit.

We are interested in the lossless behaviour of the transmission line and will, therefore, neglect the influence of the series resistance and shunt conductance. To find the voltage we use the Kirchhoff's voltage law. See equation (27).

$$v(z + \Delta z, t) - v(z, t) + L\Delta z \frac{\partial i(z, t)}{\partial t} = 0 \quad (27)$$

Knowing that Δz tends to zero, we can rewrite the equation, see equation (28).

$$\frac{\partial v(z, t)}{\partial z} + L \frac{\partial i(z, t)}{\partial t} = 0 \quad (28)$$

Now applying Kirchhoff's current law and rewriting the equation similarly to equation (28) we can get an expression in terms of the capacitance, see equation (29).

$$\frac{\partial i(z, t)}{\partial z} + C \frac{\partial v(z, t)}{\partial t} = 0 \quad (29)$$

We can obtain individual differential equations for the voltage and the current by using equations (28) and (29). See equations (30) and (31).

$$\frac{\partial v(z, t)}{\partial z} - LC \frac{\partial v(z, t)}{\partial t} = 0 \quad (30)$$

$$\frac{\partial i(z, t)}{\partial z} - LC \frac{\partial i(z, t)}{\partial t} = 0 \quad (31)$$

We can also obtain second order differential equations by deriving equation (28) by the position, z , and equation (29) by the time, t . See equations (32) and (33).

$$\frac{\partial^2 v(z, t)}{\partial z^2} - LC \frac{\partial^2 v(z, t)}{\partial t^2} = 0 \quad (32)$$

$$\frac{\partial^2 i(z, t)}{\partial z^2} - LC \frac{\partial^2 i(z, t)}{\partial t^2} = 0 \quad (33)$$

Knowing that the square root of the capacitance times the inductance is equal to the velocity of propagation, $c = \sqrt{LC}$, it is clear that equation (32) is equal to the "one dimensional wave equation", equation (12). Both voltage and current satisfy the same differential equation.

Boundary or initial conditions must be set up in order to continue developing the solution to the equations. The boundary condition is that there must be a continuity on the voltage and on the current in all the ports of the transmission line, which means that the voltage at the load, V_L must be equal to the sum of the voltages before, V^+ , and after it, V^- , equation (34), and that the current flowing through the load, I_L , must be equal to the difference between the current before, I^+ , and after it, I^- , equation (35).

$$V_L = V^+ + V^- \quad (34)$$

$$I_L = I^+ - I^- = \frac{V^+}{Z_0} + \frac{V^-}{Z_0} \quad (35)$$

Combining ohm's law, equation (36) and the voltage border condition, equation (34), we get an expression of the current flowing through the load in terms of its resistance, equation (37).

$$I_L = \frac{V_L}{Z_L} \quad (36)$$

$$I_L = \frac{V^+}{Z_L} + \frac{V^-}{Z_L} \quad (37)$$

Combining the second equation derived from the boundary conditions, equation (35), and the equation of the current of the load, equation (37), we can get an expression of the ratio between the voltage before and after the load, equation (38). This ratio is known as the reflection coefficient, Γ , and is unitless.

$$\frac{V^-}{V^+} = \Gamma = \frac{Z_L - Z_0}{Z_L + Z_0} \quad (38)$$

The boundary conditions are also useful to determine the generic solution to the differential equation when the system is excited with a sinusoidal wave, equation (39).

$$V(z, t) = V^+ \cos\left(\omega t - \frac{\omega z}{c}\right) + V^- \cos\left(\omega t + \frac{\omega z}{c}\right) \quad (39)$$

In equation (39) V^+ and V^- are the coefficients of the forward propagating wave and the backwards propagating wave respectively. The solution for the current is of the form of equation (40).

$$i(z, t) = \frac{V^+}{Z_0} \cos(\omega t - \frac{\omega z}{c}) - \frac{V^-}{Z_0} \cos(\omega t + \frac{\omega z}{c}) \quad (40)$$

Z_0 is the characteristic impedance of the transmission line and is equal to the square root of the inductance divided by the capacitance, $c = \sqrt{L/C}$.

These equations can also be rewritten as phasors and using the wave number $k = \frac{2\pi}{\lambda} = \frac{\omega}{c}$ as equations (41) and (42)

$$\tilde{V}(z) = V^+ e^{-jkz} + V^- e^{+jkz} \quad (41)$$

$$\tilde{i}(z) = \frac{V^+}{Z_0} e^{-jkz} - \frac{V^-}{Z_0} e^{+jkz} \quad (42)$$

The Thevenin equivalent results very useful to find the impedance of the load and it becomes very handy for calculating the response of cascaded transmission lines with arbitrary loads. The impedance of the load is equal to the voltage at the load, $V(z)$, divided by the current flowing through, $i(z)$. The equation simplifies itself when using the reflection coefficient instead of two arbitrary values of the amplitude of the forward and backwards propagating wave. Equations (43) through (48) describe the process to find the expression of the impedance at the load, Z_{TH} , equation (49).

The relationship between the forward and backwards propagating wave's coefficients is of the form

$$\Gamma V^+ = V^- \quad (43)$$

Replacing the backwards propagating wave coefficients in the voltage and current equations of the transmission line yields

$$\tilde{V}(z) = V^+ e^{-jkz} + \Gamma V^+ e^{+jkz} \quad (44)$$

$$\tilde{i}(z) = \frac{V^+}{Z_0} e^{-jkz} - \frac{\Gamma V^+}{Z_0} e^{+jkz} \quad (45)$$

Calculating the Thevenin equivalent using these equations we obtain

$$Z_{TH} = \frac{\tilde{V}(z)}{\tilde{i}(z)} ; Z_{TH} = Z_0 \frac{e^{-jkz} + \Gamma e^{+jkz}}{e^{-jkz} - \Gamma e^{+jkz}} \quad (46)$$

And expanding the reflection coefficient

$$Z_{TH} = Z_0 \frac{Z_0(e^{-jkz} - e^{+jkz}) + Z_L(e^{-jkz} + e^{+jkz})}{Z_0(e^{-jkz} + e^{+jkz}) + Z_L(e^{-jkz} - e^{+jkz})} \quad (47)$$

Using the Euler's formula we can express equation (47) as

$$Z_{TH} = Z_0 \frac{2j Z_0 \sin(kz) + 2 Z_L \cos(kz)}{2 Z_0 \cos(kz) + 2j Z_L \sin(kz)} \quad (48)$$

And finally dividing everything by $\cos(kz)$ we can get the following equation

$$Z_{TH} = Z_0 \frac{Z_L + jZ_0 \tan(kz)}{Z_0 + jZ_L \tan(kz)} ; k = \frac{2\pi f}{c} \quad (49)$$

4.2.11 Transmission line model for simulating phononic crystals

There are several approaches to describe the behaviour of resonant systems that make use of equivalent circuits. The concept of impedance in physics is widely used and some authors have used the transmission line theory developed for electrical circuits to develop a simulation method that can be used to calculate the frequency response of phononic crystals composed of thin layers. The method is based on performing an analogy between the propagation of waves through a mechanical system and an electrical circuit based on the similarity of the electric and acoustic impedance concept. This method simplifies the calculation of the transmission and reflection coefficients by performing a reduction in the dimensionality. The equivalences between the electrical model and the acoustic model used to develop the transmission line model, TLM, are shown in Table 1.

Table 1 Equivalences between the electrical and acoustic parameters

Mechanical Tension	$T \Rightarrow U$	Electrical Voltage
Particle velocity	$v \Rightarrow I$	Electrical Current
Acoustic Impedance	$Z = \frac{T}{v} \Rightarrow Z = \frac{U}{I}$	Electrical Impedance

Replacing the mechanical tension, T , for the electrical voltage, V , and the particle velocity, v , for the electrical current, I , in equation 41 and 42 we obtain the tension and velocity equation for the acoustic transmission line, equations (50) and (51).

$$T(z) = T^+ e^{-jkz} + \Gamma T^+ e^{+jkz} \quad (50)$$

$$v(z) = \frac{T^+}{Z_0} e^{-jkz} - \frac{\Gamma T^+}{Z_0} e^{+jkz} \quad (51)$$

In order to obtain the frequency behaviour of the multi-layered phononic crystal it is necessary to calculate the transmission and reflection coefficients of the acoustic transmission line, therefore, we use the Thevenin equivalent which on the acoustic transmission line would be related to the acoustic impedance instead of the electrical impedance. Equation 52 shows the Acoustic Thevenin equivalent of the transmission line model for simulating phononic crystals.

$$Z_{TH} = Z_0 \frac{Z_L + jZ_0 \tan(kz)}{Z_0 + jZ_L \tan(kz)} ; k = \frac{2\pi f}{c} \quad (52)$$

A graphic user interface was developed using the transmission line model for simulating the frequency response of phononic crystals and the software MatLab, which is optimised for solving engineering and scientific problems.

The procedure for performing the calculation of the transmission and reflection coefficients is as follows:

First, the user enters the material properties and dimensions of the structure in labelled text boxes. The required information is:

- # of layers
- Initial Frequency
- Ending frequency
- Frequency step
- Layer properties
 - density

- speed of sound
- thickness

After the user has entered the required information, the program starts by calculating the acoustic impedance of each layer using the density and speed of sound of the materials composing the phononic crystal.

Then, the resulting load impedance between the one transducer and the first layer is calculated. The transducers are taken as semi-infinite layers.

The next step is to calculate the load impedance of the rest of the structure.

And finally, the transmission and reflection coefficients are calculated between the load impedance from all the layers and the second transducer.

4.3 Summary

This chapter presented a brief overview of some techniques used to simulate phononic crystal sensors. Several alternatives have been used by multiple research groups to obtain the frequency response of phononic crystals. Among the simulation methods presented in this chapter, the transmission line method has been briefly described. This method plays a central role in the research work presented in this thesis and will be very important to design and understand the behaviour of the phononic crystals studied in this work.

The next chapter will focus on developing a theoretical study of the use of phononic crystals as sensors and the material, geometrical and other design properties that are key to understanding them.

Chapter 5 - Theoretical study on the use of multi-layered phononic crystals as liquid sensors

This chapter presents a theoretical study making use of two simulation methods, the 1D transmission line model for simulating phononic crystals and the finite element software Comsol Multiphysics. The PnC structures explored in this study are multi-layered structures or superlattices, whose frequency response can be simulated using calculations with a lateral miniaturisation of the model with a 1D method given the uniformity and dimensions of the layers that compose the structures, therefore the selection of the TLM.

This chapter initially presents the fundamental basis for calculating the dimensions of each one of the layers that compose the PnC structure, then a theoretical study using the transmission line model as a simulation tool is presented. In this study different multilayer structures and arrangements are simulated in order to observe the behaviour of the phononic crystals under different design conditions. A 2D theoretical study using the finite element software Comsol Multiphysics is also presented to confirm the findings obtained with the model in 1D and verify the effect of introducing a new dimension into the calculations, taking the model closer to reality.

5.1 Bandgap engineering

Bandgap engineering in multi-layered phononic crystals or superlattices is simpler than in other phononic crystal structures with different topologies because their structures are formed by consecutive thin layers with different acoustic properties. These properties can be carefully selected to form bandgaps.

Materials with different acoustic properties, especially high acoustic impedance mismatch, should be used in order to favour the generation of reflected waves between each layer of the structure. Homogeneous layers inside a superlattice present maxima of transmission when the layer thickness, d_T , is equal to a factor of the wavelength divided by two. The reflection coefficients, on the other hand, reach their maximum

value when the layer thickness, d_R , is equal to an odd factor of the wavelength divided by 4. [139] [140]

$$d_T = \frac{n\lambda}{2} \quad ; \quad d_R = \frac{(2n-1)\lambda}{4} \quad (1)$$

Bandgap engineering in multi-layered phononic crystals is based on carefully calculating the layer thickness of all the layers so that their maxima of transmission are located in the same frequencies, therefore, the layer thickness is calculated as a factor of the speed of sound of the material, c , divided by two times the desired frequency of appearance of the maxima of transmission, f .

$$d_T = \frac{n\lambda}{2} \quad ; \quad f = \frac{c}{\lambda} \quad \therefore \quad d_T = \frac{nc}{2f} \quad (2)$$

The calculation can also be performed using the equation of maximum reflection (3), the difference is that the equation of maximum transmission (2) is used to obtain the borders of the bandgap while the equation of maximum reflection (3) is used to find the working frequency of the phononic crystal or the centre of the bandgap.

$$d_R = \frac{(2n-1)\lambda}{4} \quad ; \quad f = \frac{c}{\lambda} \quad \therefore \quad d_R = \frac{(2n-1)c}{4f} \quad (3)$$

The design of liquid sensors using phononic crystals is based on the introduction of resonant modes generated by analyte layers into frequencies inside the bandgap. The frequency of the maxima of transmission is inversely proportional to the dimensions of the layers, therefore, the analyte layer should be calculated using the equation of maximum transmission divided by two (4).

$$d_{T_bandgap} = \frac{nc}{2f} \quad ; \quad d_{T_analyte} = \frac{nc}{2 \times 2f} \quad \therefore \quad d_{T_analyte} = 2d_{T_bandgap} \quad (4)$$

Bandgaps behave as filters that generate boundary conditions to increase the quality factor of the resonance modes generated by the analyte layer. Although ideally, they only increase the quality factor of the peaks, in practice they also affect their amplitude as there are losses in the materials. This attenuation becomes more visible as coupling layers on each side of the main cavity are increased. This behaviour has led some

researchers to propose ideas to solve this issue by bringing these maxima of transmission closer to the borders of the bandgap instead of leaving them in its centre. However, there is insufficient literature evidence to reach a conclusion on whether this is or not an appropriate strategy to solve this problem of attenuation.

5.2 Theoretical study using the transmission line model for simulating phononic crystals

The theoretical study using the 1D transmission line model presents an analysis of the main characteristics affecting the formation of bandgaps, the appearance of resonant modes due to analyte layers and the potential modifications that can be done to the structure of a traditional phononic crystal to modify its behaviour in frequency and use them as liquid sensors.

5.2.1 PnC sensor with analyte resonance mode located in the central frequency of the bandgap.

Figure 13 shows the simulation results using the TLM of a PnC sensor designed following equations (1) and (3). The PnC structure is composed of 7 consecutive layers with the analyte layer located in the middle of the structure. The properties of the layers are shown in Table 2.

Table 2 Designed Structure Properties

Acoustic Properties				
<i>Layer #</i>	<i>Thickness um</i>	<i>Material</i>	<i>ρ (Kg/m³)</i>	<i>c (m/s)</i>
1	inf	PZT	3333	7500
2	375	Water	998	1493
3	1250	Aluminium	3880	4000
4	750	Analyte	998	1500
5	1250	Aluminium	3880	4000
6	375	Water	998	1493
7	inf	PZT	3333	7500

The PnC was designed to have a working frequency of 1MHz and, in order to evaluate the frequency sensitivity of the resonant mode generated by the analyte layer,

variations of 10 m/s were made to the longitudinal component of the speed of sound of this layer.

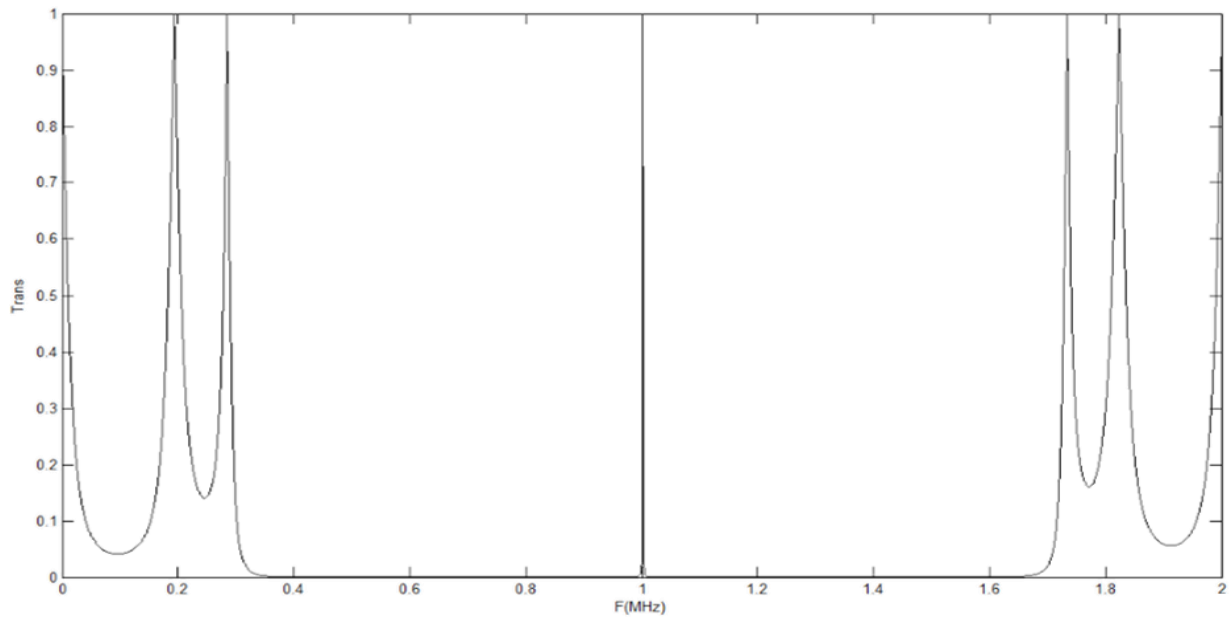


Figure 13 Simulation results of a structure composed of 7 consecutive layers with the analyte layer located in the middle of the structure. The simulation was performed using the transmission line model for simulating phononic crystals.

The sensitivity obtained in this first test was 595 Hz/ms^{-1} . It is clear how in Figure 13 the transmission band generated by the analyte layer is in the centre of the bandgap and has a very high-quality factor. When variations were made to the speed of sound of the analyte layer, changes in the position in frequency of the bandgap were also perceived. The sensitivity obtained in the borders of the bandgap was 280 Hz/ms^{-1} for the higher frequency one and 98 Hz/ms^{-1} for the lower one. This sensitivity is much lower than the one obtained by the central peak.

5.2.2 PnC sensor with analyte resonance mode located near the border of the bandgap

Experimental studies have shown that in some structures when the analyte resonant mode is located in the centre of the bandgap it suffers from severe attenuation and, therefore, Lucklum's group in the Otto-von-Guericke Universität proposed to locate the analyte resonant mode in frequencies near the borders of the bandgap so that the effect of the attenuation could be weaker.

The second simulation performed in this study was to analyse a structure with the same characteristics as the one presented in Table 2 but with an analyte layer located near the border of the bandgap. In order to displace the analyte resonance mode to higher frequencies, a layer thickness of 450 μm was selected. Although the 1D transmission line model is not suitable to observe the amplitude attenuation in the frequency spectrum, it is possible to observe the behaviour of the bandgap when the analyte resonance mode is located nearer. The simulation results can be observed in Figure 14.

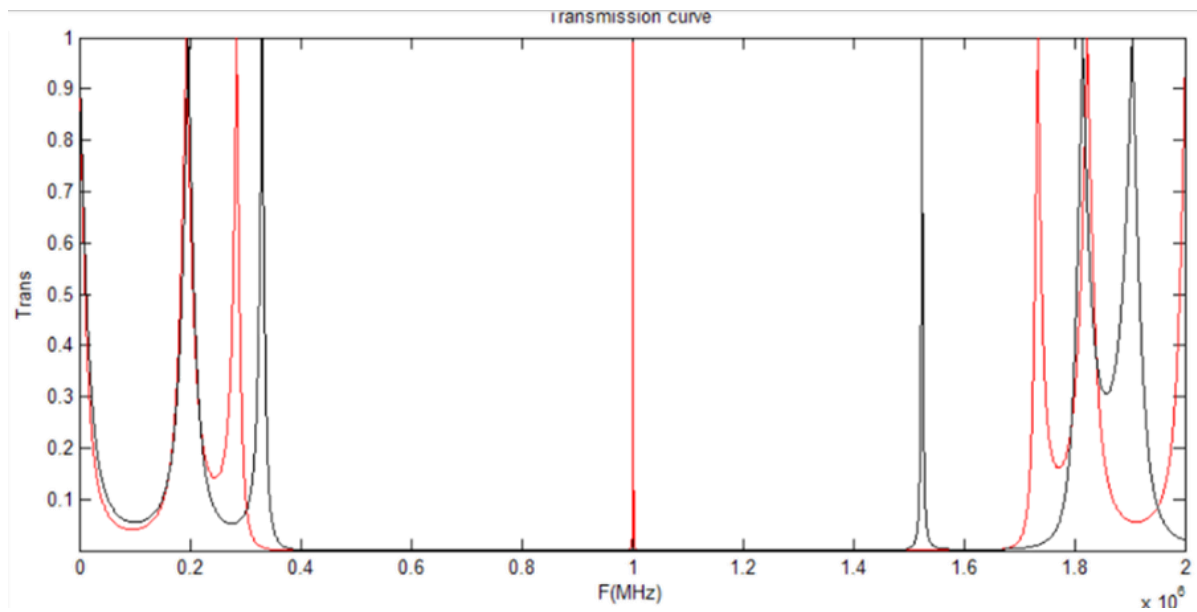


Figure 14 Simulation results of a structure composed of 7 consecutive layers with the analyte layer located in the middle of the structure. In red is the original structure, in black the effect of displacing the analyte resonance mode to frequencies nearer the border of the bandgap. The simulation was performed using the transmission line model for simulating phononic crystals.

The sensitivity obtained in the second simulation was the same as the one obtained in the first one, $595 \text{ Hz}/\text{ms}^{-1}$. Figure 14 shows how the analyte resonance mode, that was generated in the second simulation (black) and that is located near the border of the bandgap, has a lower quality factor which could proof that when the peak is located nearer the border of the bandgap it is less influenced by the attenuation effects of generated by it. The bandgap suffered minor changes in the second simulation and was displaced to higher frequencies while maintaining its filtering properties.

If the fact that lowering the quality factor of the transmission peaks increasing their bandwidth is enough to overcome the attenuation problems that arise from locating

them in the centre of the bandgap, one could think of an alternative to the solution proposed by Lucklum's group, and it is to lower the acoustic impedance of the materials composing the layers surrounding the analyte layer, thus lowering the bandwidth of the bandgap and its effect on the characteristic transmission feature generated by the defect mode.

Figure 15 shows the results of a simulation using the same structure from Table 2 but replacing the aluminium layers by a material with half the density and speed of sound. It is clear how the bandgap's bandwidth was reduced, and the analyte resonance mode presented a lower quality factor.

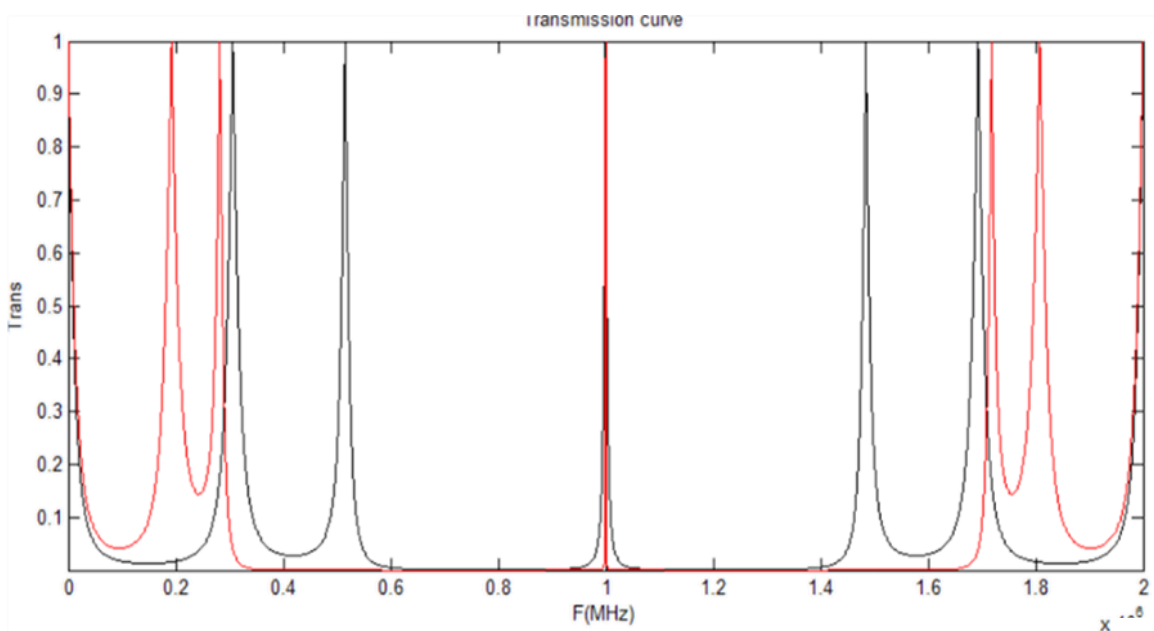


Figure 15 Comparison of the simulation results of structures composed of 7 consecutive layers with an analyte layer located in the middle. In red is the original structure, in black the effect of replacing the solid layers by materials with lower acoustic impedance. The simulation was performed using the transmission line model for simulating phononic crystals.

The sensitivity of this new structure was also tested, and it was found that reducing the acoustic impedance of the aluminium layers resulted in a lower sensitivity, 400 Hz/ms⁻¹. It appears that the bandgap's width plays an important role in the determination of the sensitivity of the system and, therefore, additional simulations were performed to confirm this hypothesis. The results of these simulations can be found at the end of this 1D study.

5.2.3 PnC sensor using overtones

The working frequency of phononic crystals sensors is inversely proportional to the dimensions of the structure, therefore, increasing the layer thickness generates a displacement of the working frequency of the PnC to lower frequency regions. Each resonance mode has overtones that appear in multiple frequencies and the next test was performed to see if these overtones could be used to design a phononic crystal sensor. Figure 16 shows the results of a simulation using a structure like the one presented in Table 2 but with the dimensions of all the layers multiplied by 3 to obtain an overtone of the analyte resonance mode around 1 MHz.

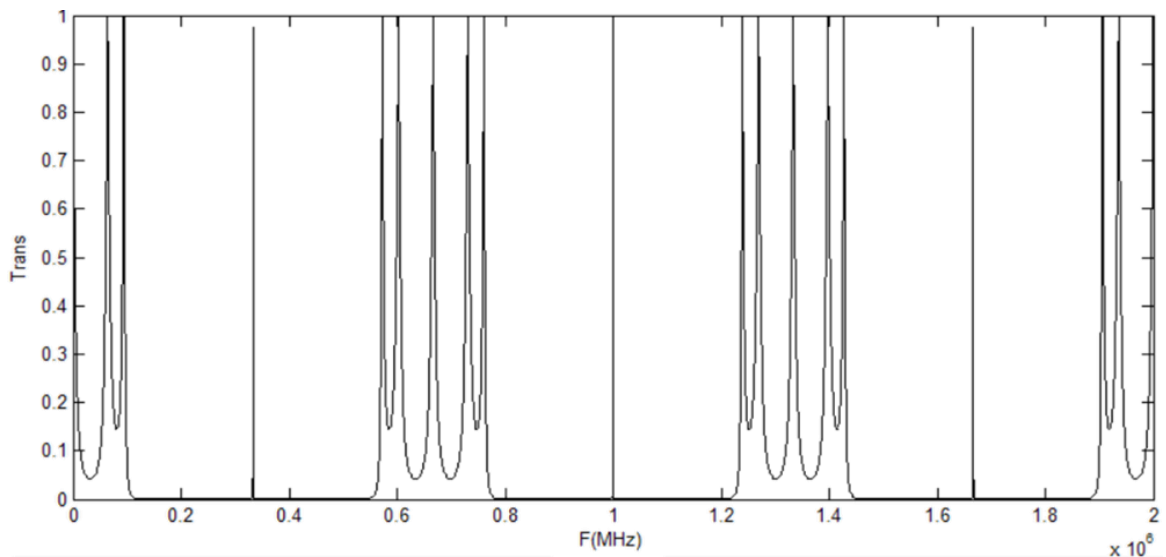


Figure 16 Simulation results of a structure composed of 7 consecutive layers with an analyte layer located in the middle. This structure is composed of layers three times larger than the others investigated before. See Figures 13, 14 and 15. The simulation was performed using the transmission line model for simulating phononic crystals.

Using values three times bigger in the layer thickness generates two additional overtones inside the same range of frequencies. The first overtone is located around 1 MHz and the bandgap surrounding it is three times narrower than the one generated in Figure 13.

The sensitivity of the analyte resonant mode located around 1MHz in this new arrangement was found to be of 595 Hz/ms^{-1} , equal to the first PnC sensor investigated. These results show that it is possible to fabricate structures with larger dimensions while maintaining the sensitivity.

The use of overtones could open the possibility to new designs, and, using bigger dimensions, enables the use of different manufacturing techniques that would otherwise be very difficult to implement like CNC routing machines and 3D printers. To confirm if the use of overtones increasing the dimensions of all the layers of the PnC structure did not affect the sensitivity over a wide range of overtones, new simulations were performed. Figure 17 shows the resulting bandgap bandwidth and sensitivity of structures whose layer thickness values were increased by a factor of 1, 3, 5 and 7.

The sensitivity was measured in the analyte resonance mode overtone generated around 1 MHz and it was constant for all the simulations, 595 Hz/ms^{-1} , while the bandgap's width around it decreased with each simulation.

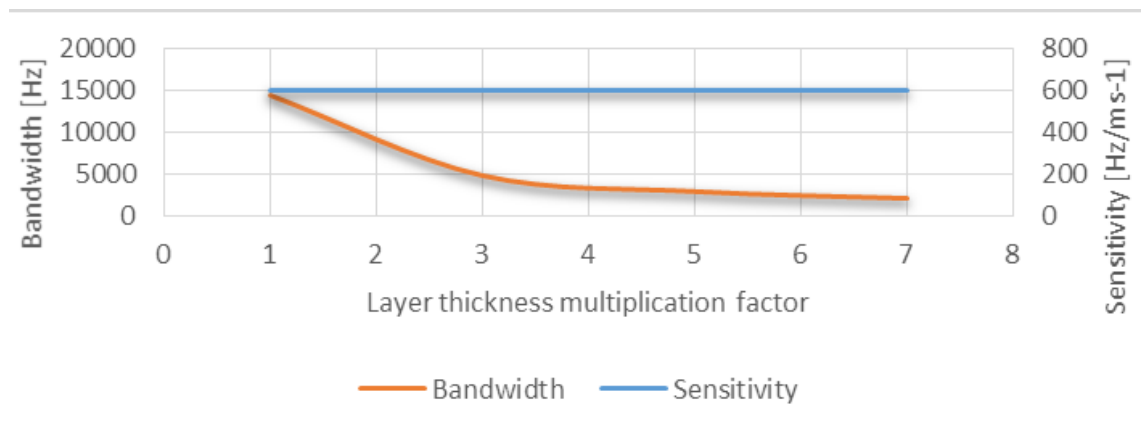


Figure 17 Behaviour of the bandwidth and sensitivity of the bandgap in a PnC structure whose layer thickness values were increased by a factor of 1, 3, 5 and 7.

Knowing that the impedance mismatch affects the quality factor of the defect mode located in the middle of the bandgap it is only foreseeable that the modification of the layer thickness could have the same effect. Figure 18 shows the results of simulating an increase in the layer thickness by a factor of 3, 5 and 7.

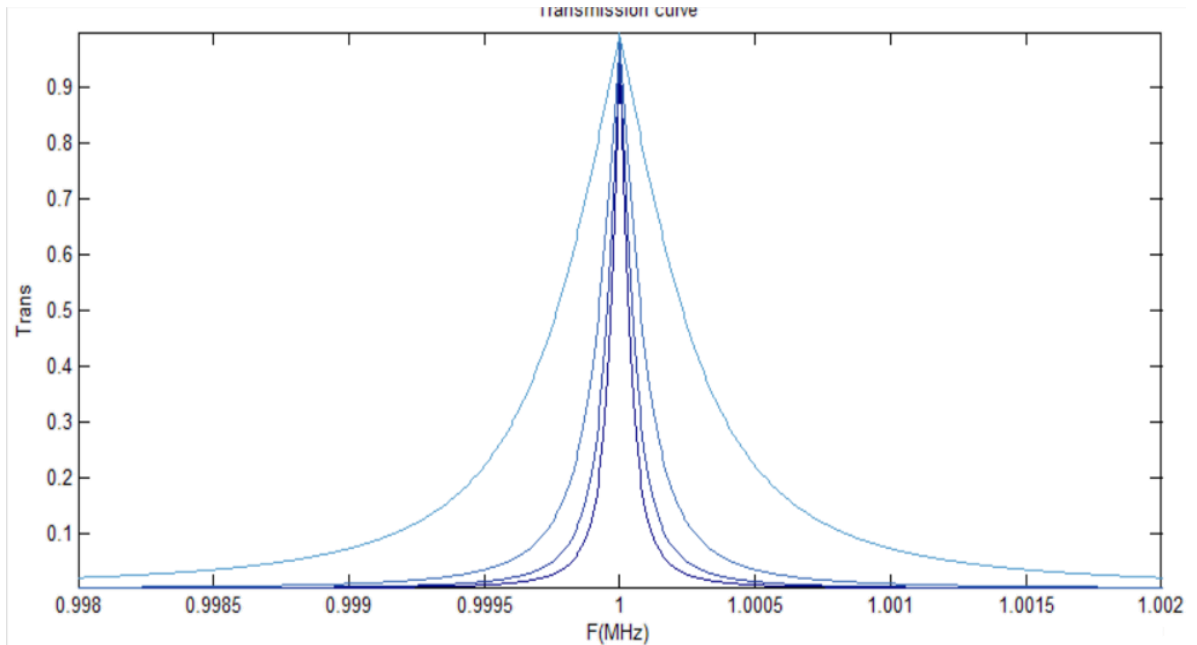


Figure 18 Simulation results of increasing the layer thickness on PnC sensors. Larger values of layer thickness are represented by darker colours. The layer thickness values were increased by a factor of 1, 3, 5 and 7. The simulation was performed using the transmission line model for simulating phononic crystals.

As predicted larger values of layer thickness produce higher quality factors in the defect modes located in the centre of the bandgap. The larger the quality factor the larger the probability of obtaining large losses in real applications thus the importance of taking this into consideration when designing phononic crystal sensors.

5.2.4 PnC sensor using bandgap overtones only

The design of the defect mode can be done independently from the design of the bandgap. The defect mode can be placed in one of the gaps created using multiple overtones having smaller thickness for the analyte layer and larger thickness for the other layers composing the phononic crystal sensor.

The next simulation performed was to study the effect of increasing only the overtones of the bandgap and leaving the analyte layer thickness unchanged. There are some applications of phononic crystal liquid sensors where the analyte is not abundant, and it is important to keep the analyte consumption as low as possible. Figure 19 shows the simulation results of a structure similar to the one presented in Table 2 but with the

values of the layer thickness of all the layers, except from the analyte layer, multiplied by a factor of three.

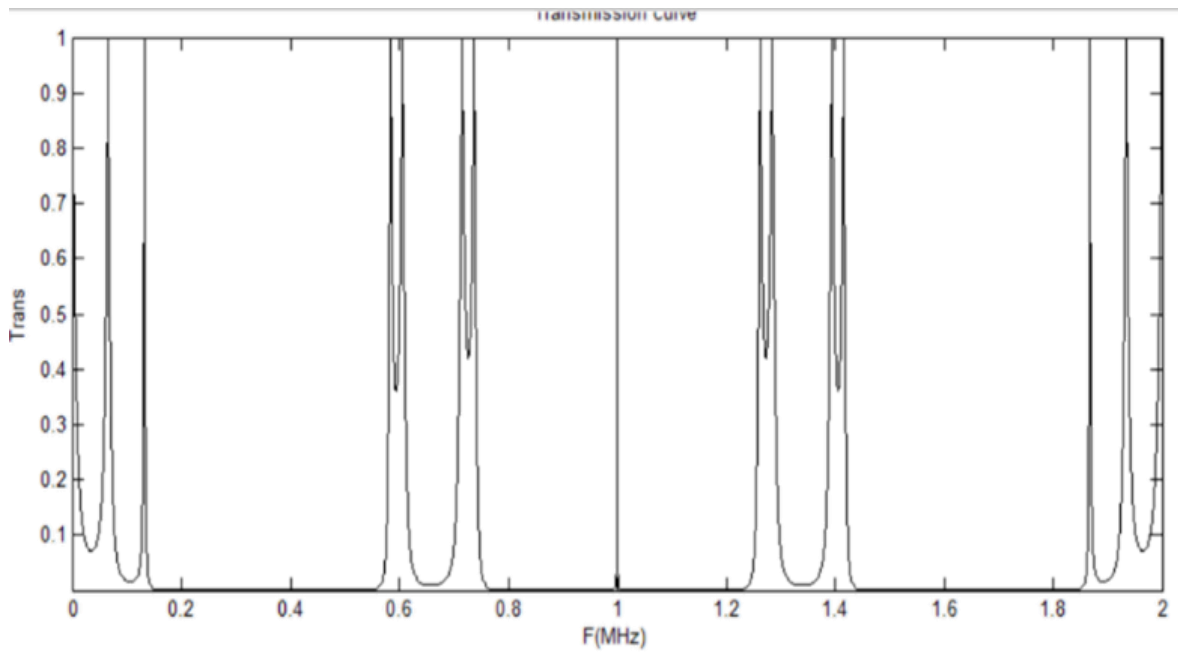


Figure 19 Simulation results of increasing the layer thickness on all the layers of the PnC sensor, except on the analyte layer. The simulation was performed using the transmission line model for simulating phononic crystals.

Figure 19 shows 3 bandgaps and one analyte resonant mode around 1 MHz, as expected. The bandgaps show a different morphology, but the effect is the same. This is due to the absence of analyte resonance modes inside the transmission bands of the bandgap borders. The sensitivity of the transmission peak located around 1 MHz is lower than in previous simulations, 500 Hz/ms⁻¹. The changes in the morphology of the bandgap borders around the 1 MHz analyte resonant mode have affected the effects of the bandgap on the transmission band inside it.

5.2.5 PnC sensor using analyte overtones only

Increasing the values of the layer thickness of the layers surrounding the analyte generated a lower sensitivity, and, therefore, it is possible that increasing only the value of the layer thickness of the analyte layer could increase the sensitivity of the PnC Sensor. Figure 20 shows the results of increasing the layer thickness of the analyte layer by a factor of two, leaving the other layers of the structure unchanged.

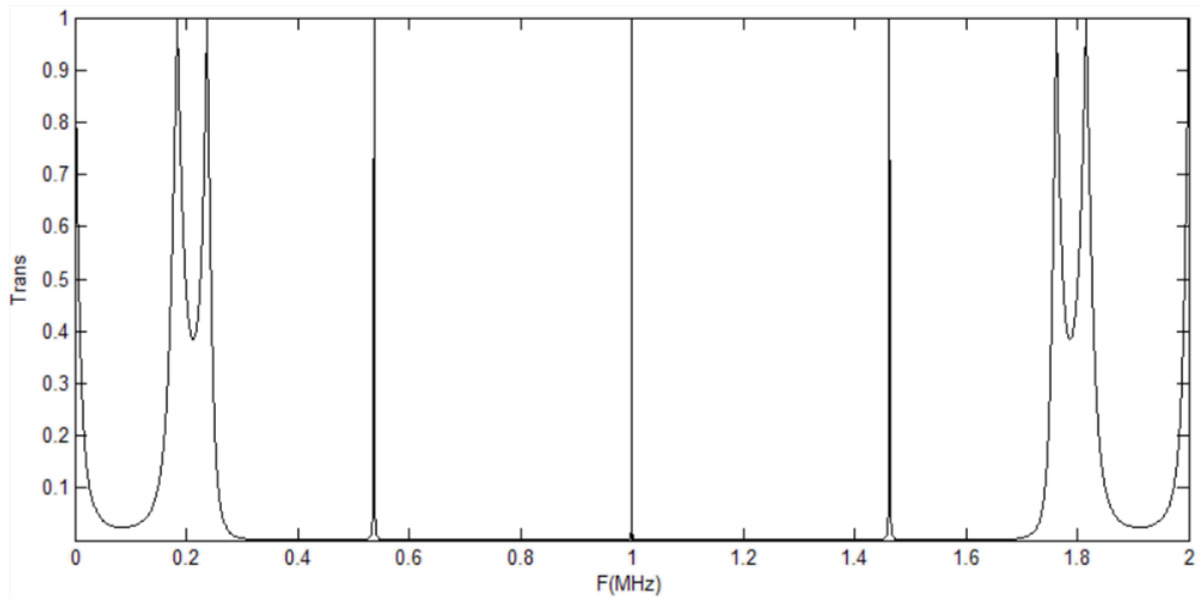


Figure 20 Simulation results of increasing the layer thickness only to the analyte layer of the PnC sensor, leaving the other layers untouched. The simulation was performed using the transmission line model for simulating phononic crystals.

The effect that generates increasing the thickness of the analyte layer two times is the displacement of the analyte resonant mode to 500 KHz and introducing two additional overtones inside the bandgap; one of which has a central frequency of 1MHz. The sensitivity of the 1 MHz peak is 630 Hz/ms^{-1} , which is higher than the original sensitivity of the structure without any increase in the layer thickness. The same test was performed again, but this time with a value of the layer thickness of the analyte layer multiplied by 5 and the sensitivity of the system increased to 650 Hz/ms^{-1} , showing that the larger the factor by which the analyte layer is multiplied, the larger the sensitivity.

5.2.6 PnC sensor using analyte overtones near the bandgap borders

Increasing the layer thickness only in the analyte layer results in the introduction of multiple overtones which are distributed evenly in the in the bandgap. The overtone that is near the higher frequency end of the bandgap should be less attenuated by the effects of the bandgap and might be a good candidate for using as measure in phononic crystal sensors.

Continuing with the theoretical study, a simulation to compare the sensitivity of an overtone of a phononic crystal having its analyte layer multiplied by a factor of two

and that is located near the high frequency end of the bandgap versus the sensitivity of an analyte resonant mode displaced changing the width of the analyte layer to avoid the effects of the attenuation generated by the bandgap. Both are located in the same frequency. The use of an overtone could be useful in structures with dimensions very difficult to manufacture and with sufficient availability of analyte.

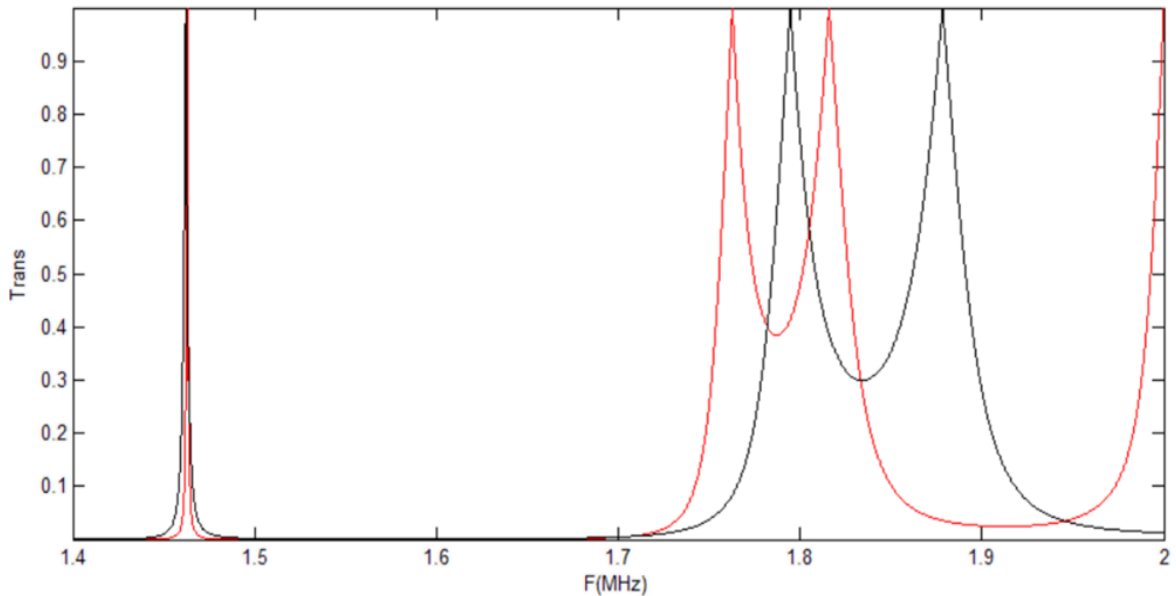


Figure 21 Comparison of the simulation results of two PnC sensors, one with the central peak displaced to higher frequencies by reducing its layer thickness (black), and the other one using an overtone and multiplying the layer thickness by two. The simulation was performed using the transmission line model for simulating phononic crystals.

Figure 21 shows the simulation results of two structures similar to the one presented in Table 2 but one with a layer thickness multiplied by two in the analyte layer (red) and the other one with a layer thickness of the analyte layer of 475um (black). Both peaks are located on the same frequency, but the bandgaps are a little separated. The peak generated by the overtone has a higher quality factor than the displaced one. When studying the sensitivity of both multi-layered phononic crystal structures it was found that the displaced resonance has a higher sensitivity of 622 Hz/ms^{-1} , which is good, but the overtone structure has an even higher sensitivity, 840 Hz/ms^{-1} . It is important to notice that increasing the frequency of the analyte resonant modes affected both the sensitivity and the quality factor of the resonant peak.

5.2.6 Effect of using phononic crystal structures with different number of layers

The next simulations were performed to observe the behaviour of multi-layered phononic crystal sensors when adding more layers on each side of the structure. Adding more layers allows PnC to have more effective bandgaps and, therefore, enables the use of materials with lower acoustic impedance mismatch.

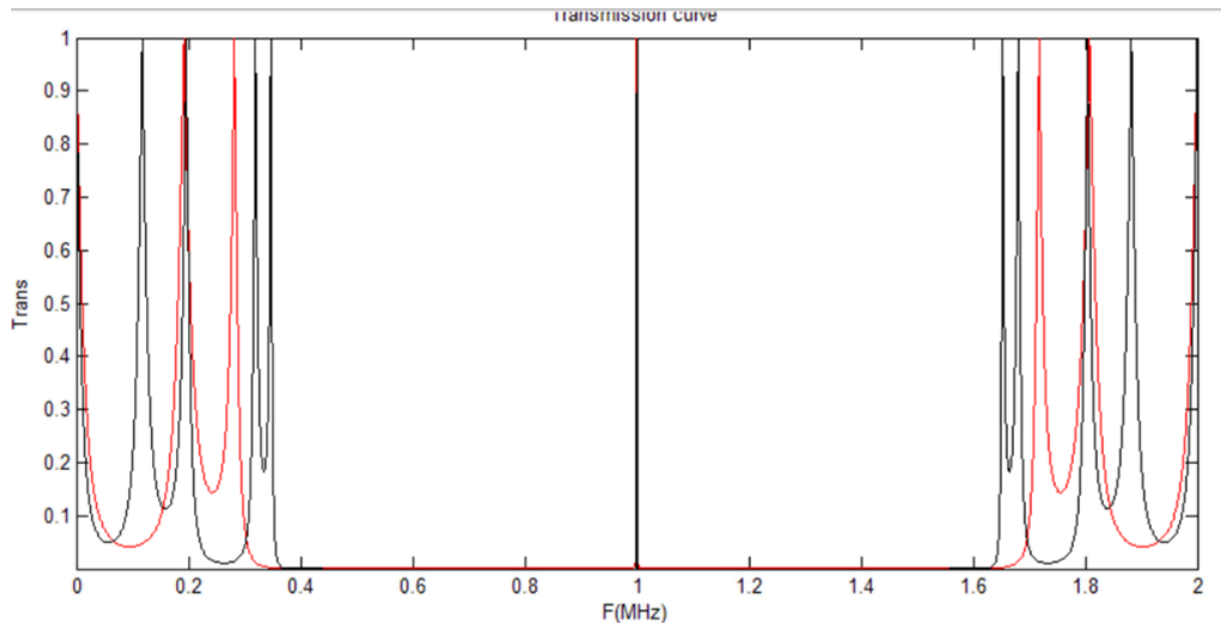


Figure 22 Comparison of the simulation results of two PnC sensors, one with 7 layers (black), and the other one with 11 layers (red). The simulation was performed using the transmission line model for simulating phononic crystals.

Figure 22 shows the simulation results of the structure presented in Table 2 and another with the same properties but with two additional layers of water and aluminium on each side with the same properties as the ones already composing the structure of the crystal. The addition of these 4 layers makes the bandgap borders to be sharper and to have a narrower bandwidth.

A comparison between the transmission peaks of both structures along with a modification of ± 10 m/s on the speed of sound of the analyte layer can be observed in Figure 23. Increasing the number of layers makes the transmission peaks a lot narrower, thus resulting in a much higher quality factor. The sensitivity, on the other hand, stays the same as in the first structure, 595Hz/ms^{-1} , a very important fact, because

it means that introducing layers to the structure doesn't affect the sensitivity, it only increases the quality factor of the analyte resonant modes.

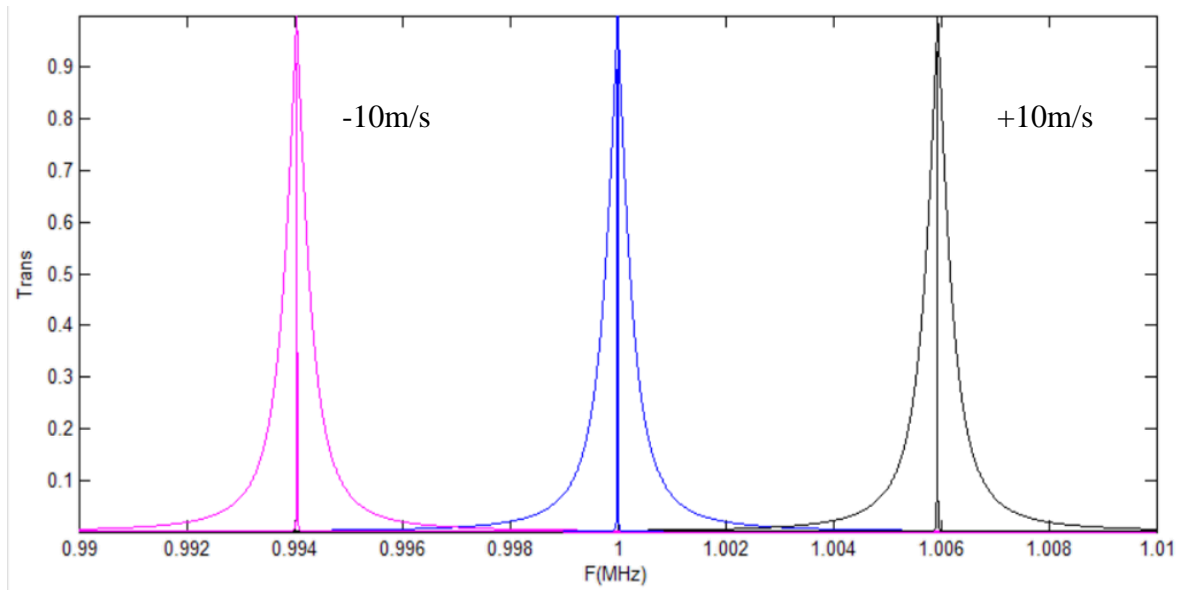


Figure 23 Comparison of the simulation results of two Phononic crystal sensors, one with 7 layers (black), and the other one with 11 layers (red). The high quality transmission peaks result from using 4 additional layers on the PnC structure. The simulation was performed using the transmission line model for simulating phononic crystals.

5.2.7 Evaluation of the effect of moving the analyte layer from the centre of the structure disrupting the symmetry on the lateral layers.

Another important aspect of the design of phononic crystal sensors is selecting where to locate the analyte layer in the multi-layered structure. The analyte layer is commonly placed in the centre of the structure, maintaining the symmetry on both sides. Figure 24 shows the simulation results of a structure similar to the one presented in Table 2 but with two additional layers on one side of the crystal, specifically on the side of the emitter.

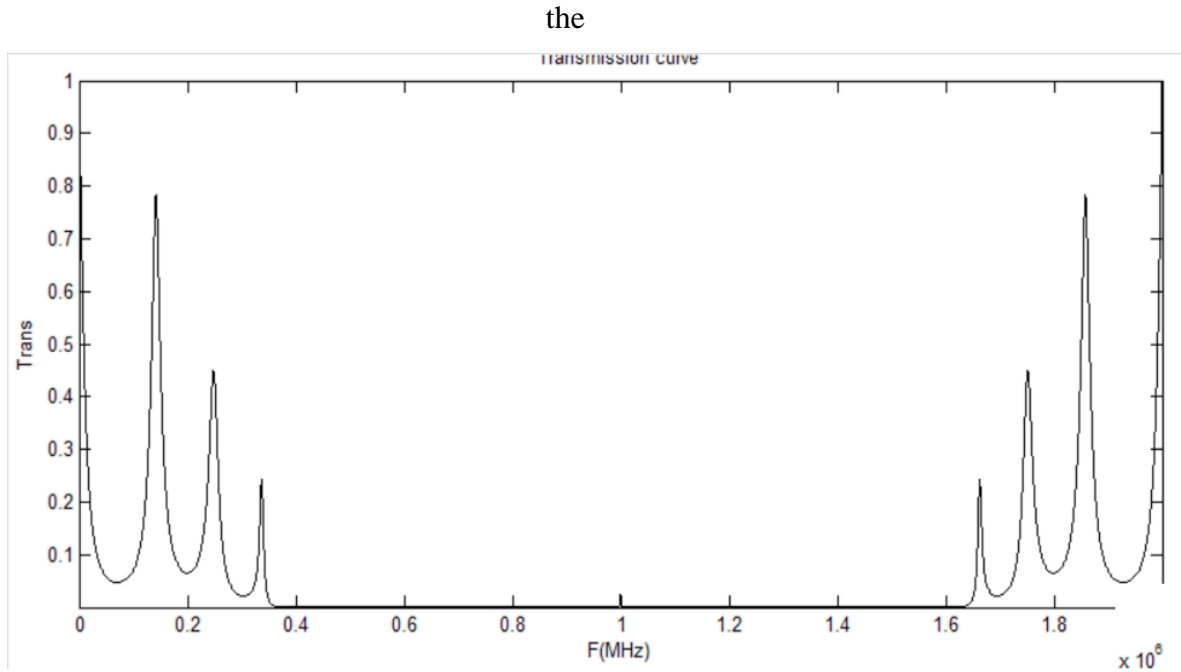


Figure 24 Simulation results of a phononic crystal structure with a symmetry reduction composed of a change on the dimensions of a liquid layer located on one side of the structure. The simulation was performed using the transmission line model for simulating phononic crystals.

Breaking the symmetry makes the analyte resonant mode to be attenuated almost completely. A second simulation was performed, only this time with the additional layers on the other side of the structure, but the effect was exactly the same. The attenuation of the analyte resonant mode makes asymmetric structures not very suitable for designing PnC liquid sensors. No further simulations were made investigating asymmetric structures given the poor results obtained in the last tests.

5.2.8 Evaluation of the effect of varying the speed of sound and density of the materials of the PnC sensor.

The objective of this new set of simulations is to analyse the effect of varying the speed of sound and density on the bandwidth of the bandgap and on the sensitivity of the analyte resonance mode.

Figure 25 shows the behaviour of the sensitivity and bandwidth when the speed of sound in the analyte layer of the crystal was varied in a structure like the one presented in Table 2, going from 1000m/s to 10000m/s of the original value.

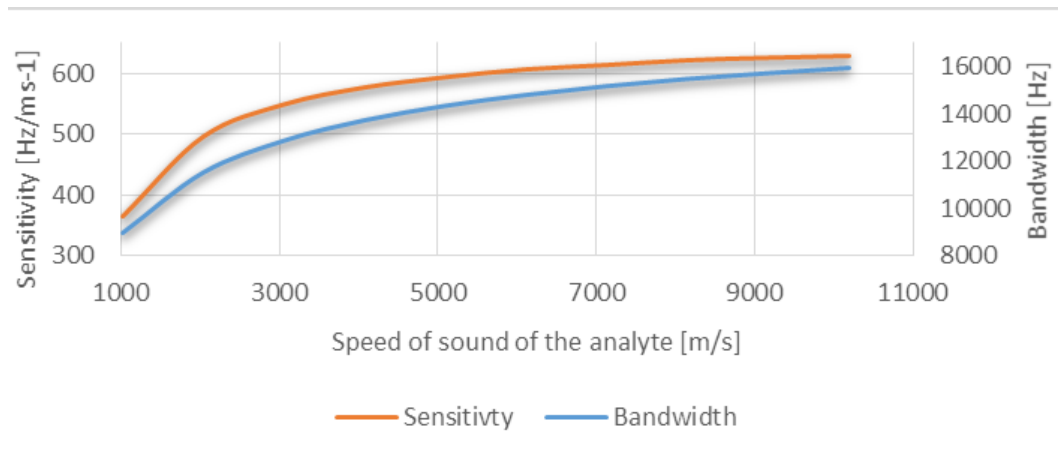


Figure 25 Effect of varying the speed of sound of the analyte layer on a phononic crystal structure composed of seven layers with an analyte layer located in the middle.

It is clear how both the sensitivity and bandwidth increased on each iteration showing that the use of higher values of the speed of sound produces better results for phononic crystal sensors. It is important to notice that the layer thickness needed to be modified along with the speed of sound in order to comply with the equations used to design the PnC sensors (1) and (3).

The same study was performed but this time, the density was varied instead of the speed of sound. It is interesting how the exact same results were found in this last test. These results were to be expected because the 1D transmission line model is based on using the acoustic impedance of each layer to obtain the transmission and reflection coefficients, which make both parameters, speed of sound and density, equally influential in the response of the system.

In general, the selection of materials to design new PnC sensors should take into account the speed of sound to calculate the dimensions of the layers and the acoustic impedance of the material to calculate the bandwidth of the bandgap.

5.3 Theoretical study using the FEM software Comsol Multiphysics to evaluate the behaviour of multi-layered phononic crystal sensors in 2D.

The transmission line model is a very useful model to simulate multi-layered structures in 1D and observe their behaviour in frequency. One of its advantages is that it reduces

the amount of computational power and time using a lateral miniaturisation of the model. This reduction of the dimensionality does not always deliver accurate results and sometimes it is necessary to use other methods like the FEM to support some of the important results obtained under more realistic conditions, especially if attenuation needs to be taken into account.

The finite element method (FEM) is a numerical approach to solve partial differential equations and integral equations both in the time domain and in the spectral domain. FEM is a powerful method for solving complex phononic crystal structure designs and is able to deliver accurate displacement fields calculations although it has some limitations in computation power and time.

Some authors have been using the finite element software Comsol TM Multiphysics which is a commercial software widely used to compute band structures of phononic crystals. The calculation of the displacement fields in phononic crystals using the solid mechanics interface, which is based on solving Navier's equations, and the pressure acoustics interface, which is based on solving the Helmholtz equation in the frequency domain, is of special interest to analyse the behaviour in frequency of the structures.

The properties of the materials and layers used for the simulations in 2D with Comsol were the same used with the TLM. Reflecting boundary conditions were selected on the borders of the layers to simulate finite structures.

5.3.1 Investigation of phononic crystal structures composed of 5 and 9 layers

The first test using Comsol was made to evaluate the behaviour of the analyte resonance mode of a 5 layered structure and a 9 layered structure. In the previous tests using the 1D TLM it was clear how the transmission peak around 1 MHz enhanced its quality factor when the number of layers was increased, but it was not possible to observe the effect of the attenuation generated by the influence of the bandgap. Figure 26 shows the 2D simulation results of a structure composed of 5 consecutive layers (green) and one composed of 9. (blue).

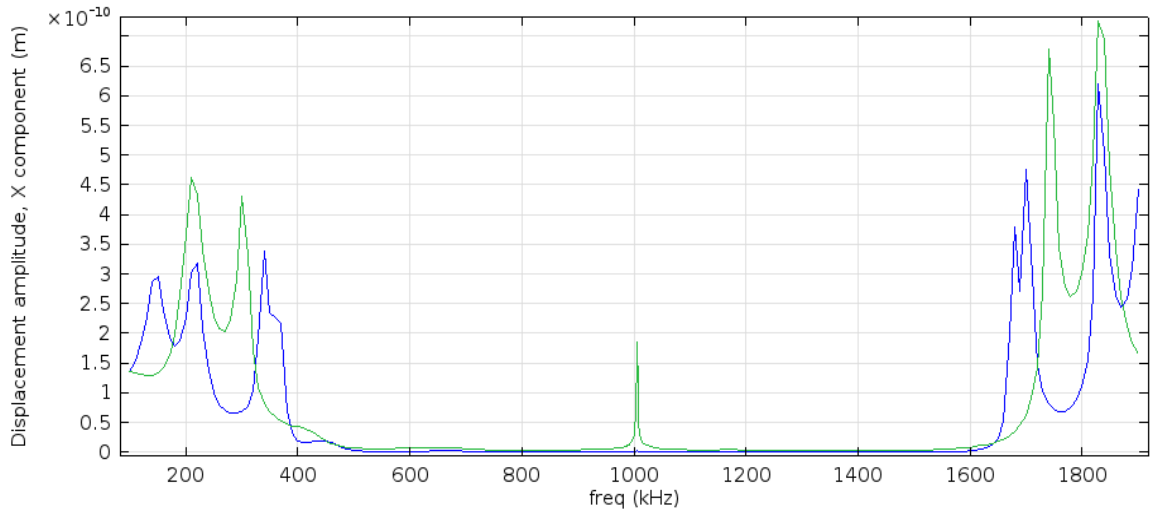


Figure 26 2D simulation results using the FEM software Comsol Multiphysics of a Phononic crystal sensor with an analyte layer on the middle structure composed of 5 consecutive layers (green) and 9. (blue).

As some researchers had previously indicated, the transmission peaks are attenuated, even completely in the case of structure composed of 9 consecutive layers, making it very difficult to use this structure as a phononic crystal liquid sensor. The bandgap and analyte resonance mode are in the same frequencies as in the results with the TLM, indicating that the one-dimensional model can be used for saving time and computational resources.

5.3.2 Phononic crystal multi-layered sensor using analyte resonance mode overtones

We previously proposed the use of overtones to generate maximum transmission peaks closer to the borders of the bandgaps, since the closer they are, the lower the influence of the bandgap allowing them to have adequate amplitudes in experimental studies. Figure 27 shows the simulation results of a PnC structure of 5 layers (green) and a structure of 9 layers (blue) with the same properties presented in Table 2 but with the analyte layer thickness multiplied by a factor of two. The results show three transmission peaks inside the bandgap confirming the findings with the 1D TLM.

The nine layers structure presents critically attenuated transmission peaks which are not very useful in sensing applications.

The transmission peaks located in frequencies nearer the borders of the bandgap have higher amplitudes and are easily recognisable in the frequency spectrum due to the filtering effect of the bandgap.

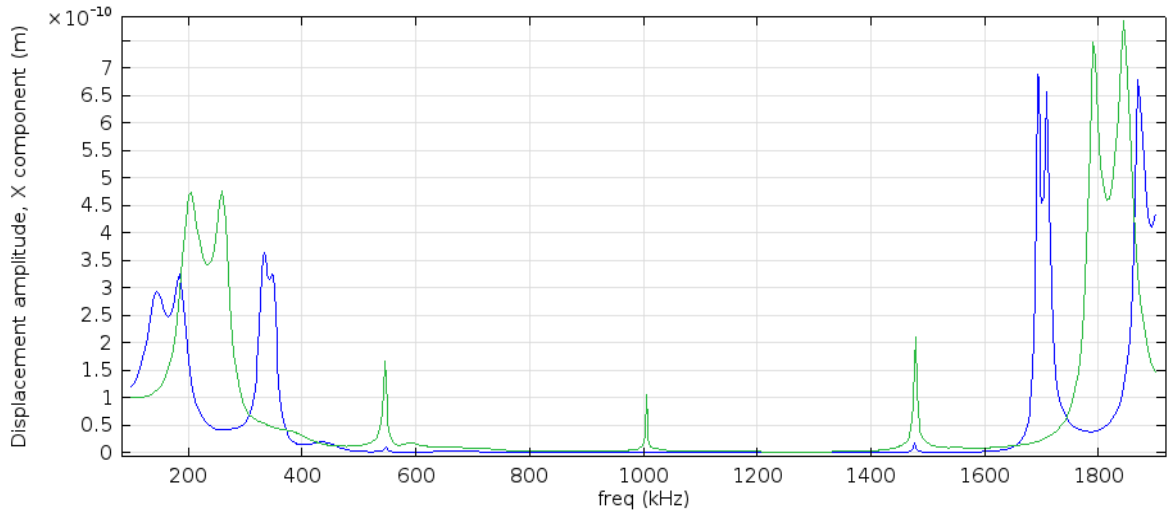


Figure 27 2D simulation results using the FEM software Comsol Multiphysics of a Phononic crystal sensor with an analyte layer on the middle structure composed of 5 consecutive layers (green) and 9. (blue). This time the analyte layer thickness was increased by a factor of 2.

An additional simulation with structures having the analyte layer thickness multiplied by a factor of three was performed. The results from this new simulation can be observed in Figure 28. The results show a bandgap with five transmission peaks inside. The peaks located nearer the bandgap have a very high amplitude, close to the amplitude of the bandgap borders itself. One notorious difference with the previous simulations is that this time the phononic crystal structure composed of nine consecutive layers has two visible transmission peaks, and the one located near 1.65 MHz has a very good amplitude and quality factor.

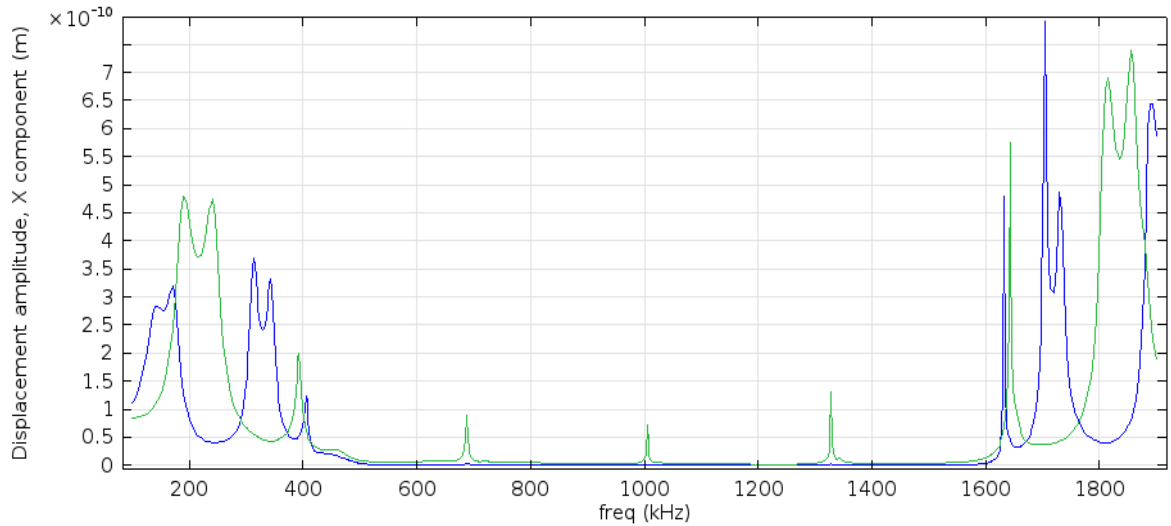


Figure 28 2D simulation results using the FEM software Comsol Multiphysics of a Phononic crystal sensor with an analyte layer on the middle structure composed of 5 consecutive layers (green) and 9. (blue). This time the analyte layer thickness was increased by a factor of 3.

5.3.3 Phononic crystal multi-layered sensor using the overtones of all layers

The use of overtones increasing the dimensions in all layers facilitates the manufacture of new structures and maintains the original sensitivity of multi-layered PnC sensors. Another important advantage of overtones is that the analyte resonance modes have an increased quality factor if located near the bandgap.

In Figure 29 the 2D simulation of a structure composed of 5 (green) and 9 (blue) layers with increased dimensions in all layers by a factor of 3 is shown. The results obtained are not very promising, the analyte resonance mode is critically attenuated in both structures and it makes it almost impossible to use these structures for sensing purposes.

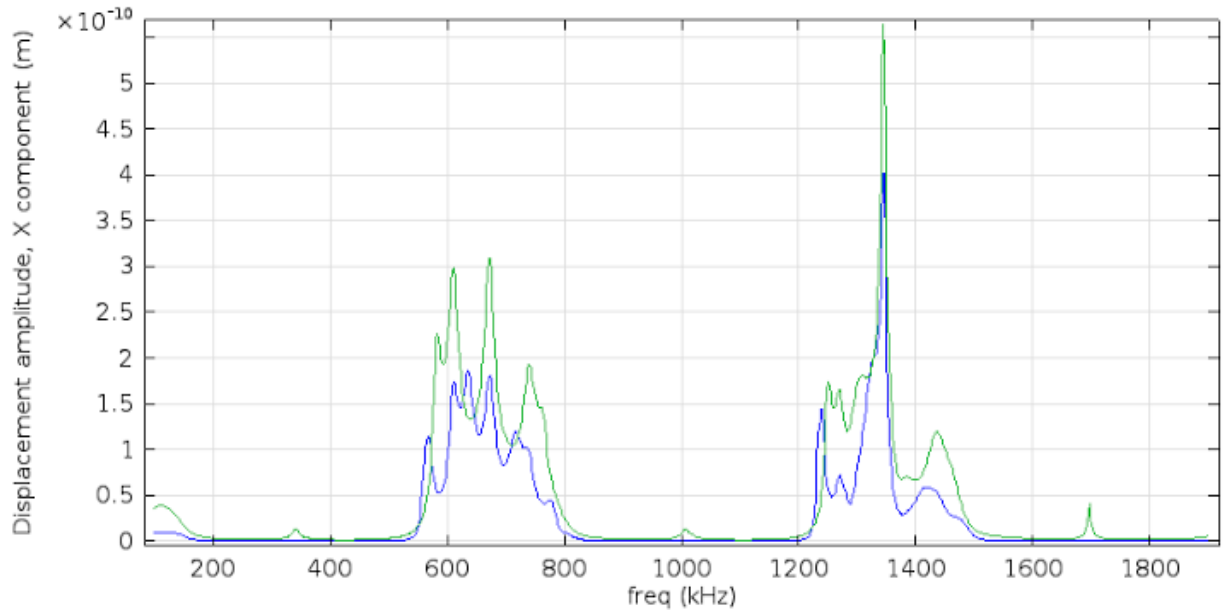


Figure 29 2D simulation results using the FEM software Comsol Multiphysics of a Phononic crystal sensor with an analyte layer on the middle structure composed of 5 consecutive layers (green) and 9. (blue). This time, the dimensions of all the PnC were increased by a factor of 3.

5.3.4 PnC sensor using analyte resonance mode and water overtones

In order to lower the effect of the bandgap and get less attenuated analyte resonance modes, a new phononic crystal structure was designed using the overtones of the liquid layers by multiplying their layer thickness by a factor of three and leaving the solid layers untouched. The results of this new approach can be observed in Figure 30.

The results obtained show a significant improvement in the amplitude of the analyte resonance modes in the 5 layers structure (green), especially in the 1.65 MHz transmission peak. This confirms that the approach using overtones is a good strategy to design PnC liquid sensors.

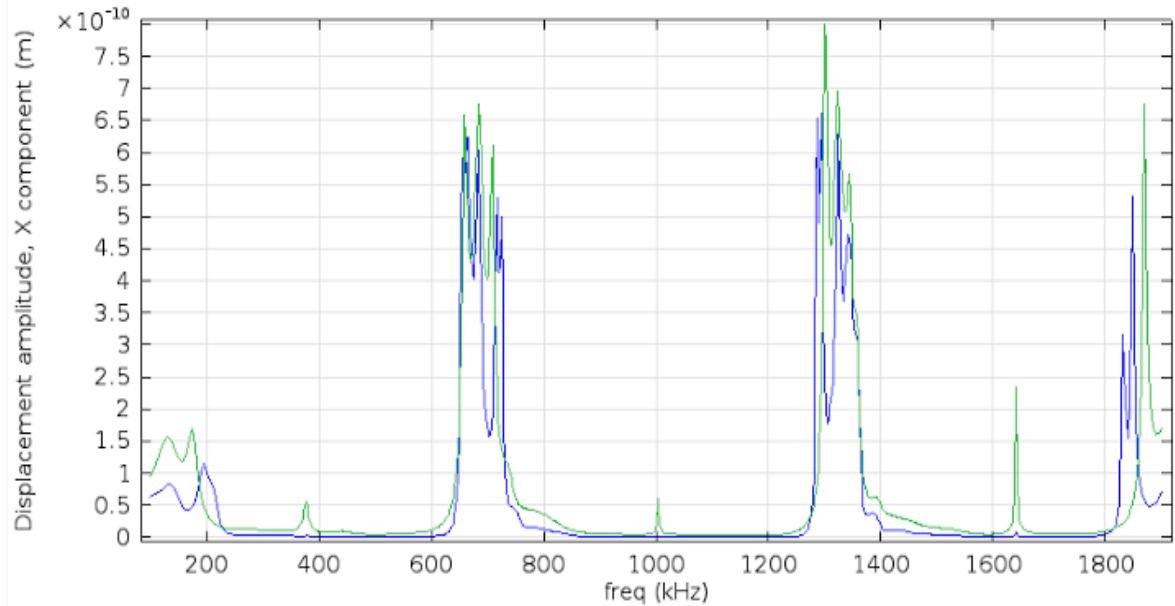


Figure 30 2D simulation results using the FEM software Comsol Multiphysics of a Phononic crystal sensor with an analyte layer on the middle structure composed of 5 consecutive layers (green) and 9. (blue). This time, the dimensions of all the liquid layers of the PnC were increased by a factor of 3.

5.4 Conclusions on the theoretical study

The theoretical studies performed on this chapter on multi-layered phononic crystal sensors presented very promising results. The use of a defect mode generated by disrupting the symmetry on the central layer and filling it with the analyte showed to be a good approach to design liquid sensors.

Similar results were obtained with the one-dimensional transmission line model and the finite element method software Comsol Multiphysics, indicating that the TLM can be used to perform the design and evaluation of phononic crystal structures composed of consecutive thin layers. This model enables researchers to save time and computational resources when developing novel phononic crystal based technologies.

The sensitivity of the phononic crystals investigated on this report showed to stay constant if the dimensions of all the layers of the structure were increased to be able to use overtones on the same frequency regions but with larger structures. However, if only the analyte layers are increased, the sensitivity of the system improved.

Another way of improving the sensitivity of the phononic crystal sensors is to increase the probing frequency, which can be done by decreasing the dimensions of the structure. This paves the way to the development of sensors with a very low analyte consumption.

The sensitivity of a resonant sensor is only as good as the quality factor of the relevant transmission peak being analysed. The bandwidth of the transmission peak generated by the analyte layer can be lowered by introducing new layers to the phononic crystal or by increasing the impedance ratio between the different layers of the structure. However, especial care must be taken since it can also affect its amplitude due to losses in the materials as was observed in the 2D simulations using Comsol Multiphysics.

The use of overtones is a good approach to develop phononic crystal sensors since the sensitivity can be kept constant and the relevant transmission peaks have enough amplitude to be tracked with the sensing instrument. Another benefit of using overtones is that higher frequencies can be used as probing frequencies with macroscopic structures that can be fabricated using conventional manufacturing techniques.

5.5 Summary

This chapter presented theoretical study to better understand the transmission of waves through phononic crystals used as sensors. Multiple designs containing overtones, symmetry disruption, changes in the material properties and number of layers were simulated and discussed. The results obtained during this study are very important to design the phononic crystal sensors that are going to be studied experimentally in this work.

The next chapter will focus on developing a phononic crystal sensor and studying it experimentally.

Chapter 6 - Acoustic spectrometer: resonant sensing platform for measuring volumetric properties of liquid samples

A sensing platform for measuring volumetric properties of liquid samples using phononic crystals is presented in this chapter. The proposed sensor concept is based on the transmission of elastic and acoustic waves through solids and liquids respectively to gather relevant information about the properties of the liquid under test.

The sensing platform demonstrates the simplest form of a phononic crystal sensor consisting of a resonant cavity formed by two glass layers, 2 coupling layers and 2 ultrasonic transducers.

The aim of this first experimental realization is to understand the behaviour of a phononic crystal sensor and to evaluate the effect of introducing a disposable element into the sensor structure in order to be able to comply with the requirements of point of care sensing applications.

A major difference between this concept and the majority of current resonant sensors, like the well-known quartz crystal microbalance, is that the proposed acoustic spectrometer measures bulk properties and not interfacial properties of the liquid.

An electronic characterization system based on the acquisition of three mixed signals to obtain the frequency response of the designed sensor is also presented.

6.1 Introduction:

During recent years, there has been a growing interest in sensing platforms based on resonant systems. The perhaps most known is the Quartz Crystal Microbalance (QCM), with a broad application range reaching from film thickness monitor to advanced biosensors which work in liquid environments [91, 124].

Phononic crystals, PnCs, are a new platform that has been proposed to be used in several applications due to their characteristic capacity of generating frequency bands in which elastic waves cannot propagate, giving scientists a way of designing a selective transmission spectrum [5, 8, 141].

QCM is a resonant sensor with extraordinary (mass) sensitivity. In order to acquire high biochemical sensitivity, it is necessary to merge the QCM with a biological compound deposited onto the QCM surface that enhances a selective response of the system to the analyte of interest. QCM therefore only measures changes at the interface between the sensor and the analyte, making it impossible to acquire bulk properties of the liquid under test. Unlike the QCM, PnC sensors merge the properties of resonant sensors and ultrasonic sensors by measuring frequency changes of relevant transmission features of ultrasonic waves transmitted through the PnC. The liquid under investigation is confined in a cavity having a well-defined resonance which depends on volumetric properties of a liquid analyte. Similar to QCM, the PnC sensor determines frequency changes of the cavity resonance which appear as a shift in the maximum of transmission and a phase change. PnC sensors are still in a preliminary stage of development, however, a series of structures have been proposed that could be implemented in real sensor applications [6, 109, 106, 92]. Besides fundamental requirements, real applications may also introduce additional constraints, specifically in biosensing [142 - 144].

Commercial electronic characterization systems that are commonly used to measure the characteristic frequency features of resonant structures are vector network analysers and high-frequency lock-in amplifiers. These conventional systems are very robust and expensive, making it very challenging to conduct tests in the field, thus, forcing the users to send the samples to specialized laboratories and, therefore, limiting the applicability of these sensing systems in various areas. However, a novel characterization system for measuring frequency changes of resonant structures like PnC has been recently introduced. This system is based on a double sideband modulation with suppressed carrier and a special demodulation process that involves a series of operations to obtain a signal that depends both on changes in the amplitude and phase induced by the resonant system under test. It enables, therefore, the use of phononic crystals in the field due to its portability [144]. The block diagram of the

electronic system can be observed in Figure 31. This system does not however deliver an actual value for the gain and phase of the system. Therefore, some modifications were done using a multiplexer in order to extract the necessary information to characterize the response of the sensor system.

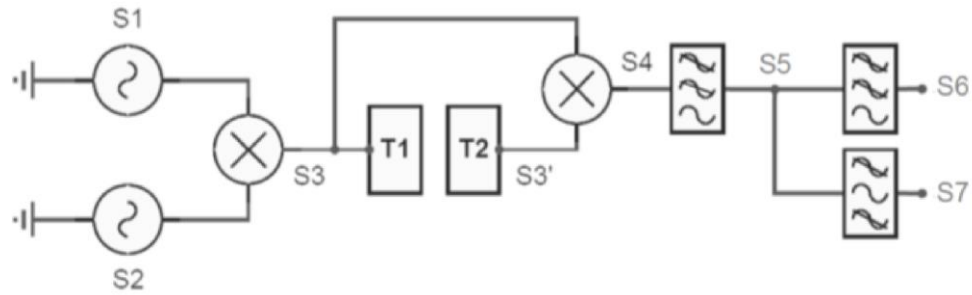


Figure 31 Block diagram of the electronic characterization with a double sideband modulation. Source: [144].

6.2 Materials and Methods

Biomedical applications often require the use of biological or hazardous samples and, therefore, it is important to consider that all the elements of the system that are in contact with the analyte must be disinfected or discarded after the test is completed.

The designed acoustic spectrometer has three main components: An electronic characterization system, a pair of piezoelectric ultrasonic transducers and a disposable analyte container made of glass that can be discarded or sterilized after each test.

Figure 32 shows a graphic representation of the container and the analyte, which can be understood as the very simplest form of a 1D PnC sensor.

The ultrasonic transducers located on each side of the analyte container generate ultrasonic waves that travel from one transducer to the other generating a cavity resonance inside the container.

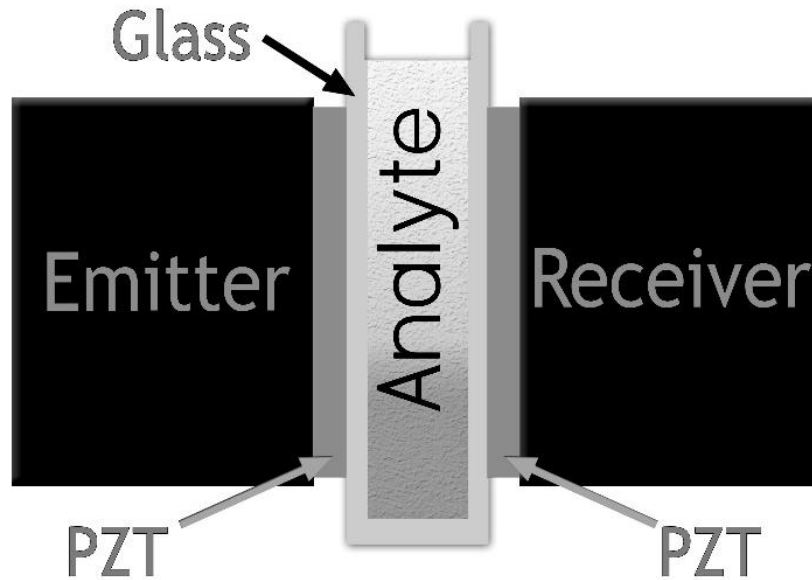


Figure 32 Graphic representation of the acoustic spectrometer structure.

The electronic characterization system presented on this chapter is based on obtaining three main signals, these signals are acquired by using the excitation signal that is fed to the transducer configured as the transmitter, S_0 , and the signal acquired by the transducer configured as the receiver, S_1 , same as in the system presented in Figure 31, but without the double sideband modulation.

The three signals that the system obtains are: the square of the RMS value of S_0 , the square of the RMS value of S_1 , and the DC component of the signal obtained by multiplying S_0 by S_1 . The signals are then passed through a series of mathematical operations to acquire the gain and phase of the system, thus generating a frequency spectrum with valuable information on the volumetric properties of the substance being analysed. The block diagram of the proposed system is shown in Figure 33.

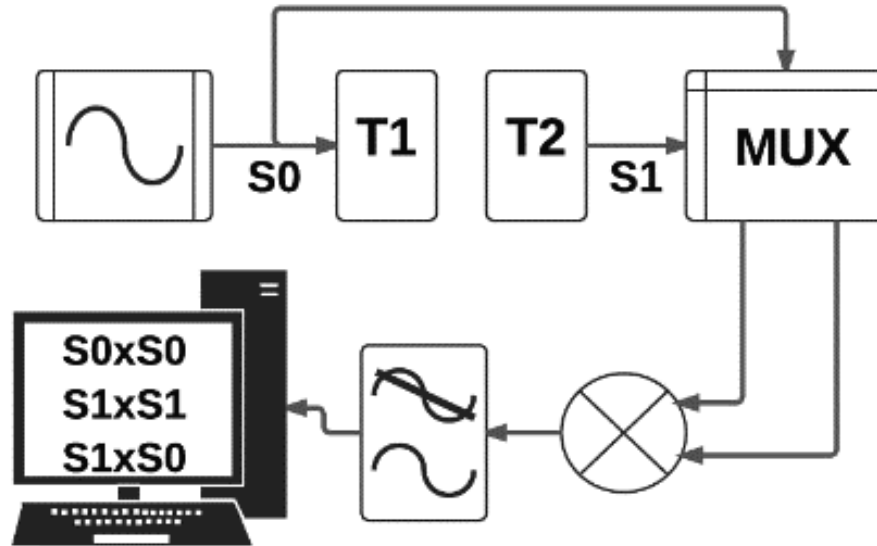


Figure 33 Block diagram of the electronic characterization system designed.

As seen in the block diagram, Figure 33, an analogue multiplexer feeds a four-quadrant multiplier with the two signals, S_0 and S_1 , to perform three multiplications and to obtain 3 mixed signals, S_2 , S_3 and S_4 . The signal acquired by the receiver, S_1 , experiences modifications when traveling through the resonant structure and the ultrasonic transducers. These variations are presented as changes in gain, G , and changes in phase φ_2 .

$$S_0(t) = A \sin(2\pi ft + \varphi) ; S_1(t) = AG \sin(2\pi ft + \varphi + \varphi_2) \quad (1)$$

$$S_2(t) = A^2 \sin^2(2\pi ft + \varphi) \quad (2)$$

$$S_3(t) = A^2 G^2 \sin^2(2\pi ft + \varphi + \varphi_2) \quad (3)$$

$$S_4(t) = (A^2 G^2 / 2) [\cos(\varphi_2 - \varphi) - \cos(4\pi ft + \varphi_2 + \varphi)] \quad (4)$$

The three mixed signals obtained by performing the multiplication between S_0 and S_1 are then passed through a low-pass frequency filter to obtain the DC component of each signal. The resulting signals are then passed through a digital to analogue converter to be processed by a microcontroller.

$$S'_2(t) = A^2 / 2 \quad (5)$$

$$S'_3(t) = A^2G^2/2 \quad (6)$$

$$S'_4(t) = (A^2G/2)\cos(\varphi_2 - \varphi) \quad (7)$$

The three signals obtained contain relevant information to extract the value of the gain, G , and phase, φ , of the system. The gain is obtained by calculating the square root of the resulting value of dividing S'_3 by S'_2 , while the phase is obtained by calculating the inverse cosine of the resulting value of dividing S'_4 by G and S'_2 .

$$G(t) = \sqrt{(A^2G^2/2)/(A^2/2)} \quad (8)$$

$$\varphi(t) = \cos^{-1} \left(\frac{A^2G}{2} \cos(\varphi_2 - \varphi) / G \frac{A^2}{2} \right) \quad (9)$$

For the experimental realisations, wide bandwidth piezoelectric ultrasonic transducers with a central frequency of 1.5MHz and a half-peak band width of 1 MHz were used.

The electronic system was set to acquire a total of 400 points starting at 0.85MHz, with frequency steps of 3 kHz and ending at 2.05MHz. The disposable analyte container used was a 700uL glass cuvette and only 500uL of analyte were used per test. The cuvette was carefully rinsed and dried using acetone before introducing a new sample and the temperature was kept constant via room temperature control.

The ultrasonic transducers were coupled to the analyte container using glycerol and a holding structure specially designed to ensure an adequate surface contact and constant pressure. The experimental arrangement of the acoustic spectrometer can be observed in Figure 34.

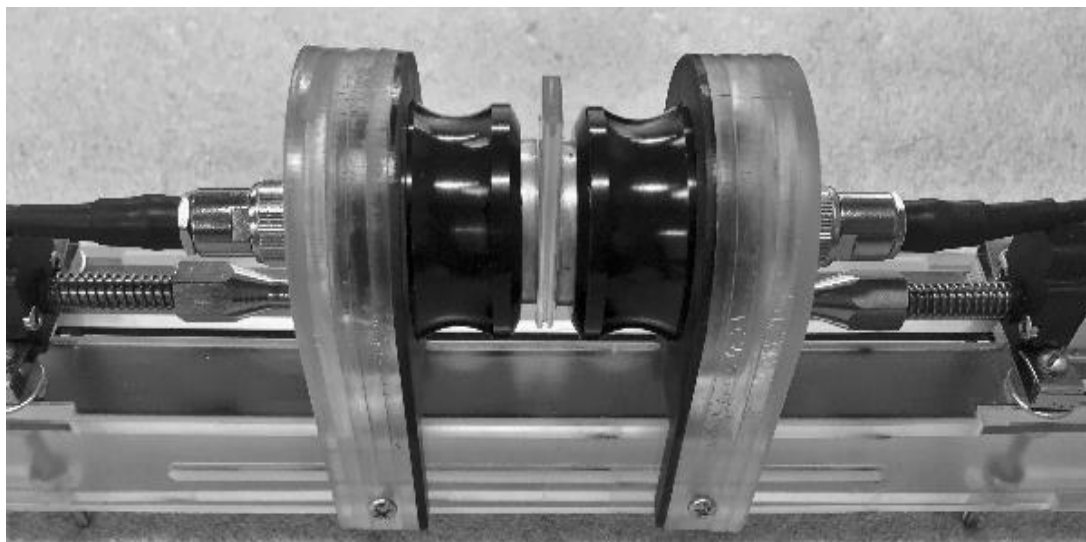


Figure 34 Acoustic spectrometer experimental arrangement.

To evaluate the performance of the acoustic spectrometer, tests using different alcohol analytes were conducted. The properties of the analytes used can be found in Table 1. There are many methods to simulate phononic crystal structures, some of them are the Layer Multiple Scattering Theory (LMST), the Finite difference Time Domain (FDTD), the Finite Element Analysis (FEA) and the 1D Transmission Line Model (TLM). Simulations using the 1D Transmission Line Model to corroborate the experimental results were performed. This method was selected because it is widely used to simulate the performance of multi-layered structures giving accurate results and it uses a reduction of the model to 1D that enhances the calculation speed and lowers the computation power required, that are commonly high when other methodologies are used. The TLM uses a chain matrix technique and an analogy between the electrical impedance and the acoustic impedance to perform the calculation of the transmission and reflection coefficients. The geometric and material properties of each layer were used to calculate the elements of the propagation matrix [126, 127, 142 - 144].

Table 3 Analytes used for the preliminary tests

Analyte	Density kg/m ³	Speed of sound m/s
Distilled	998	1493
Water		

n-Propanol	786	1170
Methanol	792	1100

Source: Adapted from [145]

6.3 Results and Discussion

The results obtained from the experimental realisations conducted are shown in Figure 35. No further digital signal processing was made to enhance the quality of the signals given the signal to noise ratio exhibited by the electronic system.

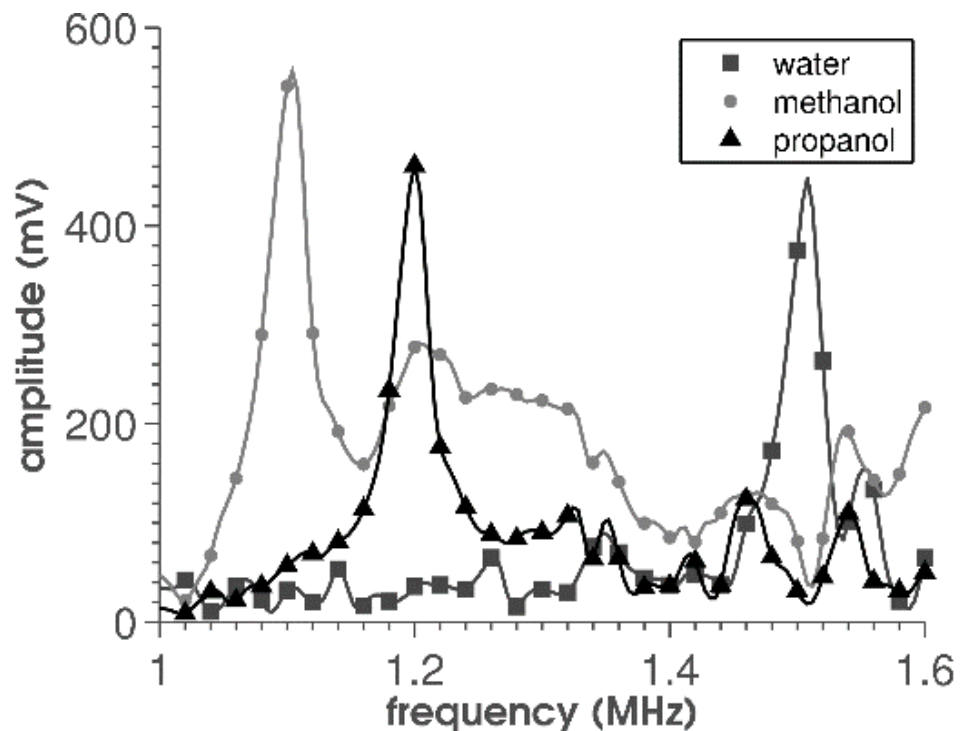


Figure 35 Experimental results using different alcohols as analytes.

Each test showed a well differentiated maximum of transmission generated by the resonance in the cavity. This characteristic transmission feature has a good quality factor and was located at different frequencies on each experimental realisation. The results from the simulations using the 1D transmission line model are shown in Figure 36.

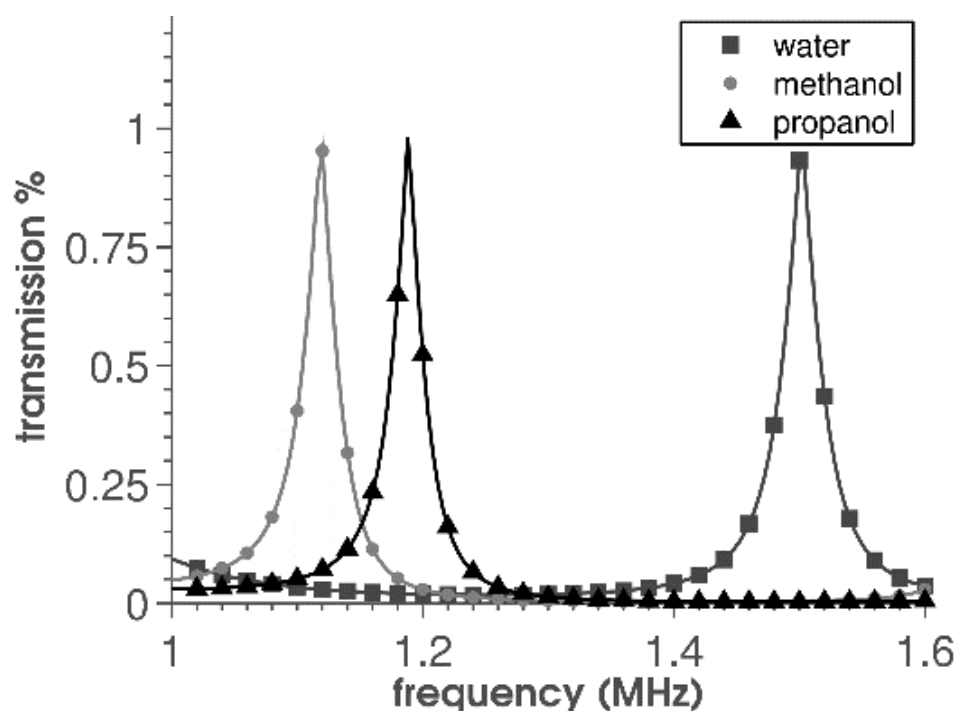


Figure 36 Theoretical results using different alcohols as analytes.

The transmission curves obtained in both theoretical and experimental realisations show significant changes in the frequency and magnitude of the main resonant peaks.

Variations in the acoustic properties of the liquid mixtures showed to be responsible of the frequency changes on the characteristic transmission features. The maxima of transmission of the experimental realisations agree well with the ones obtained in the simulations.

The sensitivity obtained in these tests is good, variations of 1 m/s⁻¹ on the longitudinal component of the speed of sound of the analyte produce variations of 1098 Hz in the frequency of the characteristic transmission peaks. This result is very important given the fact that the signal to noise ratio of the system is high and enables accurate measurements of the frequency of the transmission features without noise interference.

6.4 Conclusions

An acoustic spectrometer with a disposable cavity that measures volumetric properties of liquid analytes was studied in this chapter. The acoustic spectrometer relies on the determination of the frequency of relevant transmission features, in this case, maxima

of transmission. The 1D transmission line model showed to be useful to corroborate and even predict the results obtained with the system.

The removable component of the sensing platform enables its use in applications where hazardous substances need to be analysed, like point of care testing and other biomedical applications.

The ultrasonic transducers need to be coupled to the disposable element by using a coupling agent, in this case glycerol, which can vary its acoustic properties due to evaporation of the alcohol content of the substance. These variations can cause displacements in frequency of the resonant modes, thus increasing the measurement error. Another issue with the coupling agent is that its layer thickness is very complicated to maintain stable.

The electronic characterization system designed is portable and economic and makes it possible to use the acoustic spectrometer in the field. The designed platform could differentiate two different alcohols and distilled water with sufficient sensitivity and resolution, however, in order to use the designed system in label free applications with extraordinary sensitivity and lower analyte availability, further optimization processes need to be done.

6.5 Summary

This chapter presented an experimental realization of a simple 1D phononic crystal sensor having a resonant cavity and a disposable element. An electronic characterisation system is also presented and discussed in this chapter.

The results obtained during this study are very interesting and serve as a proof of concept of phononic crystal sensors.

One of the limitations presented in chapter 3 can be solved by using a disposable element as demonstrated in this chapter.

The next chapter will focus on developing a phononic crystal sensor having a disposable element but this time replacing the coupling agent by two additional water layers in order to eliminate the error caused by the coupling agent.

Chapter 7 - Cavity Resonance Sensor with Disposable Analyte Container

This chapter presents the experimental demonstration of a phononic crystal sensor with a disposable element and replacing the coupling agent for additional water layers. The aim of this second experimental realizations is to prove the use of additional water layer as coupling layers.

The sensor consists of seven layers with high acoustic impedance mismatch. The disposable element used was a glass spectrophotometry cuvette and, during the experimentation, it was filled with different liquid analytes showing characteristic transmission features that can be used as measures to differentiate and identify them.

Experimental transmission curves were obtained using the same electronic characterization system used in the previous chapter.

Simulations using the 1D transmission line method were performed to support the experimental realisations. The frequency of maximum transmission has been found to be strongly dependent on the speed of sound of the analyte under test.

7.1 Materials and Methods

The structure studied in this section consists of 7 consecutive layers with high acoustic impedance mismatch. Material properties, such as thickness, density and speed of sound of each layer of the structure were carefully selected in order to obtain the desired frequency response and be able to quantify changes in the liquid under test.

The designed structure was investigated both theoretically and experimentally to observe its performance and usage as a liquid sensor.

7.1.1 Materials

When designing sensors for PoCT, it is important to take into account that all the components that are in contact with the analyte must be disposable. The designed

sensor uses a disposable analyte container, a glass spectrophotometry cuvette, which is inserted in the structure and is then discarded after the test. The analyte container is made of glass, which is FDA approved, and the acoustic waves travel through the glass cuvette, as shown in Figure 37 and generate a liquid cavity resonance that can be measured and characterized to be used for sensor purposes.

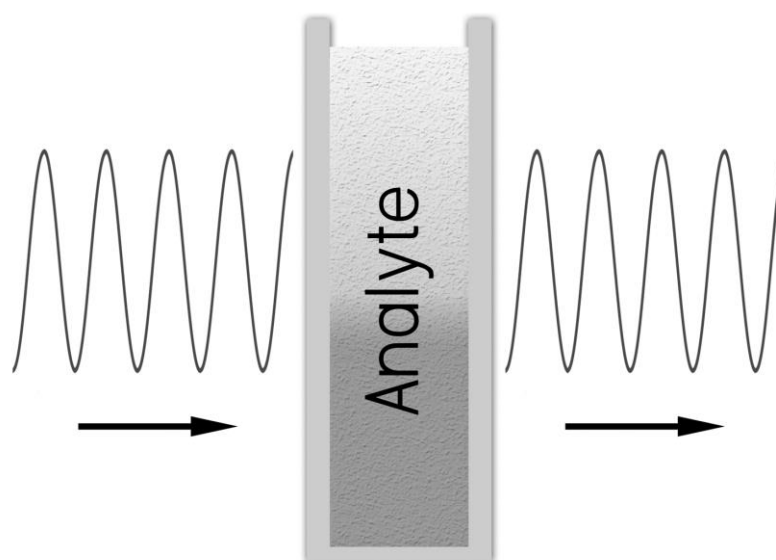


Figure 37 Representation of a glass cuvette filled with a liquid analyte and the acoustic wave path.

The analyte container is responsible for the generation of the cavity resonance and the main resonance peak is positioned at the desired frequency by adjusting its properties.

The impedance mismatch between the cavity walls and the liquid confined inside must be high in order to generate a resonance with a good half-peak band width. Available spectrophotometry cuvettes are made from high-density glass and, therefore, give a good impedance contrast compared with the acoustic impedance of distilled water.

Although glass may not have one of the highest acoustic impedances amongst common solids, its cost and easy manipulation make it a good choice to develop point of care sensors.

With a central frequency around 1.05 MHz and the materials of the cavity, high-density glass, the next step is to calculate the layer thickness of the liquid contained in the

cavity, d_T . In order to achieve maximum transmission through the layer, its thickness must be equal to a factor of the wavelength, λ , divided by 2 [139, 140].

$$d_T = \frac{n\lambda}{2} ; f = \frac{c}{\lambda} \therefore f = \frac{nc}{2d_T} \therefore d_T = \frac{n(1483m/s)}{2(1.05MHz)} = 0.706n \text{ mm} \quad (1)$$

The thickness of the walls of the cavity, d_a , is calculated to have a perfect coupling without losses. This can be achieved having a layer thickness equal to a factor of the wavelength, λ , divided by 4 [139, 140].

$$d_a = \frac{n\lambda}{4} ; f = \frac{c}{\lambda} \therefore f = \frac{nc}{4d_a} \therefore d_a = \frac{(4000m/s)}{4(1.05MHz)} = 0.952n \text{ mm} \quad (2)$$

The most impressive feature of PnC is the formation of bandgaps, the inclusion of this feature in sensing systems can increase the peak half band width of the relevant transmission peaks.

The dimensions of the layers of the bandgap are calculated the same way as the thickness of the cavity walls, using a layer thickness of a quarter of the wavelength. The more layers the better the bandgap but the lower the transmission amplitude due to losses in the structure.

The fabricated structure (a) and its graphic representation (b) are shown in Figure 38. The design was made using a factor of 14 in the thickness of the analyte layer to be able to use commercial spectrophotometry cuvettes, which have a 10mm wide analyte layer.

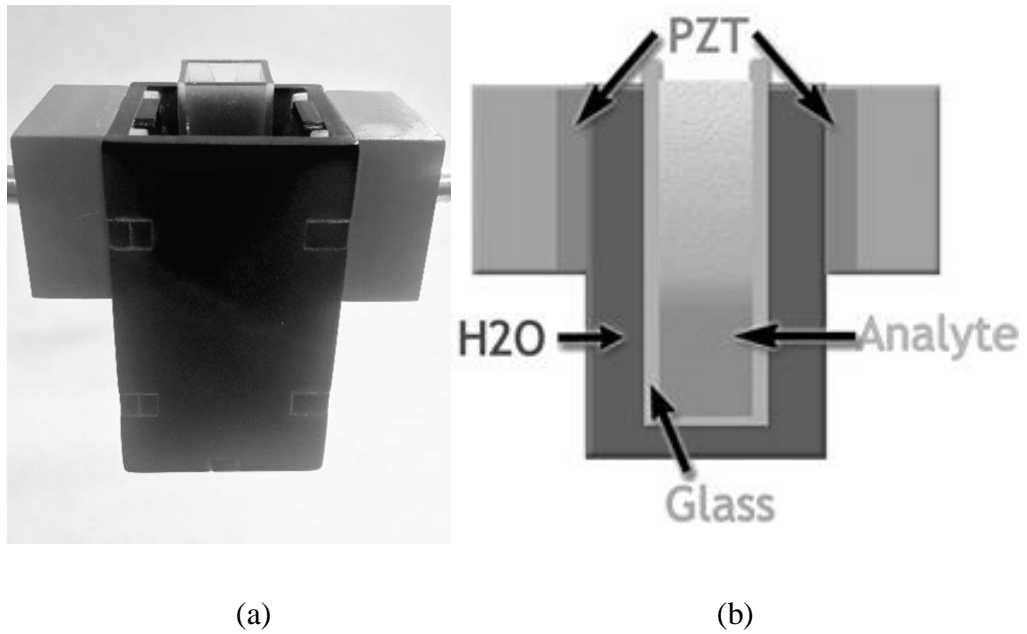


Figure 38 Fabricated Structure (a) with the glass cuvette in the middle and the ultrasonic transducers on each side and its respective graphic representation (b).

The information and details of the materials and layers composing the phononic crystal structure are summarized in Table 4.

Table 4 Designed structure properties

Acoustic Properties				
Layer #	Thickness mm	Material	ρ (Kg/m ³)	c (m/s)
1	1	PZT	3333	7500
2	10	Water	998	1493
3	1	Glass	3880	4000
4	10	Water	998	1493
5	1	Glass	3880	4000
6	10	Water	998	1493
7	1	PZT	3333	7500

7.1.2 Experimental Setup

Vector network analysers and high-frequency lock-in amplifiers are typically used as PnC acquisition systems and their high cost and size does not allow their use outside laboratories, making it impossible to use them in PoCT. Therefore, an electronic characterization system based on a high-frequency double sideband modulation with suppressed carrier was used to acquire the experimental data, Figure 39. By using a special demodulation, this system delivers accurate transmission curves and allows the use of phononic crystals in the field, thus decreasing the high costs associated with more robust devices. [144]

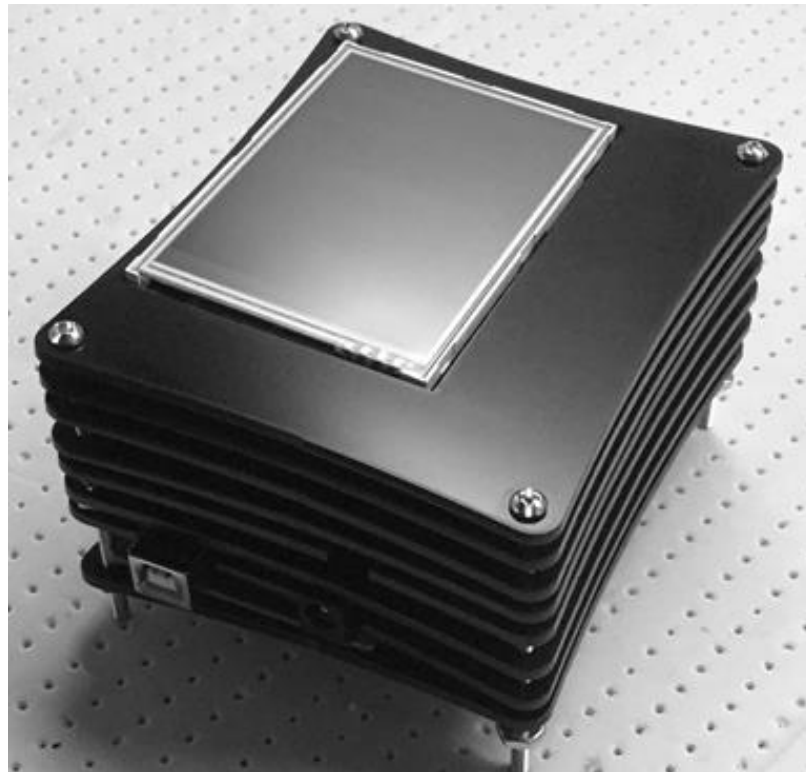


Figure 39 Electronic characterisation system for measuring frequency changes in phononic crystals.

The number of points acquired with the electronic system was 1000 starting with a frequency of 1.05MHz. The phononic crystal structure was characterized using two ultrasonic transducers having a central frequency of 1.1 MHz and a half-peak band width of 150 KHz. Temperature was kept constant via room temperature control.

Distilled water, ethanol, propanol and commercial milk products were used as analytes. Their acoustic properties are well known and they can give very relevant insights about the performance of the sensor and its potential use in PoCT. The acoustic properties of the materials used as analytes are listed in Table 5.

Table 5 Properties of the Analytes used

Analytes		
Material	ρ (Kg/m ³)	c (m/s)
5% n-Propanol solution	992	1520
5% Ethanol solution	996	1514
Distilled Water	998	1493

A total of 3 experimental tests were conducted. All data was acquired using the electronic characterization system previously described.

The analyte container was thoroughly rinsed with distilled water and then dried before introducing a new analyte.

The temperature was kept constant via room temperature control and all the tests were performed 3 times to corroborate the results.

A user interface was developed using the software Matlab® to acquire and process the data from the electronic system.

Characterization of the cavity: The cavity was characterized using the two PZT transducers separated by 10mm to form a liquid cavity with the same dimensions of the one formed with the glass spectrophotometry cuvette. Distilled water and an n-Propanol solution with a concentration of 5% by volumetric fraction were used in this test.

Characterization of the Sensor: The structure designed was characterized using an n-Propanol solution with a concentration of 5% by volumetric fraction and an Ethanol solution with a concentration of 5% by volumetric fraction.

Complex liquids test: the last consisted of using three commercial milk products with unknown properties to observe if the designed sensor could be used to characterize and identify complex liquids in the food industry. The milk products used were lactose-free milk, whole milk and flavoured milk.

7.1.3 Simulation Setup

Several methods have been developed to simulate the propagation of elastic waves through phononic crystal structures including: the eigenmodes matching theory (EMMT), the transmission line model (TLM), the plane wave expansion method (PWE), the layer multi-scattering theory (LMST), the finite difference time domain (FDTD) and the finite element method (FEM). The FEM is a numerical approach to solve partial differential equations and integral equations, both in the time domain and in the spectral domain. FEM is a powerful method for solving complex phononic crystal structure designs and is capable of delivering accurate displacement field calculations, but it has some limitations in computation power and time [17, 94, 125 - 127].

In order to reduce the amount of computation power and time needed to perform the simulations, a 1D approach based on the transmission line model, TLM, was used.

Simulations using the TLM theory were performed to corroborate experimental realisations. The software Matlab was used to run the calculations. The simulations were performed using the same material properties and analytes of the experimental tests and the frequency sweep was done taking the same number of points (1000) that were taken with the electronic characterization system.

All the imaginary parts of the acoustic impedance were set to zero, losses were not considered in the simulations. The transmission coefficient was calculated and used for comparing the theoretical results with the experimental results.

The values used for the simulations are listed in Table 6. The values used for the analyte layers are the same values presented in Table 5.

Table 6 Simulation Configuration Values

Characterization of the cavity				
<i>Layer #</i>	<i>Thickness mm</i>	<i>Material</i>	$\rho \text{ Kg/m}^3$	<i>c m/s</i>
1, 3	1	PZT	3333	7500
2	10	Analyte	-	-
Characterization of the Sensor				
1, 7	1	PZT	3333	7500
2, 6	10	Water	998	1493
3, 5	1	Glass	3880	4000
4	10	Analyte	-	-

7.2 Results and Discussion

The first test made was the characterization of the cavity filled with the analyte. Two different analytes were investigated. The acoustic properties of glass and PZT are very different but this test allows to understand the behaviour of a cavity with a high impedance mismatch between the liquid contained and the cavity walls. The two analytes used in this first test were distilled water and a solution of n-propanol in distilled water with a concentration of 5% by volume fraction. The results of this first test can be observed in Figure 40. The simulations were performed using the TLM.

The simulative and experimental transmission curves of the first test agree very well with respect to the frequencies of maximum transmission. The simulative results using the 1D model have some limitations and do not take into account the frequency response of the ultrasonic transducers, which could explain the differences between simulative and experimental results. The central peak looks very interesting from the sensor point of view because it has the best peak half band width and its frequency of maximum transmission varies with the changes in the acoustic properties of the analyte. Although this arrangement looks very promising, the peak half band width of the experimental results is still too large for sensing purposes.

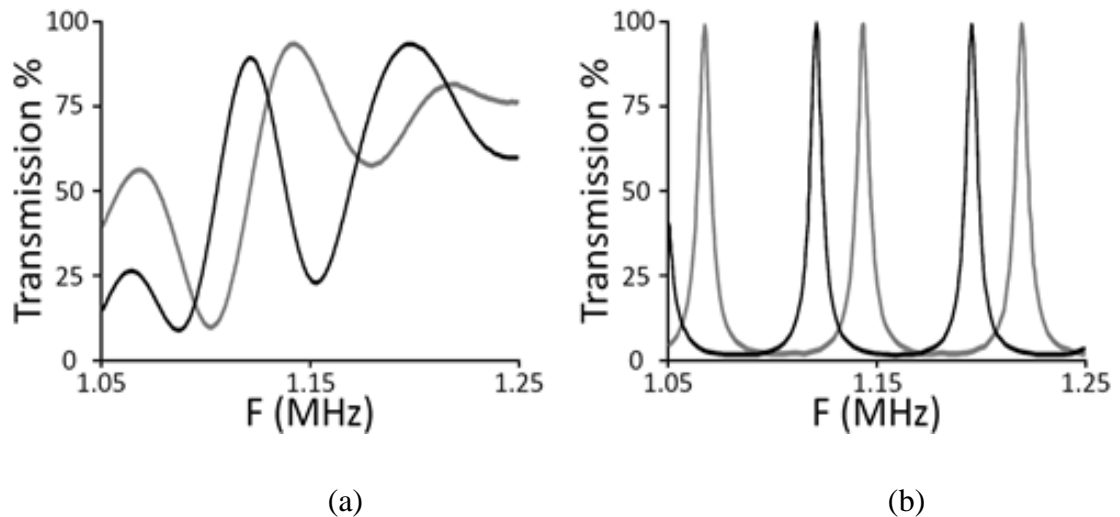


Figure 40 Experimental (a) and simulative (b) results of the test using distilled water and n-propanol. The cavity is filled with an n-propanol solution in distilled water with a concentration of 5% by volumetric fraction (grey) and with distilled water (black).

In order to test the full structure, an experiment using a solution of n-propanol in distilled water with a concentration of 5% by volume fraction and a solution of ethanol in distilled water with the same concentration was conducted.

The results of the simulation using the TLM, dotted lines, and the experimental results, solid lines, are presented in Figure 41.

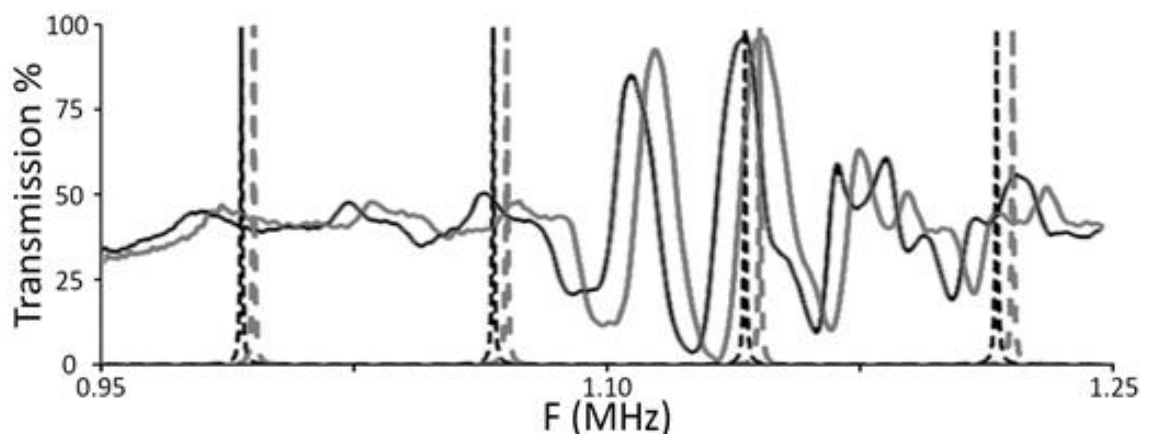


Figure 41 Experimental (solid lines) and simulative (dotted lines) results of the test using n-propanol and ethanol solutions. The glass cuvette is filled with an n-propanol solution in water with a concentration of 5% by volumetric fraction (grey) and with an

ethanol solution in water with a concentration of 5% by volumetric fraction (black). Dotted lines display 1D simulation and the solid lines the experimental results.

The position of the main experimental transmission peaks agrees with the 1D simulations, although not all the transmission peaks are covered by the simulations.

The final arrangement presents a more complex structure and the lateral miniaturization of the model is no longer valid to present accurate calculations which result in simulations with mayor discrepancies.

The displacement in frequency generated by the changes in the analyte can be easily measured by means of a maximum of transmission, it is clear how the transmission peaks of the n-propanol solution appear at higher frequencies than those of the ethanol solutions due to the difference in acoustic impedance of both solutions.

Figure 42 shows the comparison between the experimental transmission curves for water in the cavity (black) and the arrangement of 7 layers (grey). The peak half band width decreases considerably with the additional layers increasing the functionality of the system as a point of care sensor.

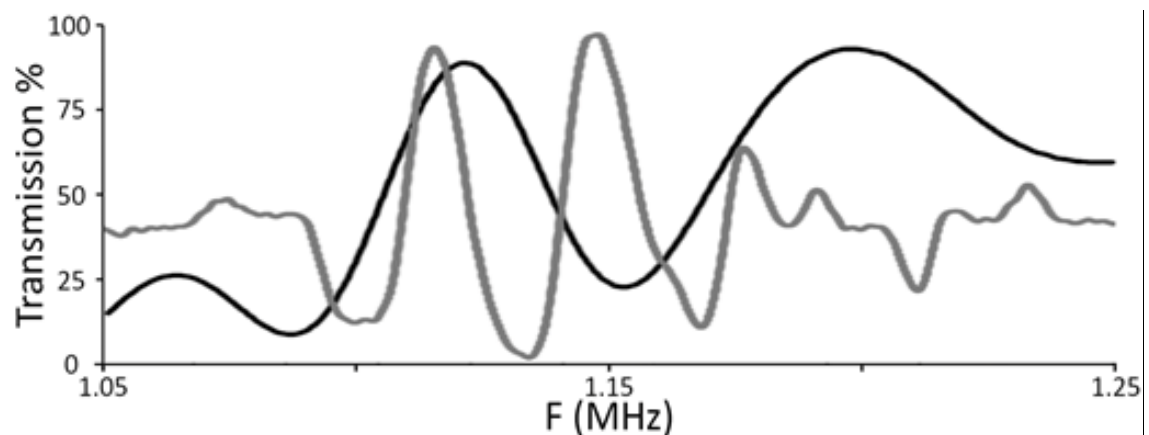


Figure 42 Comparison between the experimental transmission curves for water in the cavity (black) and the arrangement of 7 layers (grey).

The third test was conducted to analyse if the sensor could be used to characterize or differentiate complex liquids. For this purpose, three commercial milk products of the same brand were used. The first product was whole milk, the second lactose-free milk

and the third strawberry flavoured milk. The experimental results can be observed in Figure 43.

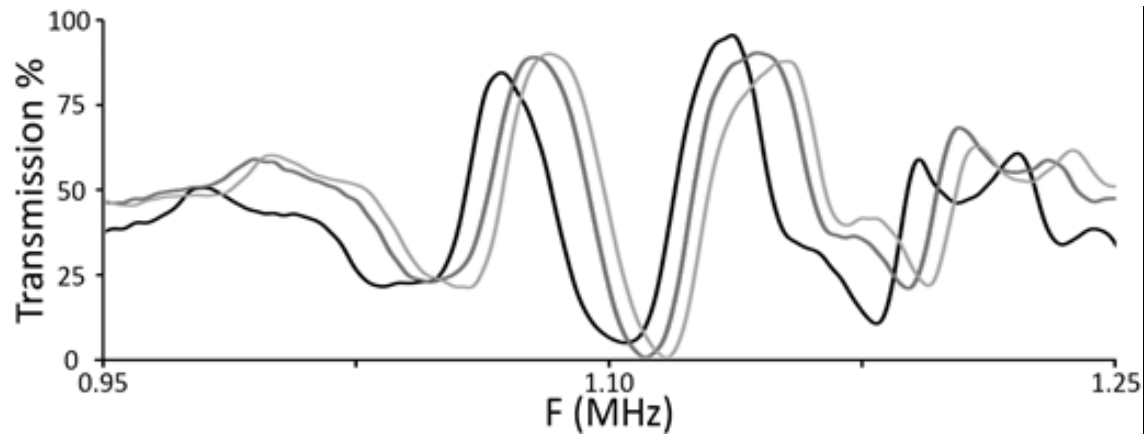


Figure 43 Experimental results of the tests using commercial milk products. The glass cuvette is filled with whole milk (grey), lactose-free milk (black) and strawberry flavoured milk (light grey).

The transmission curves of the three different milk products are well distinguishable and each one of them has transmission peaks with different amplitudes and frequencies that can be used as measures. The flavoured milk appears to have its maximum transmission peaks at higher frequencies while the lactose-free milk has its maximum transmission peaks at lower frequencies. The lactose-free milk also shows a different amplitude in both of its main transmission peaks, feature that could be used to differentiate it from the other milk products.

The frequency difference between the whole milk and the lactose-free milk is 3.36 KHz and the frequency difference between whole milk and flavoured milk is 2.23 KHz. The results are as expected given that flavoured milk has a higher sugar content than whole milk which modifies the speed of sound and density of the mixture.

The results of the third test are very promising because being able to differentiate complex liquids opens the door to the use of this sensor in biomedical applications.

7.3 Conclusions

A cavity resonance phononic crystal sensor with a disposable element that is able to quantify differences between alcohol solutions and complex fluids like milk was developed.

The use of a disposable element and the fact that it is fabricated using approved materials opens the door to the possibility of using this kind of sensors in biomedical applications and PoCT.

The experimental investigations show that the use of the 7 layered structure enhances the peak half bandwidth of the resonance induced by the cavity and that changes in the acoustic properties of the liquid confined in it generate displacements in the central frequency of these maxima of transmission.

The sensor design has large capabilities for optimization given the flexibility and robustness of phononic crystals and it enables to adapt the whole system to a large number of applications where the real-time measurement of liquid samples in the field is required.

The spectrophotometric cuvette used for this experimental realization was a square cuvette with each side measuring 10mm. This characteristic made the lateral miniaturisation very unreliable and presented discrepancies in the simulations.

Although the results presented transmission curves that can be used to characterise fluids, the design needs to be improved to be able to use the sensor in real applications.

7.4 Summary

This chapter presented an experimental realization of a simple 1D phononic crystal sensor having a resonant cavity, a disposable element and using additional layers of water to replace the coupling agent.

The results obtained during this study are not very satisfying but serve as a proof of concept of the replacement of the coupling layers by water layers as means to solve another of the limitations presented in chapter 3.

The next chapter will focus on an improved design of a multi-layered phononic crystal sensor that instead of having a disposable element, its completely disposable itself.

Chapter 8 - Fully-disposable multi-layered phononic crystal liquid sensor with symmetry reduction and a resonant cavity

This chapter reports the design, manufacture, and evaluation of a fully disposable multi-layered phononic crystal liquid sensor with symmetry reduction and a resonant cavity that can be used in applications that require the measurement of small liquid samples in the field. In order to realize the measurement of the frequency spectrum of the system, the same characterization system for measuring frequency changes from previous chapters was used.

The designed sensor contains a resonant cavity filled with the analyte that generates a defect mode that appears as a maximum of transmission located inside the bandgap.

Increasing the quality factor of this transmission peak is essential for the precision of the measurement. Our structure of this multi-layered phononic crystal is made of glass and PLA and can be discarded after the test, thus avoiding disinfection methods and improving the usability of this system in field applications with biological substances like in point of care testing.

8.1 Materials and Methods

The sensing system presented in this paper has 3 main components: the multi-layered PnC sensor, a pair of ultrasonic transducers and an electronic characterization system. The multi-layered PnC sensor was designed to develop the measurement of liquid samples with similar acoustic properties to water, with a longitudinal component of the speed of sound near 1500 m/s and a value of its mass density around 1000 Kg/m³. Knowing that the analyte becomes part of the phononic crystal structure, special care must be taken when selecting the properties of the materials composing the layers that are in contact with it so that there is a large enough impedance mismatch that allows the generation of bandgaps with adequate bandwidth and depth for sensing applications. Besides the acoustic properties of the constituent materials, it is also very

important to take into account that if the sensing system is intended to be used in applications where the analyte is a biological fluid, like in biomedical applications, all the components of the system that are in touch with the analyte must be sterilisable, and, in the case of point of care applications, fully disposable.

Taking into account all these considerations, optical glass was selected as the material to form the layers that are located next to the analyte. The selected glass has an acoustic impedance of 13.5 MRayls, resulting in an acoustic impedance ratio of 9 with the analyte. As a multi-layered PnC, the sensor can be approximated to a 1D structure by making the lateral dimensions of the layers much larger than their thickness.

The phononic crystal sensor structure was designed using 11 layers: 4 glass layers, 5 analyte layers and 2 PZT outer layers corresponding to the ultrasonic transducers. A schematic representation of the layer arrangement of the PnC structure can be observed in Figure 44.

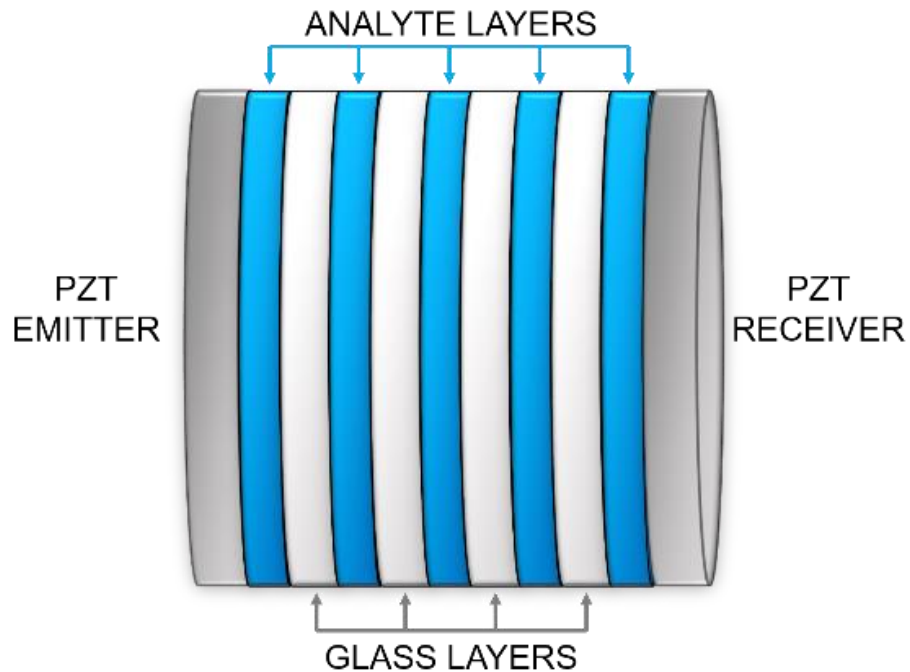


Figure 44 Schematic representation of the layer arrangement of the PnC structure.

To give support to the structure and glasses, a container made of polylactic acid (PLA) was designed. PLA is a low-cost thermoplastic polyester composed of lactic acid molecules that can be obtained from renewable resources like corn and sugarcane

making it biodegradable and ideal to form part of the disposable element of the sensor. For manufacturing the PLA container, a fused filament fabrication (FFF), 3D printer with a 0.4 mm extruder head and a 0.08 mm layer resolution was used.

The selected ultrasonic transducers have a central frequency of 1.1 MHz and a large bandwidth, therefore, the calculation of the dimensions of the layers of the PnC sensor was performed using as central frequency or working frequency the same frequency of the ultrasonic transducers. The selected transducers generate longitudinal waves in order to favour the transmission of waves through the liquid layers of the structure.

The dimensions of the glass and analyte layers were calculated following the equation of minimum transmission, or maximum reflection through thin layers, which states that in order to obtain a minimum of transmission at a specific frequency, the layer thickness, d_R , must be equal to an uneven factor of the wavelength, λ , divided by four, eq. (1) [139, 140]

$$d_R = (2n - 1)\lambda/4 \quad (1)$$

Knowing that the wavelength is equal to the speed of sound of the material divided by the frequency and that the speed of sound of the glass layers is around 5000 m/s and of the analyte layers is 1500m/s, a layer thickness of 1.13 mm was selected for the glass layers, eq. (2), and of 1.022 mm for the analyte layers, eq. (3) [139, 140]

$$d_g = (2n - 1)5000(m/s)/4(1.1(MHz)) = (1)1.13mm \quad (2)$$

$$d_a = (2n - 1)1500(m/s)/4(1.1(MHz)) = (3)341\mu m \quad (3)$$

After calculating the values of the dimensions of the layers to have a bandgap with a central frequency around 1.1 MHz, the next step was to conduct a series of simulations to observe the behaviour of a phononic crystal with these characteristics. The simulations were performed using the 1D transmission line model, and distilled water and ethanol were used as analytes to evaluate its frequency behaviour. In addition to the theoretical realisations, the PnC structure was fabricated using the 3D printer and a series of experimental tests were conducted to confirm the theoretical results. The fabricated structure can be observed in Figure 45.

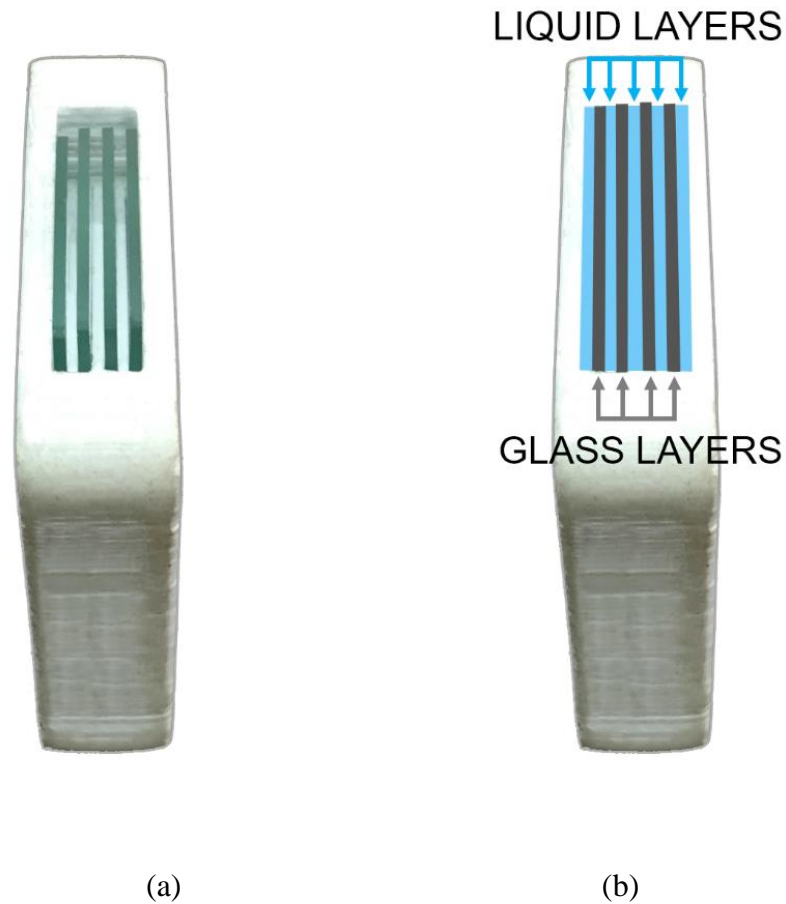


Figure 45 First phononic crystal structure fabricated using the 3D printer and glass.

The first structure designed has an uninterrupted periodicity in its design, and the calculations were performed to form a bandgap around 1.1 MHz, however, in order to be able to achieve a well-defined transmission feature in the frequency spectrum that can be characterized and used as a measure in a sensing system for biomedical applications, it is necessary to implement a symmetry reduction by means of introducing a defect mode in the phononic crystal.

For the design of the second structure, and assuming that the multi-layered PnC is a 1D structure, a point defect was introduced by changing the dimensions of one of the liquid layers, generating an additional maximum of transmission in the middle of the bandgap. In order to do so, the equation of maximum transmission, or minimum reflection through thin layers, was used. This equation states that in order to obtain a

maximum of transmission in a certain frequency, the layer thickness, d_T , must be equal to a factor of the wavelength, λ , divided by two, eq. (4). Following the equation, a value of 2.045 mm was obtained for the layer thickness of the defect layer, twice the original value, eq. (5). We have found from experience that there is a higher chance of obtaining good experimental results when using the same value of n for the analyte layer and the layers forming the bandgap.

$$d_T = n\lambda/2 \quad (4)$$

$$d_T = n1500(m/s)/2(1.1(MHz)) = (n)682 \mu m \quad (5)$$

Just as in the previous structure, theoretical realisations were performed in order to evaluate the behaviour in frequency of the designed PnC sensor. After the calculations, the PnC multi-layered sensor was manufactured using the 3D fabrication method and was evaluated experimentally using binary mixtures; ethanol solutions in distilled water at low concentrations were used to estimate its sensitivity in frequency. The fabricated structure can be observed in Figure 46.

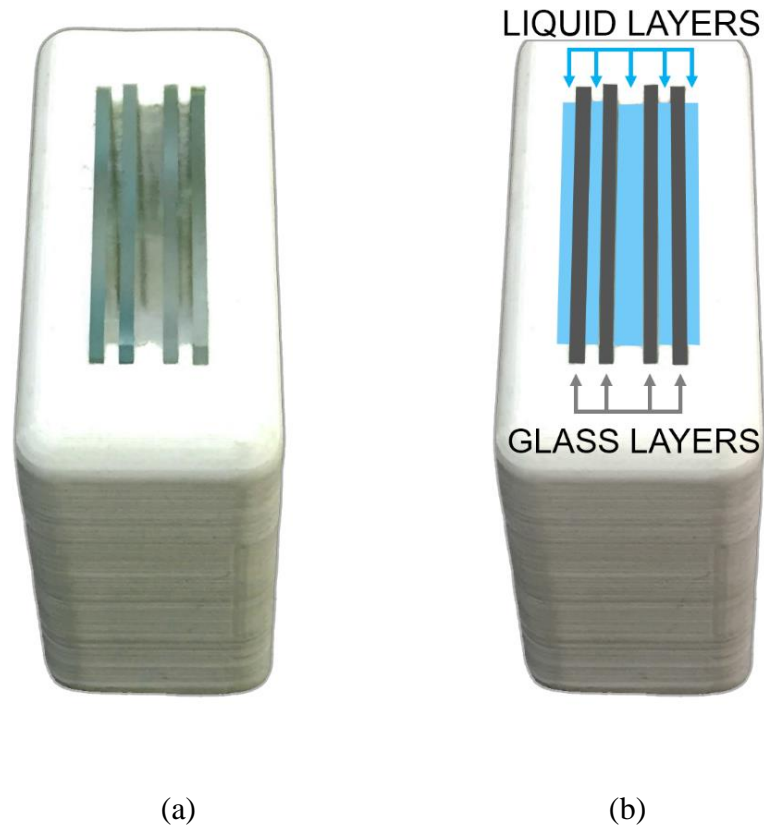


Figure 46 Second phononic crystal structure designed with a defect mode and fabricated using the 3D printer and glass. The central liquid layer has a different thickness than the other liquid layers in order to generate a transmission band inside the bandgap.

To perform the experimental realisations, a portable electronic characterization system that allows carrying out accurate measurements of frequency changes in resonant structures and phononic crystals using a pair of high-frequency ultrasonic transducers was used. This system bases its operation on a double sideband modulation with suppressed carrier and a special demodulation process using filters that allow acquiring gain and phase values of the system in a predetermined frequency range [144].

The electronic system was set to acquire 1300 points going from 0.5 MHz to 1.8 MHz. The frequency steps were set to 100 Hz and the PnC sensor was thoroughly rinsed and dried before introducing new samples. The temperature of the system was kept constant using room temperature control and the alcohol samples were carefully handled in order to avoid evaporation. The experimental arrangement used for the tests can be observed in Figure 47 and is composed of the two ultrasonic transducers, the

phononic crystal and a 3D printed holding structure to give support to the transducers. The properties of the analytes and materials used for the simulations of both phononic crystal structures can be observed in Table 7.

Table 7 Properties of the Materials used for the simulations

Material	c (m/s)	p (Kg/m ³)	Zc (MRayls)
Glass	5000	2700	13.5
PZT	3055	7500	22.91
Water	1493	998	1.49
Ethanol	1156	790	9.13

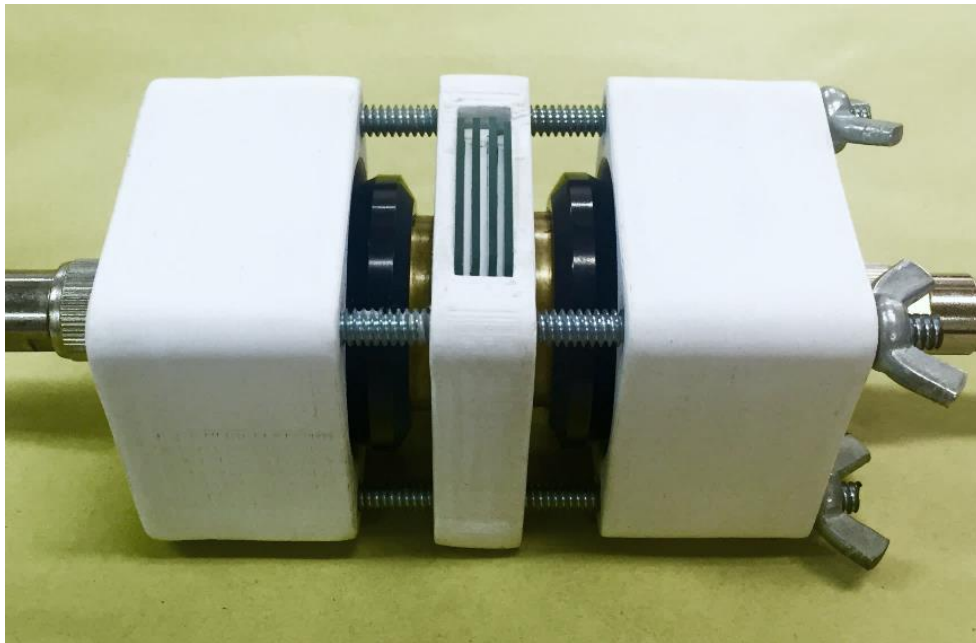
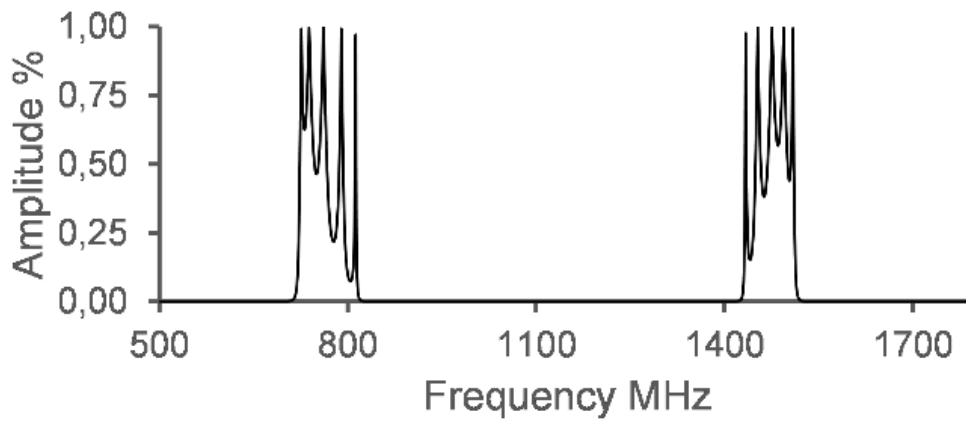


Figure 47 Experimental arrangement containing the designed structure, the transducers, and the electronic characterization system.

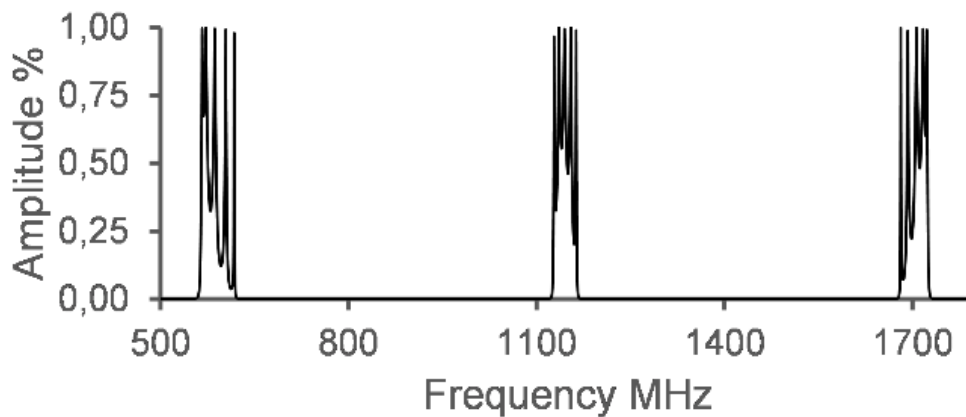
8.2 Results and Discussion

Figure 48 shows the simulation results of the first structure using the 1D transmission line model. Water (a) and ethanol (b) were used as analytes to evaluate its frequency response. The computational results show a typical behaviour of a phononic crystal with both analytes producing well-defined bandgaps with similar bandwidth. The central frequency of the bandgap produced when using water was located around 1.1

MHz and the ones produced when using ethanol were located around 850 KHz and 1.45 MHz. The difference between the frequency response of water and ethanol can be explained due to the dependence of the behaviour in frequency of the structure to the speed of sound of the analytes.



(a)



(b)

Figure 48 Simulation results of the first structure using distilled water (a) and ethanol (b) as analytes.

Figure 49 shows the simulation results of the second structure using the 1D transmission line model. This time, distilled water was used as analyte to evaluate its frequency response. The computational results show that the inclusion of a defect mode has generated the appearance of a transmission peak in the middle of the bandgap. The transmission peak has a good amplitude and a high-quality factor. The surrounding bandgap isolates it from possible noise sources generating suitable boundary conditions for sensing applications.

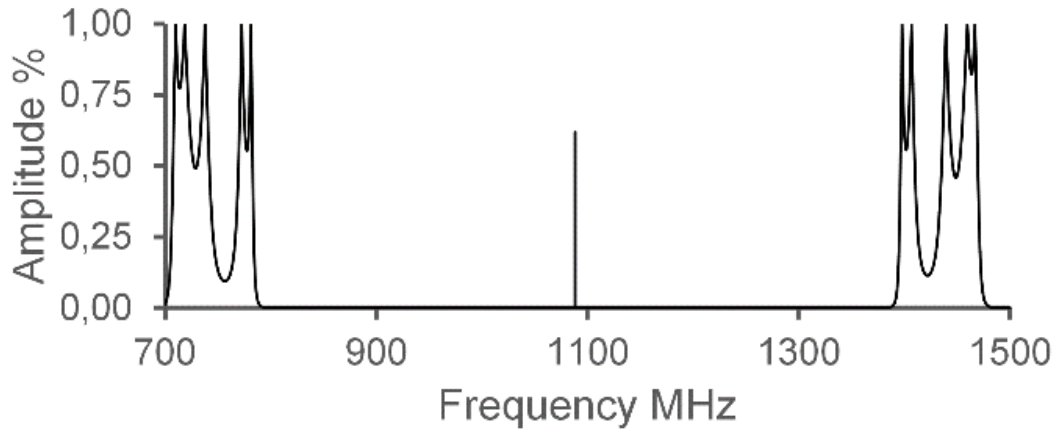
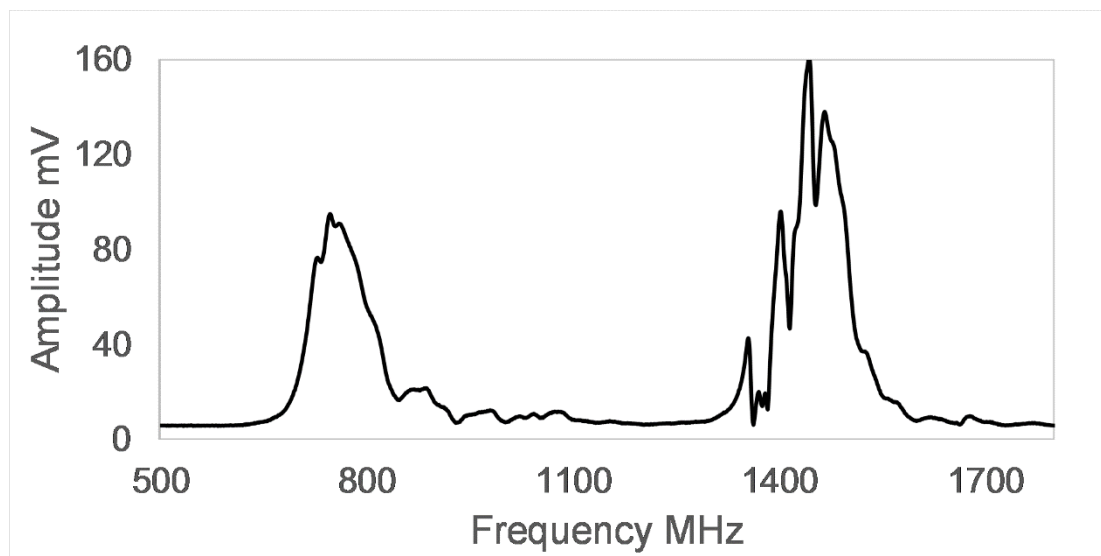


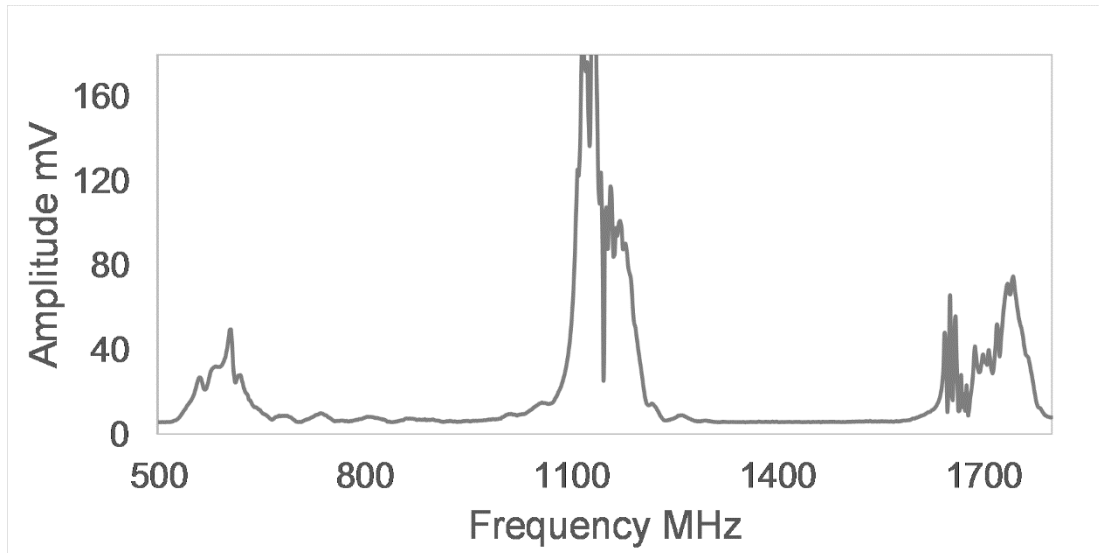
Figure 49 Simulation results of the second structure using distilled water as analyte.

After performing the simulations, the designed structures were fabricated and evaluated using the double sideband electronic characterization system previously described [144].

First, the performance of the phononic crystal structure designed without using defect modes was experimentally evaluated. Figure 52 shows the experimental results of the first structure using water (a) and ethanol (b) as analytes.



(a)



(b)

Figure 50 Experimental results of the first structure using distilled water (a) and ethanol (b) as analytes.

The experimental results using the first structure show the characteristic behaviour in frequency of phononic crystals, which is a selective transmission of waves with bandgaps located in different frequencies depending on the properties of the constituent materials and dimensions of the layers. Ethanol has a lower speed of sound than distilled water, therefore, the central frequency of the bandgaps generated by the PnC structure when ethanol is used in the liquid layers is lower. The experimental results are according to the simulations, with bandgaps located in the same frequencies and having a similar bandwidth. The simulations use a reduction in the dimensionality and the lateral miniaturization of the model could explain the differences between the amplitude of the computational results and the experimental ones.

Following the same protocol as in the 1D simulations, binary mixtures of ethanol in water with a concentration of 0.02% and 0.5% in volume fraction were used to experimentally evaluate the performance of the second structure, Figure 51.

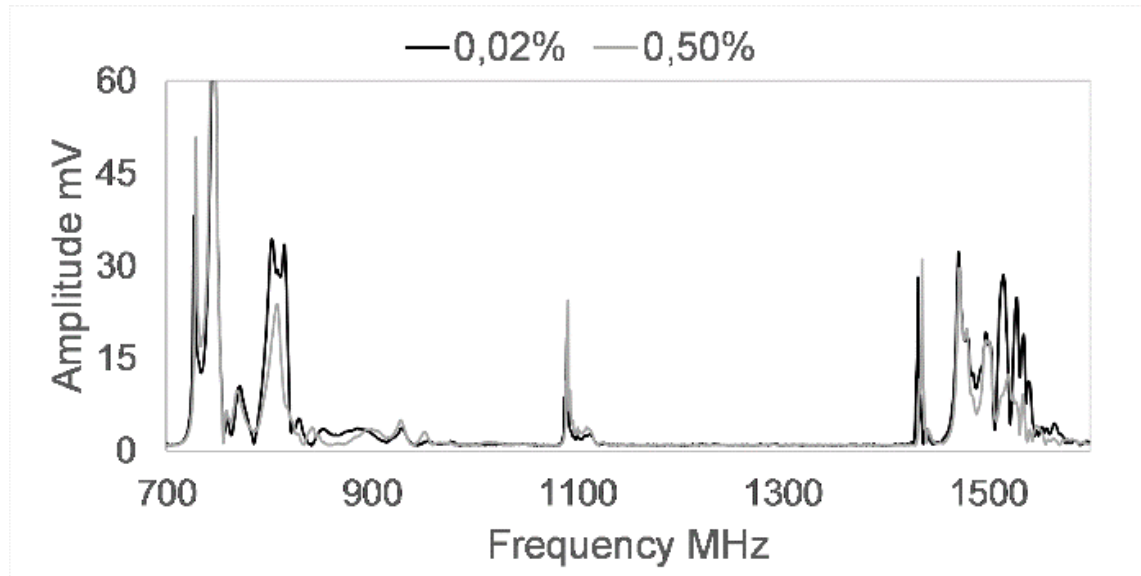


Figure 51 Experimental results of the second structure using ethanol solutions in water with a concentration of 0.02% (a) and 0.5% (b) in volume fraction.

The experimental results obtained with the second structure show a bandgap between 0.8 MHz and 1.4 MHz with a transmission band located near 1.1 MHz, as expected given the similar results obtained in the simulations. The transmission peak inside the bandgap is easily differentiated and the bandgap generates adequate boundary conditions to isolate it. Figure 52 shows a close-up on the central peak of the experimental results of the second structure and compares the frequency response of both analytes.

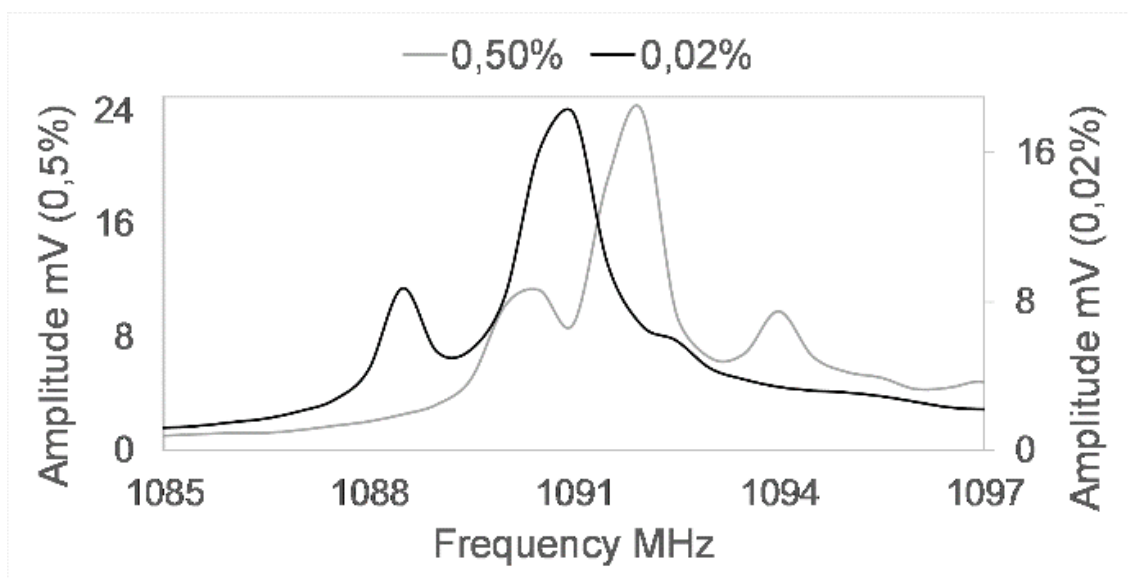


Figure 52 Comparison of the experimental results of the second structure using ethanol solutions in water with a concentration of 0.02% (black) and a concentration of 0.5% (grey) in volume fraction.

The central transmission peak has a good quality factor and it facilitates its use in sensing applications where very low concentration measurements are required. Little variations in the concentration of an analyte, like the one used in this experiment, produce small displacements in frequency of relevant transmission features, and therefore, the importance of having sharp transmission peaks to be able to differentiate these changes. The experimental results show that the designed PnC sensor can easily recognize small variations of ethanol (0.02% to 0.5%) in distilled water.

8.3 Conclusions

A multi-layered phononic crystal liquid sensor utilizing defect modes to generate transmission peaks with high-quality factor inside bandgaps for measuring variations in the concentration of analytes in small liquid samples was developed. The introduced sensor system offers a new possibility to introduce such as sensing modality in biomedical applications where point of care testing is needed and where limited analyte volume is available, and a high resolution is required.

This technology measures mechanical properties of the liquid samples instead of optical or electrical properties like most of the current point of care technologies. The

specificity of the system can be increased by using chemical/biochemical enhancements like enzymes, DNA or antigen-antibody reactions between others.

This research demonstrates that Phononic crystal sensors have the potential to be used as liquid sensors given the flexibility on the design and robustness. The applications that are most appealing are those where in-situ measurements of small liquid samples are required.

8.4 Summary

This chapter presented the design, fabrication and evaluation of a multi-layered phononic crystal sensor with low analyte consumption that can be used in biomedical applications.

The key feature of the sensor system is a fully disposable multi-layered phononic crystal liquid sensor element with symmetry reduction and a resonant cavity. The phononic crystal structure consists of eleven layers with high acoustic impedance mismatch. A defect mode was utilized in order to generate a well-defined transmission peak inside the bandgap that can be used as a measure. The design of the structures has been improved with simulations using a transmission line model. Experimental realizations were performed to evaluate the frequency response of the designed sensor using different liquid analytes. The frequency of the characteristic transmission peaks showed to be dependent on the properties of the analytes used in the experiments. Multi-layered phononic crystal sensors can be used in applications, like point of care testing, where the on-line measurement of small liquid samples is required.

Some of the main achievements of this chapter are the development of low analyte consumption tests and the reduction of the dimensions of the sensing system, which were two of the limitations presented in chapter 3.

The next chapter will focus on overcoming another of the limitations present in the state of the art which is the high dependence of environmental control units to avoid speed of sound alterations due to modifications in temperature.

Chapter 9 - Differential Phononic Crystal Sensor: Towards a Temperature Compensation Mechanism for Field Applications Development

In order to be able to implement this new technology in more challenging applications, such as biomedical applications, it is necessary to have a very precise and accurate measurement. One of the great challenges when working with liquid samples is that their properties vary in a significant way when ambient conditions are not stable, especially with a fluctuating temperature. Bulky temperature control systems have been implemented as a solution, however, these systems cannot be used in applications where portability is mandatory, like in point of care testing or other field applications. Bilanuk et al. showed the effect that temperature, T , has in the speed of sound, c , of distilled water, Equation (2) [149, 150].

$$c = 1.40238744 \times 10^3 + 5.03836171T - 5.81172916 \times 10^{-2}T^2 + 3.34638117 \times 10^{-4}T^3 - 1.48259672 \times 10^{-6}T^4 + 3.16585020 \times 10^{-9}T^5, \quad (2)$$

Different alternatives to mitigate the effect of temperature without using bulky temperature control systems have been proposed. The use of differential measurements has been one of the most effective solutions. They use a second signal and a reference with known properties that allows compensation for the effect of temperature. The advantage of using these devices is that any external influence of pressure, or temperature, among others, will affect both the reference and the sample. Kaya et al. recently developed a theoretical study about an acoustic phononic crystal Mach–Zender interferometer with two signal paths, one for the reference and one for the sample and could be used as a temperature compensation mechanism [151].

This chapter presents a phononic crystal sensor with a temperature compensation mechanism that allows performing differential measurements. The PnC was designed using three defect modes instead of one like previous approaches. The differential PnC sensor presented in this chapter uses a single wave path for obtaining the information

about the temperature and the analyte which facilitates the development and implementation of new sensors since all the information needed for characterising the liquid sample and compensating the temperature is contained in a single frequency spectra.

9.1 Materials and Methods

The PnC sensor presented on this work is comprised of a series of consecutive thin layers with different acoustic properties. The spatial modulation of the acoustic properties allows it to exhibit a wide bandgap.

For the generation of the relevant characteristic features that are used in the measurement of the acoustic properties of the liquid samples the technique of symmetry reduction was used. A total of three defect modes were introduced into the crystal by altering the dimensions of the three central liquid layers. The designed structure can be observed in Figure 53.

The central layer is composed by the analyte, while the two adjacent liquid layers are filled with a reference material. The dimensions of the reference and central layers were calculated using distilled water, therefore, making the three layers equal. The properties of the materials of each layer, as well as their dimensions, are shown in Table 8.

Table 8 Material properties of the PnC sensors used.

Layer #	Thickness (mm) PnC Sensor	Thickness (mm) Control Sensor	Material	ρ (Kg/m ³)	c (m/s)
1	-	-	PZT ¹	7500	3333
2	0.187	0.187	Water	998	1483
3	0.715	0.715	Glass	2200	5720
4	0.187	0.374	Water	998	1483
5	0.715	0.715	Glass	2200	5720
6	0.374	0.374	Analyte/Water	998	1483
7	0.715	0.715	Glass	2200	5720
8	0.187	0.374	Water	998	1483

9	0.715	0.715	Glass	2200	5720
10	0.187	0.187	Water	998	1483
11	-	-	PZT ¹	7500	3333

¹ The layer thickness of the PZT layers is considered as semi-infinite for the simulation.

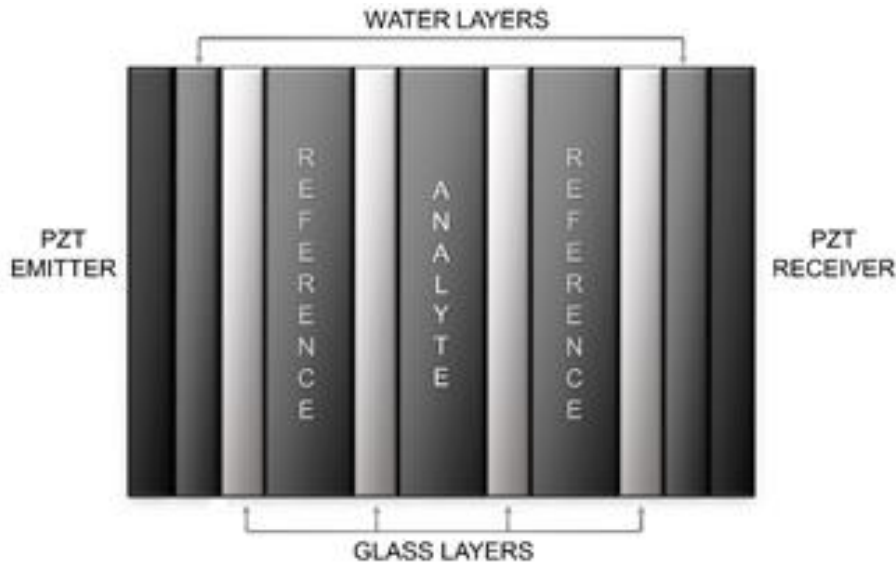


Figure 53 Differential phononic crystal sensor designed with three defect modes.

The differential PnC sensor was studied numerically using the transmission line model, TLM. This method was selected due to its performance on multi-layered structures. The TLM delivers the reflection and transmission coefficients of structures composed of thin isotropic layers. These coefficients are used to follow the frequency of characteristic transmission features generated by the technique of symmetry reduction on the frequency response of the sensor. To calculate the effective acoustic impedance of each layer, a program was coded in the mathematical software, MATLAB. The parameters used in the simulations are the properties of the layers (density, speed of sound, and layer thickness), the properties of the frequency sweep (initial frequency, steps, and step value) and finally the temperature at which the simulation is performed.

The speed of sound of the materials is closely related to the temperature, therefore, the value of the speed of sound of the layers composed of distilled water is adjusted using the equation described by Bilanuk et al. Equation (2).

To be able to compare the results and observe the benefits obtained with the proposed differential PnC sensor, the simulation of an additional control sensor, Figure 54, was performed. The properties of the layers of the structure of the control PnC sensor are shown in Table 1. The control PnC sensor was designed using only one defect mode instead of three.

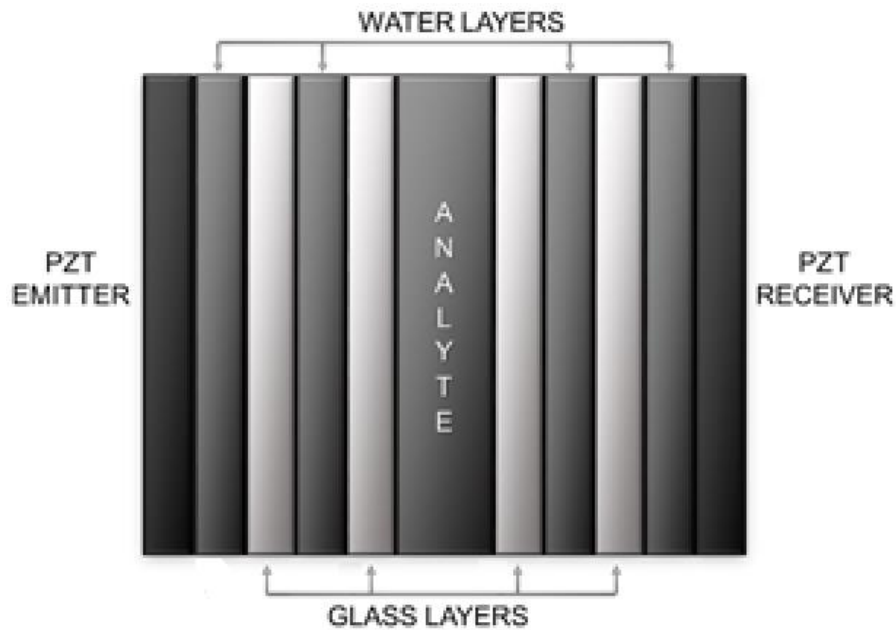


Figure 54 Control phononic crystal sensor designed with only one defect mode.

A theoretical study was performed to evaluate the behaviour in frequency of the differential phononic crystal sensor designed. Each simulation was realised using the same parameters for the control PnC sensor and the differential PnC sensor. Distilled water was used as analyte and the response of both sensors was compared, paying special attention to the transmission maxima present in the centre of the bandgap, since these are the ones that carry the most relevant information about the changes in the speed of sound of the analyte. Temperature ranges going from 3 °C to 43 °C were used to evaluate the impact of temperature on the frequency spectrum of the structures. The formula of Bilanuk et al. Equation (2) was used to calculate the speed of sound of distilled water at the different temperatures of the study. Both crystals have a working frequency around 2 MHz, therefore, the initial frequency selected to perform the studies was 100 KHz, with steps of 1 Hz. Attenuation and losses were not included in the simulations because the aim of the study was to determine the impact of temperature on the frequency of relevant transmission features and how the

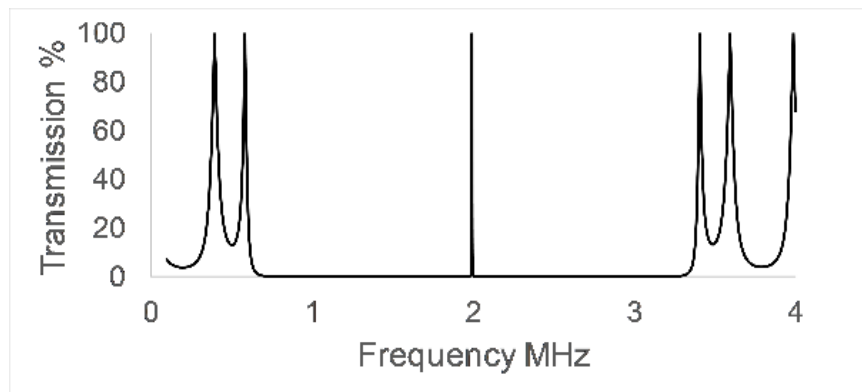
temperature compensation mechanism could help improve the performance of the sensor.

9.2 Results and Discussion

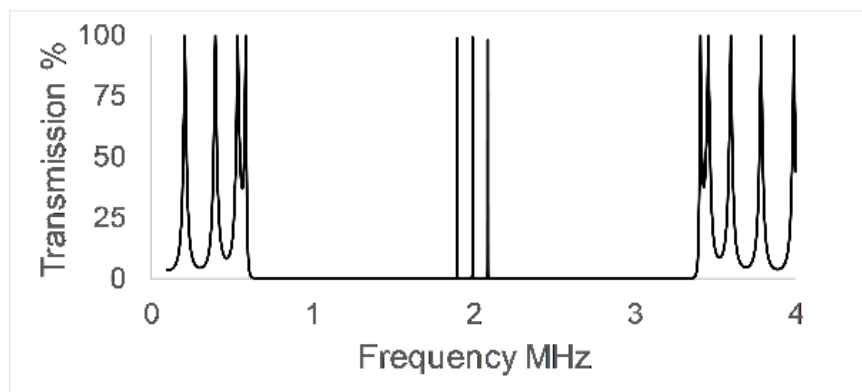
Figure 55 shows the frequency response of the control (a) and differential (b) PnC sensors at room temperature. The results of the computational simulation using the transmission line model show a well-defined bandgap on both sensors, ranging from 500 KHz to 3.5 MHz, resulting in a good bandwidth of 3MHz. The transmission spectrum of the control sensor structure has a maximum transmission located in the centre of the rejected band, while the frequency response of the differential sensor structure has three transmission maxima instead of one. The response presented by both sensors shows that when using the symmetry reduction technique, transmission maxima are generated within the rejected band, as already shown in previous studies [9], however, it is interesting to note that the use of three defect modes with the same characteristics generates three maxima in the centre of the band.

The transmission maxima generated by the disruption in the symmetry of the PnC structure present a high-quality factor. This is mainly due to the effect exerted by the rejected band on them. Although the glass used in the solid layers of the PnC does not have an acoustic impedance as high as steel or other common solids, the impedance ratio between glass and distilled water is high enough to generate a bandgap with good depth and bandwidth.

The temperature compensation mechanism relies on the measurement of the frequency of the three transmission maxima observed at the centre of the bandgap of the differential sensor, Figure 3 (b). The design of these sensors is made so that only one of these three peaks is affected by the variations in the speed of sound of the analyte. This is achieved by introducing three defects and filling only one of them with the analyte, leaving the other two with a known material. In this case, distilled water. The peaks that are not sensitive to the changes in the analyte layer are used as a reference, thus, enabling the performance of differential measurements.



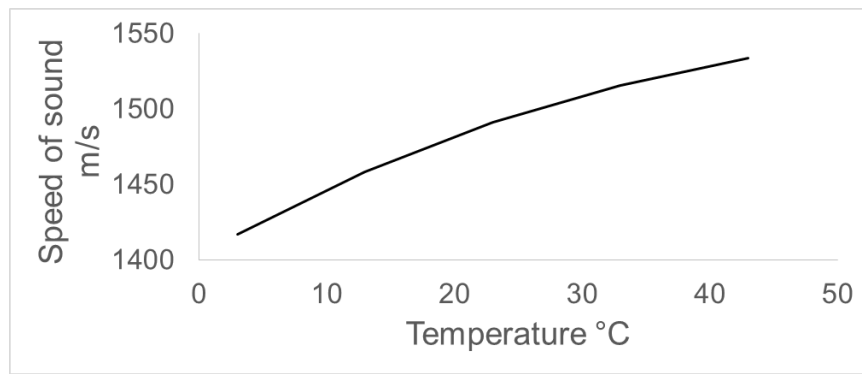
(a)



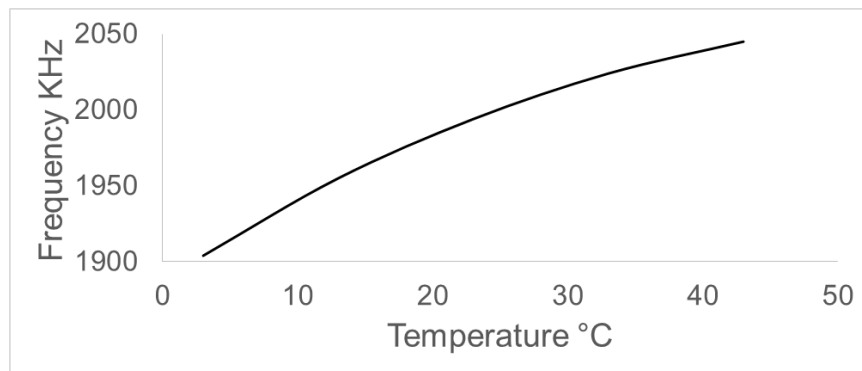
(b)

Figure 55 Simulation results using the TLM of the control PnC sensor (a) and the differential PnC sensor (b). Distilled water was used as analyte.

Changes in temperature significantly affect the speed of sound of distilled water, causing the relevant frequency characteristics in PnC sensors to shift in frequency. Figure 56 shows how temperature variations ranging from 3 °C to 43 °C are related to the speed of sound of the analyte (a) and the frequency of the central maxima of transmission of the control PnC sensor (b).



(a)



(b)

Figure 56 Behaviour of the speed of sound of distilled water (a) and the frequency of the central peak of the control phononic crystal (b) when temperature is varied from 3 °C to 43 °C.

By increasing the temperature at which the simulations are performed, the speed of sound in distilled water increases from 1416 m/s to 1533 m/s, which causes the relevant transmission maxima to move towards higher frequencies in the spectrum.

Figure 57 shows the effect that a change of 1 °C would have in a test in which it is required to identify a variation of 1 m/s in a liquid sample using the control sensor shown in Figure 54. Increasing the speed of sound by 1 m/s makes the peak displace itself in frequency by 1.182 kHz. Further increasing the temperature by 1 °C makes it go to higher frequencies, displacing itself by another 3.353 KHz. The quality factor of the central transmission maxima is good, which makes it easy to identify and quantify

small changes in frequency, however, a change of only 1 °C, generates great difficulties in identifying these changes, since its influence in the frequency position of the transmission maxima is almost three times greater than that of a change of 1 m/s

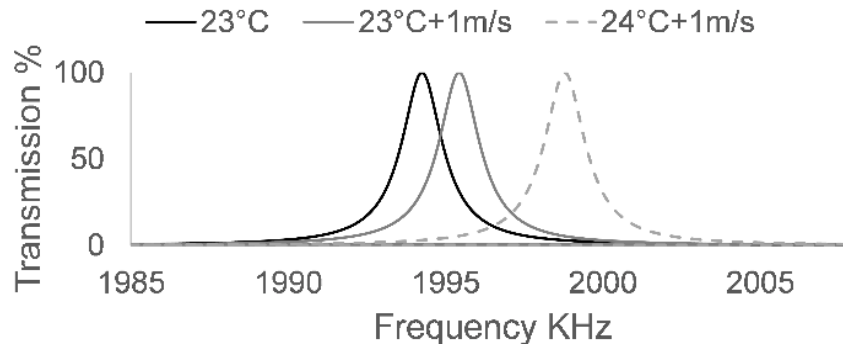
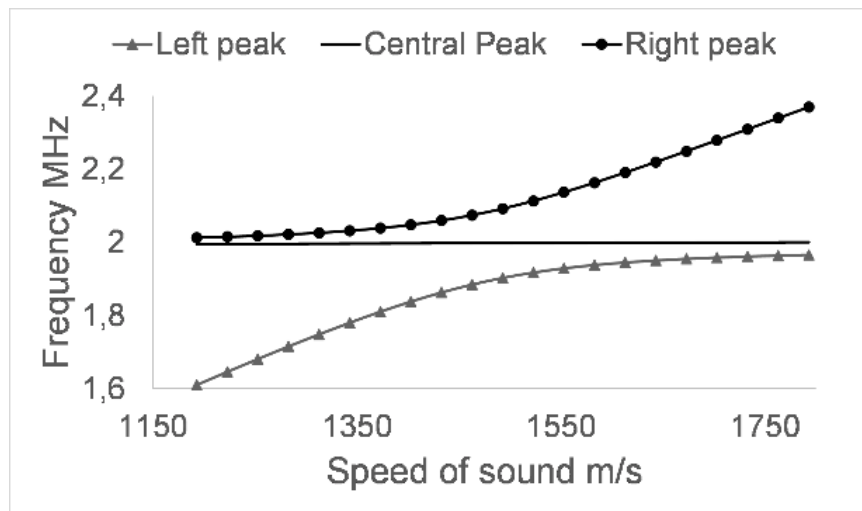


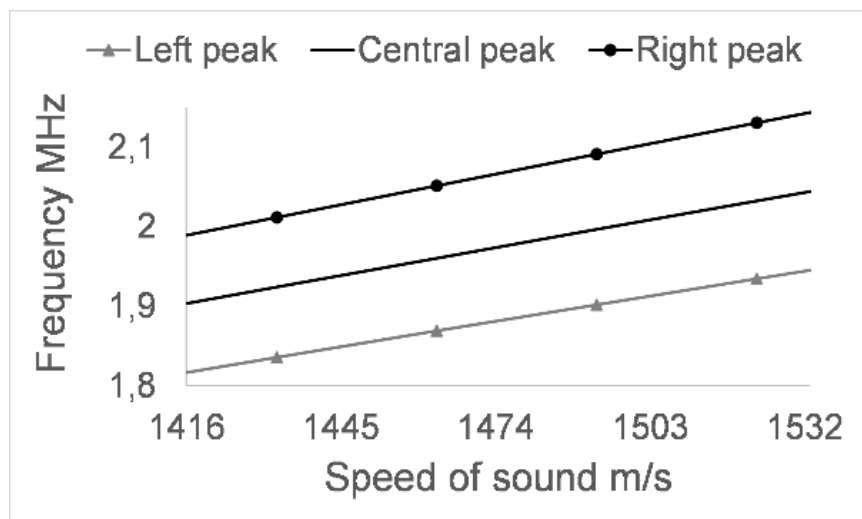
Figure 57 Effect of increasing 1 °C on simulations using the control PnC sensor. The black line shows the analyte at 23 °C, the grey line shows an increase of 1 m/s on the analyte and the dotted line shows the effect of adding 1 °C to the simulation.

After analysing the impact of varying the temperature in the control PnC sensor, the behaviour of the differential PnC sensor proposed in this work was analysed. In order to observe the performance of the temperature compensation mechanism in the differential sensor, two simulations were carried out. The first simulation was realised performing a variation of the speed of sound in the analyte layer, Figure 58 (a). The second simulation, Figure 58 (b), was performed by changing only the temperature, assuming that the analyte does not undergo further variations.

The frequency response of the three central transmission maxima, Figure 58 (a), shows that the central maximum remains stable at 2 MHz when making changes in the speed of sound of the analyte. However, the other two transmission maxima suffer significant variations in frequency, which increase in magnitude as the lateral maxima move away from the central one. It is very interesting to observe how the behaviour of the two peaks that accompany the central peak is asymptotic with respect to the frequency response of the central peak of the control PnC sensor, Figure 59.



(a)



(b)

Figure 58 (a) Influence of changes in the speed of sound of the analyte layer (a) and the temperature (b) on the relevant transmission peaks of the differential PnC sensor.

Figure 58 (b) shows how, by varying the temperature from 3°C to 43 °C, the frequency position of the transmission maxima was steadily increased, including the central transmission maximum. This behaviour allows the use of the central maximum, which is sensitive to changes in temperature, but not to changes in the properties of the

analyte, as a reference to perform differential measurements and thus to have a temperature compensation mechanism.

It is important to note that although in Figure 58 (a) the central maxima appear to be stable at 2 MHz over the entire range of sound velocities that were interrogated, it actually undergoes small frequency changes that can induce small errors in the measurement if they are not taken into account. It is also important to note that the increase in the frequency of the three central transmission maxima related to changes in the temperature, Figure 58 (b) is not the same, so it must also be taken into account in the calculation of the properties of the analyte under test.

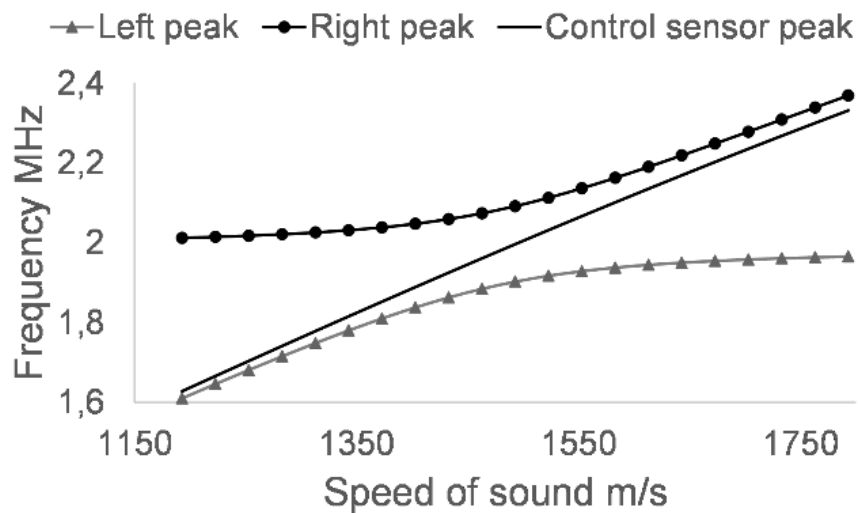


Figure 59 Relationship between the lateral peaks of the differential PnC sensor and the central peak of the control PnC sensor when the speed of sound of the analyte layer is varied.

9.3 Conclusions

A PnC liquid sensor with a temperature compensation mechanism by means of differential measurements was studied.

The PnC structure has three resonant defect modes. These modes are due to the breaking of the structural periodicity or translation symmetry of the PnC by three defect layers. The three peaks are located within the phononic bandgap and are very sharp in shape, indicating strongly localized defect modes. The introduction of three defect modes instead of one causes the modes to have energy transfer between them.

This interaction between modes or mode coupling splits the single peak into three new resonances around 2 MHz. When the properties of one of the three defect layers are varied the symmetry of these three defect mode resonances is disrupted and the peaks displace themselves in frequency.

The avoid crossing behaviour is due to the energy transfer between modes critically slowing down the displacement of the peak that comes closer to the central maxima located at 2 MHz.

The working principle of the differential PnC sensor is performing a frequency tracking of three transmission maxima located at the centre of the bandgap. The introduction of these defect modes allows following the changes in the speed of sound that occur in the liquids contained in the central cavity of the structure, showing the effectiveness of the use of the symmetry reduction technique for the design of sensors with phononic crystals.

Only the central cavity was filled with analyte, maintaining the two adjacent cavities as a reference, which allowed to make the central transmission maxima sensitive only to changes in temperature but not to those of speed of sound in the analyte. The temperature compensation mechanism used enables the realization of differential measurements with a single signal path. This facilitates the use of this sensor in applications where temperature control is a problem, such as conducting point of care tests at home or in the field.

9.4 Summary

This chapter presented the design and evaluation of a multi-layered phononic crystal sensor having multiple defect modes that enable the realization of differential measurements.

Theoretical studies using the transmission line model and analytes at various temperatures show that the proposed temperature compensation mechanism enhances the performance of the sensor in a significant way. This temperature compensation strategy can also be implemented in crystals with different topologies.

The next chapter will focus on the generating an enhancement to the phononic crystal sensor so that it is able to perform measurements of analytes in complex mixtures. This is the last of the challenges outlined in chapter 3.

Chapter 10 - Phononic crystal biosensors: functionalization of resonant cavities to enhance selectivity in challenging applications

Point of care testing devices are portable and do not require a dedicated space or are fixed to a healthcare facility. This type of tests could also increase patient's care while reducing the costs to the healthcare system. The most common use of PoC devices is for detecting levels of Glucose, blood gas analysis, pregnancy tests and lactate levels, to mention a few [3, 152].

One of the most relevant resonant sensing technologies for developing PoC devices is the Quartz Crystal Microbalance (QCM). This technology is a bulk acoustic wave gravimetric sensor that changes the frequency of oscillation of a piezoelectric crystal depending on the mass deposited over its surface. When used as a biosensor, a recognition agent, usually an antibody, is immobilized on the surface of the piezoelectric crystal transducer. When an analyte containing the molecule of interest, usually an antigen, flows over the functionalized transducer, a reaction occurs, attaching that molecule to the surface and increasing the mass. The mass change generates a variation in the resonant frequency of the piezoelectric crystal, which is being tracked by an electronic characterization system. Phase is also used to characterize high-frequency QCM sensors [91, 153].

The most important setback of using phononic crystals is that the frequency of maximum transmission of the relevant transmission features generated using the symmetry reduction technique is mainly sensitive to changes in the longitudinal component of the speed of sound of the analyte. Molar mass, molar volume, molar ratio and adiabatic compressibility determine sound velocity in liquids, which is directly related to intermolecular interactions in complex mixtures. It is very complicated to obtain specificity when complex mixtures are used as the analyte. Most PoC tests are performed using complex mixtures, e.g., blood. QCM have also the same problem, and the way to overcome this issue is the functionalization of the surface of

the transducer with a recognition agent, making it specific to a selected biological compound [124].

This chapter reports a novel phononic crystal biosensor that, through the functionalization of a resonant cavity with a recognition agent, can perform selective measurements and it can be used in challenging applications like PoC testing to detect specific proteins and biomarkers.

The functionalized resonant cavity is made of glass walls and the immobilization of bovine serum albumin, BSA, antibodies was carried out. Multiple experimental realizations using solutions of BSA in phosphate-buffered saline, PBS, were performed. When the target antibody is present in the sample, it attaches itself to the functionalized walls of the cavity producing changes in the frequency of maximum transmission of the defect mode.

10.1 Materials and methods

The phononic crystal biosensor designed consists of a periodic arrangement of nine consecutive stacked layers. It presents a single defect mode in the middle of the structure forming a central resonant cavity. The analyte is introduced in the central resonant cavity and becomes part of the phononic crystal structure. The materials selected to design the multi-layered phononic crystal biosensor are glass and distilled water because of the large impedance mismatch between these two materials. The properties of the materials, as well as the dimensions of the layers, can be observed in Table 9.

The dimensions of the layers are inversely proportional to the working frequency of the crystal; therefore, high frequencies result in very thin layers. A small volume of analyte consumption is fundamental for the development of point of care tests; however, a frequency higher than 10 MHz will result in a central resonant cavity thickness of only a few micrometres. Therefore, a working frequency of around 800 KHz was selected. With this working frequency, the central resonant cavity thickness is 1 mm, and the minimum analyte consumption is 45 uL, which is lower than the volume of a regular drop of blood, which is between 50 uL and 70 uL.

The outer layers of the crystal are PZT layers. These layers correspond to the ultrasonic transducers used to characterize the PnC biosensor. Olympus V103-RB longitudinal wave transducers were used to perform the experimental measurements. The central frequency of the wideband contact transducers is 1.1 MHz. It is important to take into account that the transducers need a coupling agent to ensure an adequate transmission of the waves to the phononic crystal. Otherwise, air might get in-between, and the transmission of the waves would be heavily attenuated. A thin layer of USP glycerine was applied to the transducer surface as coupling means with the outer glass layers to ensure maximum transmission of the waves. The experimental setup can be observed in Figures 60 and 61.



Figure 60 Close up of the experimental setup showing the phononic crystal biosensor, the wideband ultrasonic transducers and a 3D printed support structure used to hold to the setup in position.

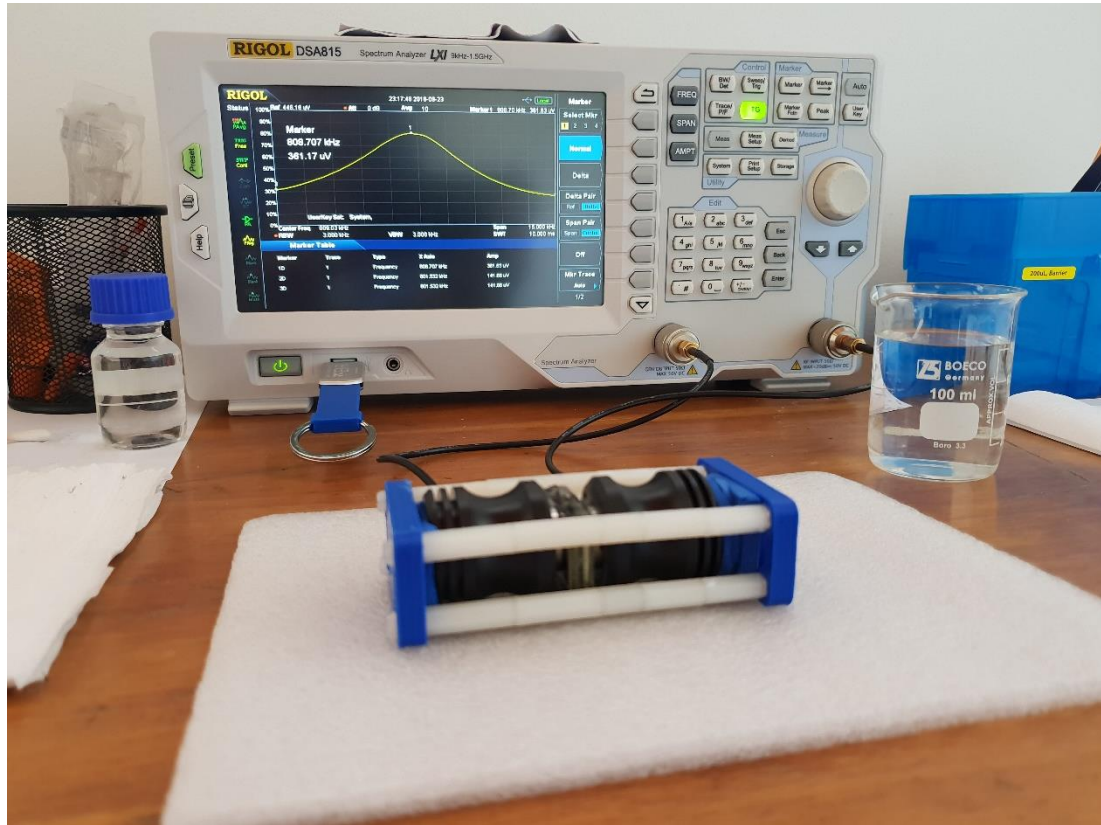


Figure 61 Experimental setup showing the phononic crystal biosensor, the wideband ultrasonic transducers, the 3D printed support structure and the Rigol Spectrum Analyser.

Table 9 Properties of the materials and layers

<i>Layer</i> (#)	<i>Thickness</i> (mm)	<i>Material</i>	<i>c</i> (m/s)	<i>p</i> (Kg/m ³)	<i>Zc</i> (MRayls)
1	-	PZT	7500	3333	25
2	1	Glass	5720	2200	12,6
3	0,5	Water	1493	998	1,5
4	1	Glass	5720	2200	12,6
6	1	Analyte			
5	1	Glass	5720	2200	12,6
7	0,5	Water	1493	998	1,5
8	1	Glass	5720	2200	12,6
9	-	PZT	7500	3333	25

A support structure was manufactured to position and align the ultrasonic transducers against the phononic crystal biosensor. It was 3D printed using an additive

manufacturing process, fused filament fabrication (FFF). The material used was acrylonitrile butadiene styrene (ABS), one of the most common thermoplastic polymers used for 3D printing.

Surface modification and antigen coupling

The immobilization process was performed using a protocol similar to the one found in [154], where a 38-kDa protein of *Mycobacterium tuberculosis* was immobilized over a glass surface. This protocol was selected to immobilize BSA antigen to the glass walls of the cavity because the antigen used in the study presented in [154] shares similar amine groups with the BSA antigen. The glass surface of the resonant cavity walls was modified with a silanization procedure that uses a piranha solution and APTES, (3-Aminopropyl) triethoxysilane to cover the walls with organofunctional alkoxy silane molecules. Then the PDITC, p-Phenylene diisothiocyanate, crosslinker was used to bond the surface with the amine groups of the BSA antigen. In addition to the steps described in the referenced protocol, ethanolamine 10 % (v/v) was used to saturate the unoccupied binding sites as a blocking reagent avoiding an active participation of these binding sites in the specific assay reaction. When the target antibody is present in the sample, it attaches itself to the biorecognition agent on the walls of the cavity, in this case, the antigen, and generates an additional thin layer to the phononic crystal sensor structure, modifying its frequency response and making it specifically sensitive to that target molecule.

Performance Test Protocol

An experimental test was realized to evaluate the performance of the developed phononic crystal biosensor by adding the respective antibody (Anti-BSA) diluted in PBS buffer in different concentrations (5 ug/ml, 0.5 ug/ml, 0.05 ug/ml, 0.005 ug/ml and 0.0005 ug/mL) in the resonant cavity. All tests were carried out at room temperature, at about 25 °C. The temperature was kept constant using room temperature control. The protocol used for the tests was as follows.

- 1) Apply HCl with a concentration of 0.1M for 3 min to clean and break previous bonds.
- 2) Remove the HCl and wash with PBS buffer five times.

- 3) Introduce 45ul of PBS buffer and measure the frequency response of the PnC biosensor. This measurement corresponds to the baseline.
- 4) Add the desired antibody-PBS solution taking into account that it will be diluted with the already introduced PBS buffer.
- 5) Take measurements every 5 minutes for a total of 20 minutes.
- 6) Remove the solution and wash the resonant cavity with PBS 5 times.
- 7) Introduce 90ul of PBS buffer and measure the frequency response of the PnC biosensor. This measurement corresponds to the control and is designed to evidence if the antigen-antibody reaction occurred.

The protocol above protocol was repeated for each concentration of the analyte. The displacement in the frequency of the resonant mode inside the bandgap that takes place after adding the additional 45ul of the antibody-PBS solution in step 4 will show if the PnC biosensor is sensitive enough to develop the measurements. However, it is the difference between the frequency of maximum transmission of the baseline measurement and the control measurement on step 7 that will show the real biosensor response.

10.2 Results and discussion

The first experimental test performed was to evaluate the frequency response of the phononic crystal. Figure 62 presents the experimental results of this first test using PBS buffer as the analyte. The frequency response of the phononic crystal biosensor presents a well-defined bandgap between 350 KHz and 1300 KHz, a very large bandgap with almost 1 MHz of bandwidth. The bandgap seems to have a larger transmission on the higher frequency border; however, this effect appears due to the bandwidth of the ultrasonic transducers used. The 350 Hz region is almost on the edge of the bandwidth of the V103 Olympus transducers, while the 1300 KHz region is near its maximum response, which is 1100 KHz.

The defect layer of the phononic crystal biosensor generates a large transmission feature around 800 KHz. This transmission feature is a narrow transmission peak with a high-quality factor and a very high signal to noise ratio. The surrounding bandgap

attenuates all the transmission around the resonant peak and makes it ideal for its use to characterize the PnC biosensor.

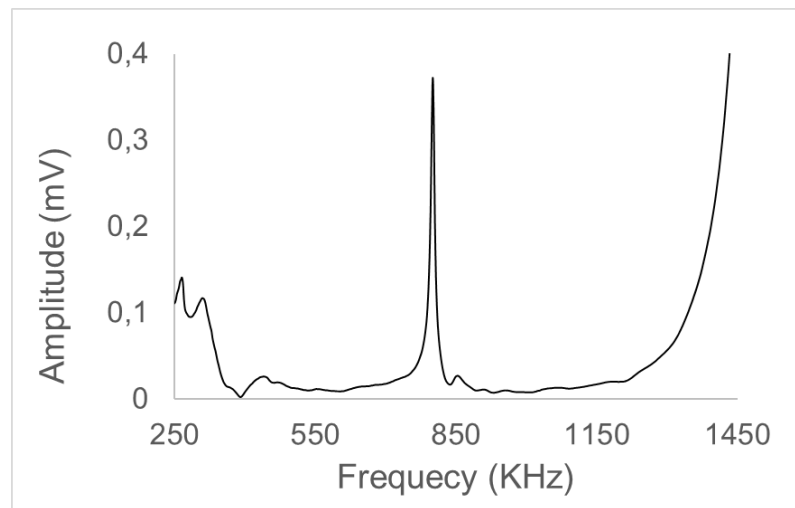


Figure 62 Frequency response of the designed phononic crystal

After evaluating the frequency response of the PnC, another experimental test was conducted to analyse the stabilization process of the phononic crystal biosensor. According to the designed protocol, four measurements, with 5 minutes between each one, were made after adding the BSA to the functionalized resonant cavity. Having the highest concentration, the 5 ug/ml solution has the slowest stabilization time; however, the experimental data showed that the phononic crystal biosensor stabilizes very quickly and that 20 minutes is more than enough to be able to obtain a good performance.

Changing the concentration of the BSA solution that is introduced into the resonant cavity affects the frequency response of the phononic crystal biosensor. An experimental test was performed using four BSA solutions in PBS buffer with a different concentration. The results of this test can be observed in Figure 63. The transmission data was acquired after 20 minutes of having introduced the analyte in the resonant cavity.

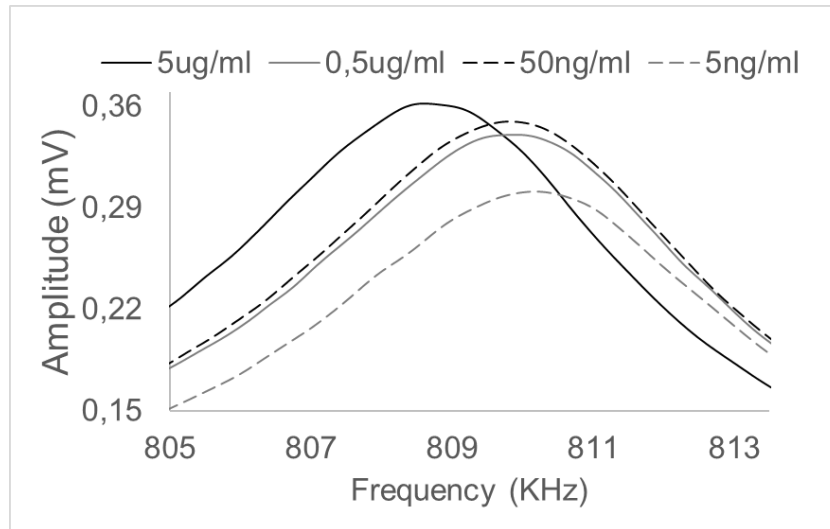


Figure 63 Experimental results of the phononic crystal biosensor using different concentrations of BSA solutions in PBS buffer. The data was acquired 20 minutes after introducing the analyte in the resonant cavity.

A single maximum of transmission is observed for each concentration. Even though the changes in the concentration of the analyte are very small, displacements in the frequency of transmission are visible in the experimental results. Figure 64 shows the frequency of the maximum of transmission at each concentration. When the concentration increases, the frequency of the relevant transmission feature is displaced to lower frequencies. The results are very promising and show that the PnC biosensor has a very high sensitivity. The frequency of maximum transmission displaced itself a total of 1500Hz, which is a considerable displacement considering that other resonant sensors like the QCM produce displacements of a few tens of Hz and with working frequencies of at least 5MHz [124].

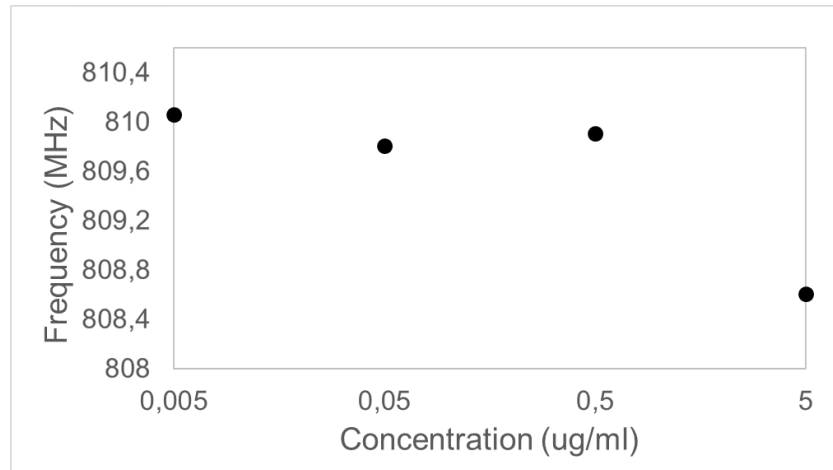


Figure 64 Frequency of maximum transmission of the phononic crystal biosensor using different concentrations of BSA solutions in PBS buffer. The data was acquired 20 minutes after introducing the analyte in the resonant cavity.

The measurements taken after 20 minutes show that the phononic crystal is sensitive enough to be able to detect small changes in the concentration of the analyte. After the 20 minutes, the recognition agent has attached itself to the BSA antibodies. In order to evaluate if this process did in fact occur, a control measurement was taken after washing the resonant cavity five times and finally filling it with a PBS buffer with no BSA in it.

Figure 65 shows how the transmission peak of the 50 ng/mL solution changes after 5 and 20 minutes of introducing the analyte and finally after washing and adding a new PBS buffer. The control measurement with the buffer is located in between the 5 minutes and the 20 minutes measurements. The results obtained with this test, demonstrate that there was an antigen-antibody reaction and that part of the BSA antibodies that were in the solution remained in the phononic crystal after being washed. The same test was performed with the other concentrations with the same effect.

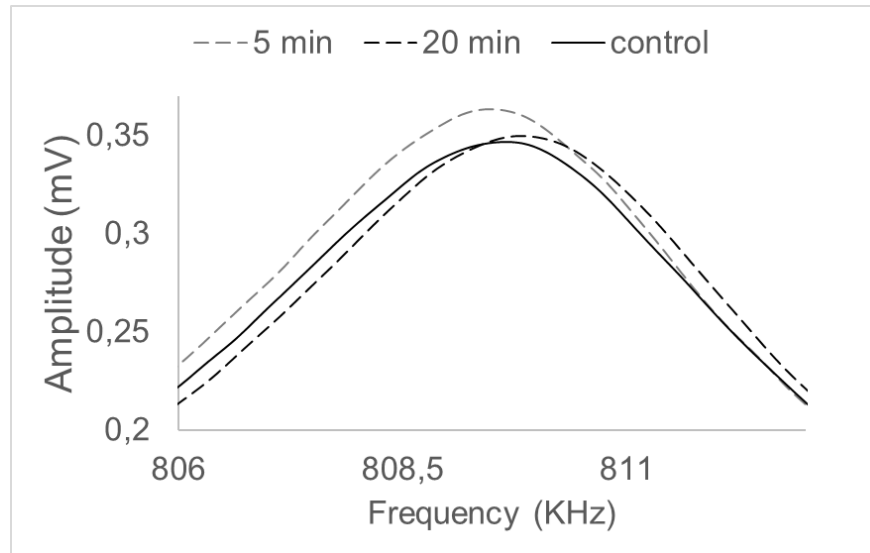


Figure 65 Control measurement of the phononic crystal biosensor with a BSA solution in PBS with a concentration of 50ng/ml.

A new experimental study using more challenging BSA concentrations in PBS buffer was performed. Figure 66 shows the results obtained during this test. Same as in the measurements after the 20 minutes of introducing the analyte, these results show that the concentration decreases with each increase in the frequency of maximum transmission of the phononic crystal. The results show that the crystal still needs to be improved to be able to be used effectively in PoC testing. However, they are very promising since the sensitivity of the PnC biosensor is very high.

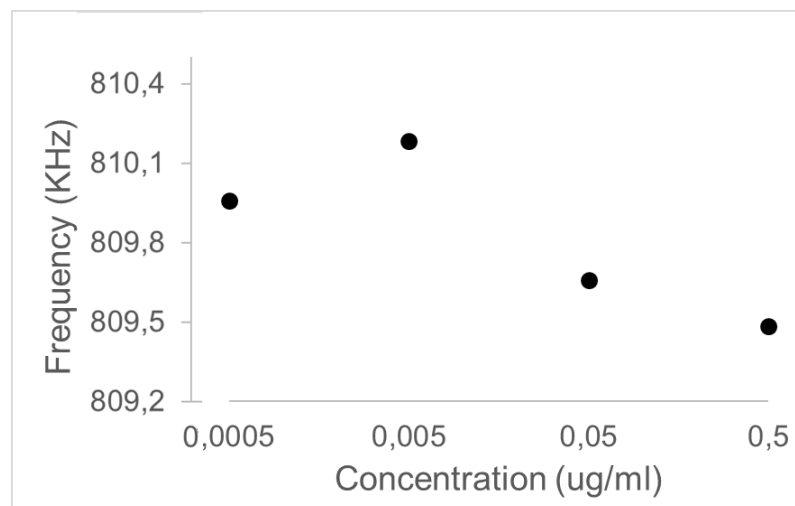


Figure 66 Frequency of maximum transmission of the phononic crystal biosensor using different concentrations of BSA solutions in PBS buffer. The data was acquired after washing the PnC biosensor and introducing PBS in the resonant cavity.

The experimental results show that the narrow transmission band generated by the resonant cavity, which is located in the centre of a conventional phononic bandgap, suffers a displacement in frequency when different concentrations of the anti-BSA solutions in PBS are measured using the phononic crystal biosensor.

10.3 Conclusions

A new phononic crystal biosensor that uses a biorecognition agent and with the capability to measure small changes of a specific protein was presented in this article. The PnC biosensor has a defect layer in the middle configuring a resonant cavity. Experimental results evaluating the performance of the multi-layered phononic crystal biosensor showed that the functionalization of the resonant cavity carrying the analyte of interest is an excellent approach to enhance the specificity of phononic crystal sensors. The confined analyte properties govern the cavity resonance frequency. Thus, small variations in the properties of the analyte can produce displacements in the frequency of maximum transmission of the defect mode in the PnC biosensor.

The modification of the resonant cavity walls makes the PnC to have a high affinity towards a specific protein. Therefore, the changes in frequency are mostly affected by the coupling of the specific protein to the recognition agent and not by other elements present in the sample. The use of a functionalization process opens the possibility of using phononic crystal sensors in applications where target analytes need to be detected in complex mixtures like, e.g., in point of care applications where specific pathogens, and proteins need to be detected in blood or other biological fluids.

The PnC biosensor showed a considerable sensitivity and the relevant transmission features that are used to characterize the sensor have a very high signal to noise ratio, therefore, facilitating the use of simpler electronic characterization systems and enabling their use in field applications.

Ongoing studies focus on improving the functionalization process and the experimental setup in order to improve the repeatability of the measurements and be able to develop real competitive applications with PnC biosensors.

10.4 Summary

In summary, this chapter described the design and development of a new phononic crystal biosensor. Experimental realizations were performed to study the properties and behaviour of the PnC biosensor by using bovine serum albumin antibody diluted in phosphate-buffered saline in different concentrations. The experimental results show that the narrow transmission band generated by the resonant cavity experiences a displacement in frequency when different concentrations are used. The functionalization of the resonant cavity showed to be an excellent approach to enhance the specificity of these type of acoustic sensors and hence, opening the possibility of using phononic crystal sensors in applications were specific pathogens, and proteins need to be detected in blood or other biological fluids.

The next chapter will present an overview of the methods used to simulate the frequency response of phononic crystals.

Chapter 11 - Use of Transient Time Response as a Measure to Characterize Phononic Crystal Sensors

Phononic crystals are periodic composite structures with specific resonant features that are gaining popularity in the field as liquid sensors. The introduction of a structural defect in an otherwise periodic regular arrangement can generate a resonant mode, also called defect mode, inside the characteristic bandgaps of phononic crystals. The morphology, as well as the frequency in which these defect modes appear, can give useful information on the composition and properties of an analyte. Currently, only gain and frequency measurements are performed using phononic crystal sensors. Other measurements like the transient response have been implemented in resonant sensors such as quartz microbalances showing great results and proving to be a great complimentary measure to the gain and frequency measurements [91, 155].

In the present chapter, a study of the feasibility of using the transient response as a measure to acquire additional information about the analyte is presented.

11.1 Materials and Methods

11.1.1 Phononic Crystal Sensor Used

A multi-layered phononic crystal sensor was used to evaluate the utilization of transient time as a measure to characterize phononic crystals. The structure of the phononic crystal is composed of nine layers, and the materials used to build it are glass, distilled water, and lithium carbonate solutions as the analyte. The properties of the layers are shown in Table 10. The generation and acquisition of the mechanical waves are performed using wide bandwidth contact ultrasonic transducers configured as transmitters and receivers as can be seen in Figure 67. These transducers are represented in Table 10 as the outer layers of the crystal and are made of piezoelectric material.

The transducers are considered as having semi-infinite dimensions for the simulations and their resonant frequency is located around 1.1 MHz.

Table 10 Properties of the layers.

Layer #	Material	Speed of sound (m/s)	Density (Kg/m ³)	Thickness (mm)
1	PZT	3333	7500	-
2	Glass	2200	5720	1.25
3	Water	998	1493	1.25
4	Glass	2200	5720	1
5	Analyte			2.5
6	Glass	2200	5720	1
7	Water	998	1493	1.25
8	Glass	2200	5720	1.25
9	PZT	3333	7500	-

The layer thickness of the PZT layers is considered as semi-infinite for the simulation.

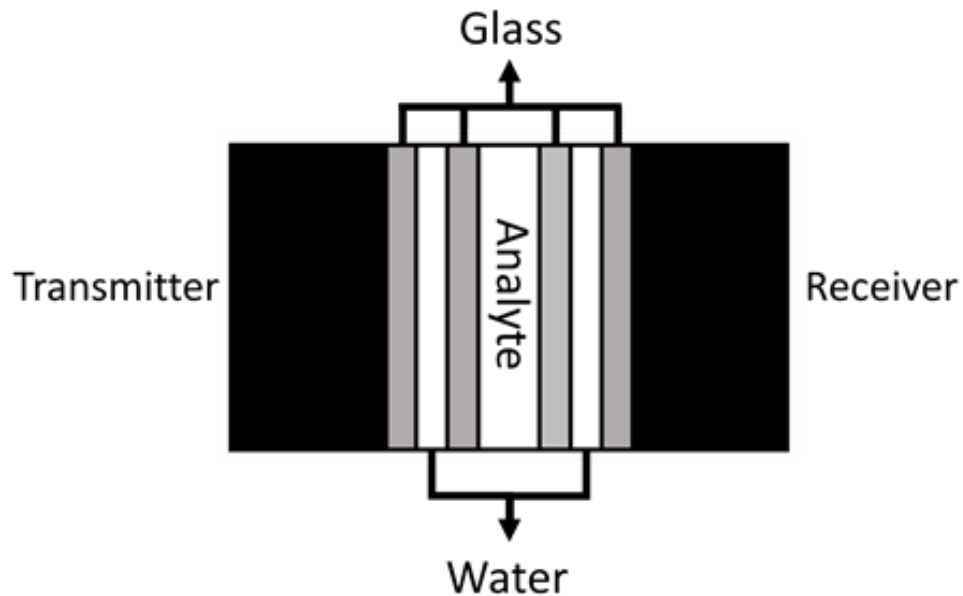


Figure 67 Phononic crystal structure representation.

Lithium carbonate was selected as the analyte since it is a very interesting and challenging PoCT application. Multiple approaches have been used to try and detect it in blood due to its use as a therapeutic means for multiple psychiatric disorders [157 – 159]. The lithium carbonate solutions are made using distilled water and have a very low concentration. Therefore, their longitudinal speed of sound is almost the same as

that of the distilled water. The analyte layer has a layer thickness of two times of that of the water layers so that a defect mode can be introduced in between the bandgap borders. Figure 68 shows the phononic crystal sensor used for the experimental realizations and Figure 69 shows the frequency response of the sensor obtained using the transmission line model.

This simulation method uses a lateral miniaturization of the structure [17] and has been widely used to simulate resonant structures and phononic crystal sensors showing accurate results despite the use of a 1D model [6].



Figure 68 Phononic crystal sensor used for the experimental realizations.

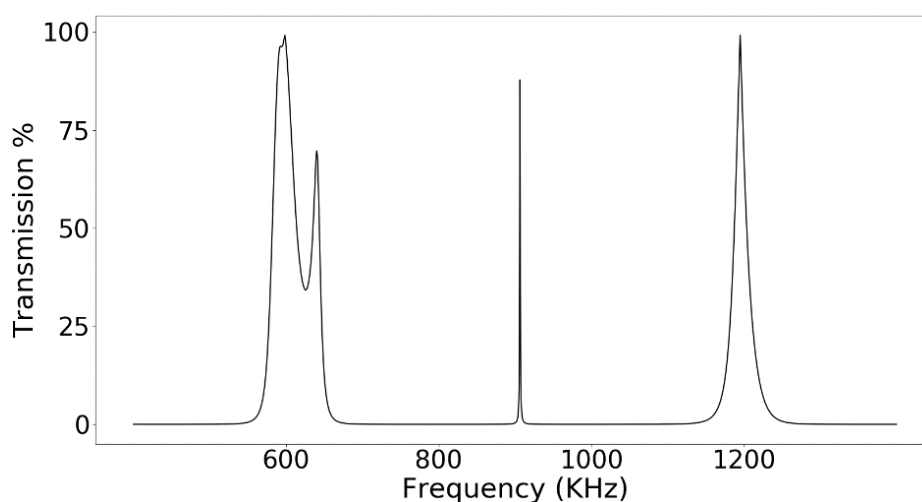


Figure 69 Simulated frequency response of the phononic crystal sensor.

11.1.2. Signal Generation and Acquisition

A Tektronix oscilloscope (TDS 2012B), an AD8302 integrated circuit from Analog devices, and a Tektronix precision signal generator (Tektronix AFG 3101) were used to generate the signal and acquire the response of the system. All the instruments were connected to the computer via USB using an ATmega2560 microcontroller from Atmel. A python code was written to control both the generation and the acquisition of the signal to synchronize the input and output and be able to obtain the transient response of the system. The Tektronix precision signal generator is shut down and both the AD8302 connected to the ATmega2560 microcontroller and the Tektronix oscilloscope continuously record the amplitude of the waves until it reaches zero. Then the time

11.1.3. Solutions Preparations

Lithium Carbonate (Li_2CO_3) solutions at different concentrations were made following the next protocol:

First, different containers were marked and separated depending on each concentration. Then, different amounts of Li_2CO_3 were weighted in a precision scale placing the lithium carbonate powder on top of an aluminium square. The different amounts needed for preparing the solutions were weighted, and finally, they were

introduced in the containers together with the distilled water that was measured using a precision pipette. The different solutions were mixed until the solution was homogenized.

Table 11 Lithium carbonate solutions.

Solution #	Concentration (g/mL)
1	0
2	0.00025
3	0.00125
4	0.0025
5	0.0075
6	0.01125

11.1.4. Protocol for the Tests

For the frequency and transient response tests, the following protocol was used. First, a syringe is used to introduce distilled water into every liquid layer of the phononic crystal shown in Figure 68. Then glycerol was applied as a coupling means between the ultrasonic transducers and the outer glass layers. Without a coupling agent, the signal is mostly attenuated due to the imperfect match of the layers and the air in between. Then connect the transmitter to the Tektronix generator and the receiver to the AD8302 integrated circuit together with a reference generator with a constant gain. Run the python program and watch if the signal is correct. When the sensor and instruments are fully operational, the analyte was carefully deposited in the central layer of the crystal. Each measurement was taken three times, and the phononic crystal was carefully cleaned and dried before each measurement. The tests were performed under a controlled room temperature since changes in temperature could affect the speed of sound of the materials and influence the results of the study.

11.1.5. Signal Processing

The signals were acquired and filtered by a second order low pass Butterworth filter with a cut-off frequency of 400 Hz to eliminate unwanted noise. A high-frequency value was selected as the cut-off frequency of the filter in order to avoid affecting the morphology of the resulting frequency spectra.

11.2 Results and Discussion

11.2.1. Frequency Sweep

The operating frequency of the phononic crystal sensor is between 600 KHz and 1.3 MHz

As shown in Figure 70, running a frequency sweep along the phononic crystal resulted in a rejected band with a very distinct transmission band inside it. The transmission peak located around 1 MHz is generated by the defect mode introduced in the central layer of the phononic crystal. It is well separated from other transmission bands resulting in a significant signal to noise ratio. The solid line represents the resulting spectra using distilled water as the analyte. It is clear how adding a low concentration of lithium carbonate affected the resulting frequency spectra and made the defect mode displace itself to higher frequencies. The total displacement of the resonant mode is about 15 KHz.

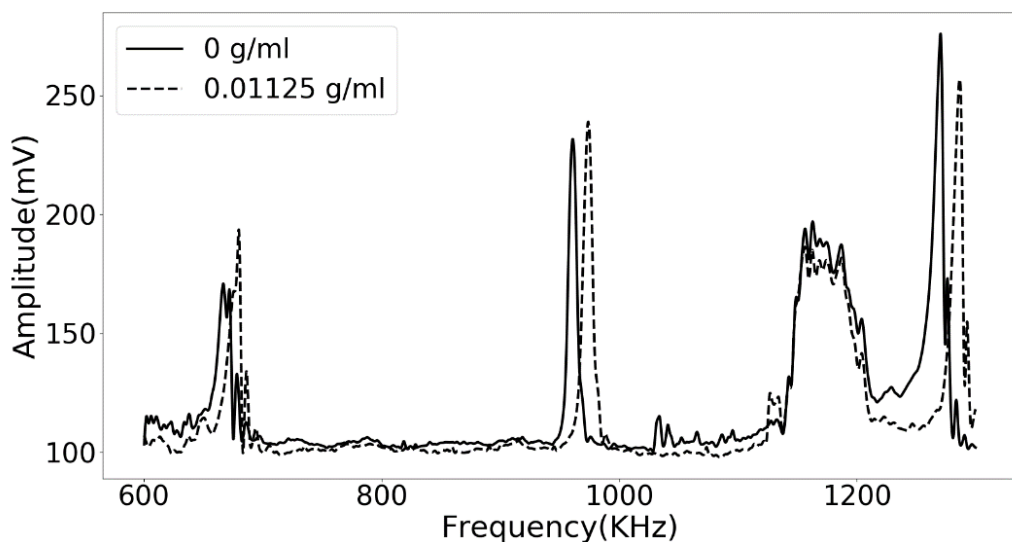


Figure 70 Experimental results of the phononic crystal sensor using distilled water (solid line) and a lithium carbonate solution with a concentration of 0.01125 g/mL (dashed line).

Figure 71 shows a zoomed-in view of the defect mode of the phononic crystal sensor. It is very interesting how changes in the concentration of the lithium carbonate can be

tracked by measuring the frequency of this transmission features, showing the potential of using phononic crystals as sensors and for developing PoCT applications.

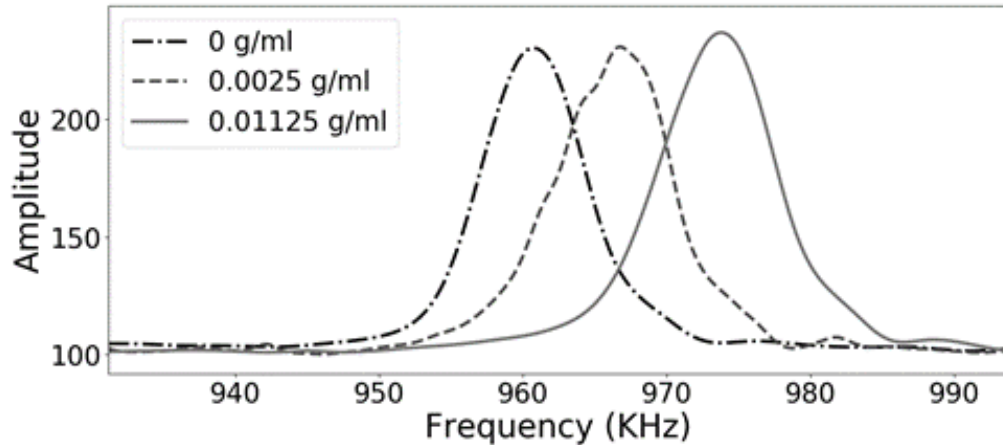


Figure 71 Zoomed-in experimental results of the phononic crystal sensor using distilled water (black dashed and dotted line), and lithium carbonate solutions with a concentration of 0.01125 g/mL (grey solid line) and 0.0025 g/mL (grey dashed line).

11.2.2. Transient Response

In Figure 72, the transient response of the acoustic waves traveling across the phononic crystal sensor at three different concentrations is shown. The system was set to a fixed frequency of 960 KHz, frequency of maximum transmission when using distilled water as the analyte, and the gain was recorded against the time. The generator system is suddenly turned off, and the transient response is obtained. The concentration-dependent damping observed in Figure 72, is related to the displacements in the frequency of the resonant transmission feature located in the middle of the bandgap. Because the amplitude of the starting signal is higher when distilled water is used as the analyte (0 g/mL), the transient response is more extended, and the slope of the signal is more inclined. When the lithium carbonate concentration increases, the initial amplitude is very low, resulting in a shorter decay time and a less steep slope.

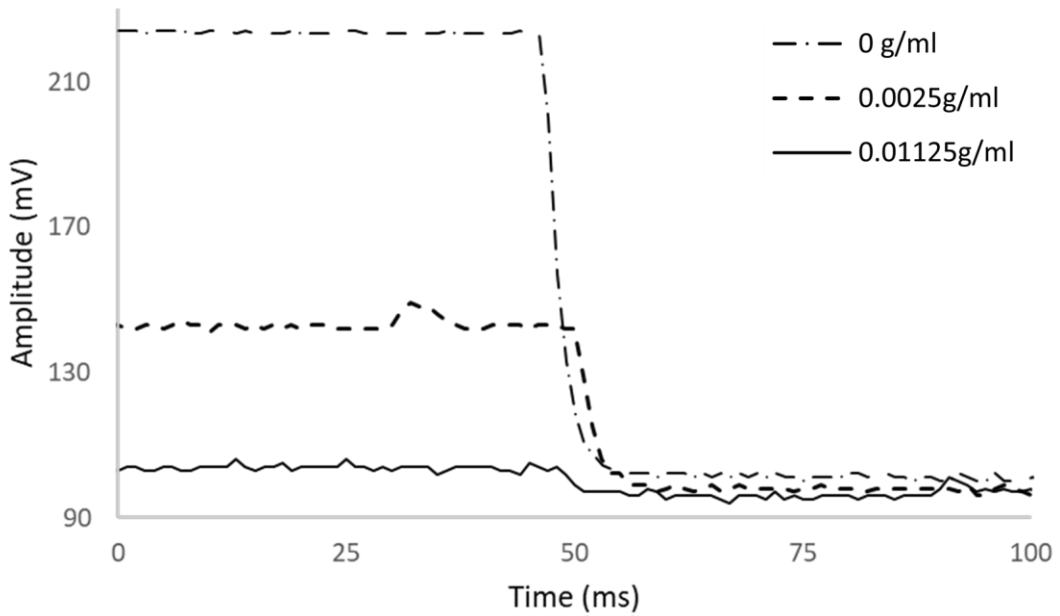


Figure 72 Transient time experimental results of the phononic crystal sensor using distilled water (dashed and dotted line), and lithium carbonate solutions with a concentration of 0.01125 g/mL (solid line) and 0.0025 g/mL (dashed line).

The same experimental realization was performed with the six lithium carbonate solutions that were previously prepared. The decay time of each signal was measured and is shown in Table 12.

Table 12 Decay time at different concentration values.

Concentration (g/mL)	Time (s)
0	0.008750
0.00025	0.008125
0.00125	0.006250
0.0025	0.004375
0.0075	0.002500
0.01125	0.001875

Figure 73 shows how the decay time changes when the concentration of the analyte is varied.

The decay time values show a clear tendency and could be used as a measure to characterize the phononic crystal sensor and retrieve the concentration value of the analyte.

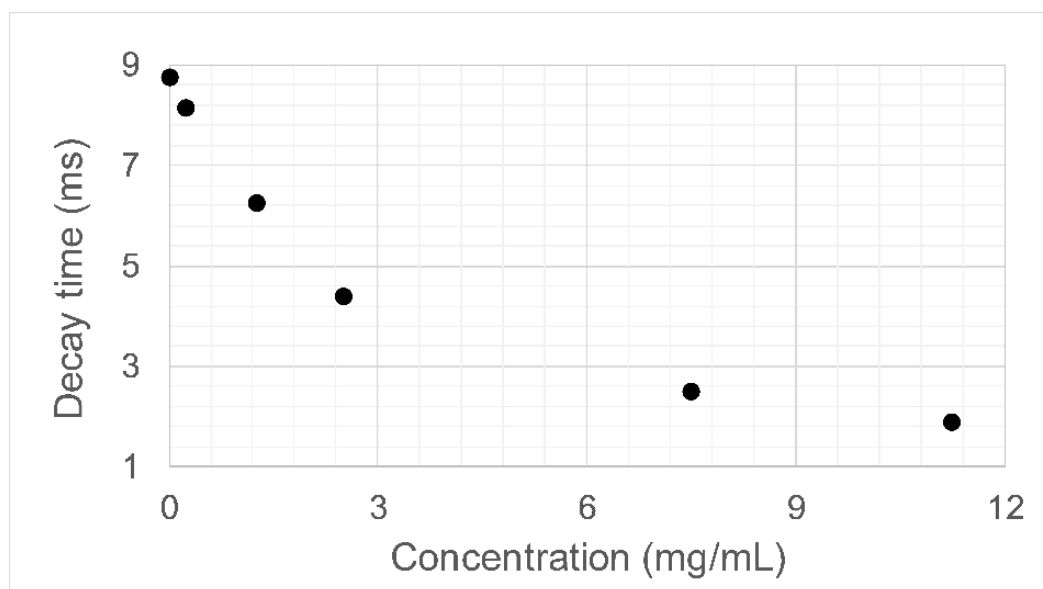


Figure 73 Relationship between the concentration of the lithium carbonate solution used as the analyte and the decay time obtained.

11.3 Conclusions

A phononic crystal sensor that uses the transient response to quantify small changes in the properties of liquid analytes was developed. The sensor was tested using solutions of Lithium Carbonate in distilled water at different concentrations.

The use of a new variable to measure changes in properties of an analyte opens the door to an entirely new type of sensing modality that can complement the traditional gain and frequency measurements that are performed nowadays.

The transient response experimental realizations show that the slope and time decay vary when the concentration of the analyte is modified, allowing its use as a measure in sensing applications.

The experimental results show that the use of phononic crystal sensors for developing PoCT applications for measuring lithium carbonate has a high potential. However, it is essential to take into account that the transmission feature frequency is sensitive to variations in the speed of sound of the sample. Blood is a complex mixture and, therefore, proper care needs to be taken to be able to make the system specific to

changes in the concentration of lithium and avoid false readings due to changes in other elements of the mixture.

11.4 Summary

This chapter presented a study of the use of transient time as a new way of characterising phononic crystal sensors. Theoretical studies using the transmission line model were realized to show the impact of variations in the concentration of an analyte, in this case, lithium carbonate solutions, in the transient time of the system.

Experimental realizations were also performed showing that the proposed measurement scheme presents significant changes in the resulting data, indicating the potential use of this measure in phononic crystal sensors.

12 Discussion

This thesis proposes the utilisation of phononic crystals as point of care sensors, by estimating variations in the speed of sound of small liquid samples. The hypothesis is that by using defect modes and modifying the acoustical properties of the resonant structure, current limitations of phononic crystal sensors could be improved to enable their use in challenging applications like point of care testing. In order to investigate this, both theoretical and experimental realizations were carried out, in which multiple phononic crystal designs were developed and discussed under various testing settings.

In order to acquire the phononic crystal frequency response needed to understand its behaviour, an electronic characterisation system was designed and developed. The acoustic waves were generated and acquired using two wideband ultrasonic transducers having central frequencies around 1MHz. The system was designed to acquire the frequency response of the phononic crystal and perform a series of mathematical operations in which both the signal that was fed into the PnC and the resulting signal were used to obtain relevant information about the behaviour in frequency of the phononic crystal.

A software application, developed in Matlab, was used to simulate the frequency response of phononic crystal sensors. The simulator was developed using a lateral miniaturisation of the structure and the transmission line model. This software was used to design and evaluate the different phononic crystal sensors studied in this research work [17].

The theoretical investigations realized in chapter 5 showed interesting insights into the characteristics that need to be taken into account to design and develop phononic crystal sensors as shown below:

- Displacing the defect mode to frequencies nearer the bandgap border allow to decrease the quality factor of the transmission peak maintaining the sensitivity of the system. This effect is of importance in design were the losses are too high with the defect mode located in the middle of the bandgap. The losses are

higher when the effect of the bandgap is larger, and this can be translated in a higher quality factor in the simulations.

- Lower impedance mismatch is another way to lower the effect of the bandgap, however, this approach presents a decline in the sensitivity of the system, which is usually not negotiable when designing point of care sensors.
- The use of overtones is a good alternative to design larger structures, maintaining the frequency of operation of the phononic crystal and also the sensitivity. The bandgap width is largely affected but most applications don't require a very large bandwidth in the bandgap.
- Increasing the width of the layers composing the bandgap produces a higher quality factor, which can result in significant losses in experimental realizations, therefore, not only materials with good impedance mismatch should be used, but also having layer thickness that is not too large.
- Using a larger overtone in the analyte layer, results in an increase in sensitivity, while using a larger overtone in the bandgap layers, results in a decrease. This means that the ratio between the analyte and bandgap overtones is important to maintain a high sensitivity.
- Contrary to what is commonly thought, additional layers added to the PnC don't affect the sensitivity. The careful selection of the layers needs to be done in order to have adequate boundary conditions that result in a useful transmission peak that can be tracked in frequency with sufficient resolution.
- Asymmetric structures result in a great attenuation of the defect mode, thus impeding their use in sensing applications.

The development of novel sensing technologies that can be implemented in application such as point of care sensing is vital to improve health conditions in the global population. The increasing life span of people and the rapid increase of treatment

methods makes it more important to be able to detect diseases and risk factors at early stages. [1 - 4]

Resonant technologies like phononic crystals arise as one of the most promising alternatives to develop new point of care tests. Some of their most interesting qualities, that arise from the unprecedented control of waves traveling through periodic composite materials, are listed below:

- Wide variety of designs with several measurement setups
- Can be scaled with respect to application requirements
- Robust for harsh environments
- Measure acoustic properties instead of optical or electrochemical bringing new information of the samples.

Although the use of phononic crystals as sensors has already been studied in previous investigations [6], they are still in very early stages of research and multiple limitations arise when challenging sensing applications like point of care tests are to be developed using these novel resonant sensors.

Biomedical applications, such as point of care testing deal most of the time with biofluids. The use of blood, saliva or urine among other typical biofluids requires a special care of the sample and the materials that enter in contact with it. Typical PoCT devices are composed of two parts, a main unit having all the electronics and processing capabilities, and a sensor chip. The sensor chip is the only element that enters in contact with the analyte and can either be discarded or appropriately sterilized after the test is performed [7]. Phononic crystals structures investigated so far consist mainly of materials that are not compatible with regulations and are designed in geometries and topologies that difficult their compliance with the required hygiene specifications [57, 141].

The utilisation of a multi-layered structure with a central defect mode to generate a frequency traceable transmission band can be designed having a disposable element to

isolate the biofluid sample from the rest of the sensor system. This concept presented in chapter 6 and used again in chapter 7 comprises 3 main elements; a main unit having the circuitry and the electronic transducers to enable the generation, acquisition and processing of the signals, a phononic crystal for controlling the transmission of waves throughout the structure, and a sensor chip composed of a glass cuvette which contains the sample and, through a defect mode, enables the creation of a relevant transmission characteristic that is related to the properties of the sample. The results obtained using this configuration were very promising and showed that the analyte properties could be measured while keeping it isolated from the rest of the structure. The experimental realizations also studied modifying the standard acoustic coupling, which is glycerol, for additional liquid phononic crystal layers, in this case water. Despite the positive results, the water layers and the geometry of the phononic crystal presented in chapter 7 presented issues with the resulting frequency spectrum. These issues were related to the structure being far from a multi-layered phononic crystal or superlattice, therefore, having a different behaviour than the results expected from the transmission line model which uses a reduction in the dimensionality [17].

The analyte consumption and portability of current phononic crystal sensors is still far from ideal to develop field applications and use biological fluids as samples. The availability of these samples is usually very limited, and the sensor should be as small as possible to be able to carry it everywhere. This research presented an electronic characterization system that can replace bulky equipment such as impedance analyzers, network analyzers and high frequency lock-in amplifiers. Along with the measurement equipment, chapter 8 presents an alternative sensor which is completely disposable after its use. The sensor can be 3D printed and the materials used take into account the lessons learned from the theoretical study performed in chapter 5. The phononic crystal structure designed uses an overtone to be able to manufacture the structure with larger dimensions and still obtain bandgaps and defect modes in the frequencies of interest. The experimental results are remarkable and well according to the simulations using the transmission line model. The large difference between these results and the previous ones relies on the geometry of the crystal. This time the structure had larger lateral dimensions than the width of the layers, causing the PnC to behave more similar to a 1D structure. These results showed the large potential of phononic crystal sensors to be used as liquid sensors given the flexibility on the design

and robustness. The applications that are most appealing are those where in-situ measurements of small liquid samples are required.

The use of defect modes showed to be a good approach to design transmission bands that, when the analyte is located in the defect layer, can be used to track the speed of sound of samples under test. One of the large differences of phononic crystals with other resonant sensors like the quartz crystal microbalance is that they measure volumetric properties of liquid samples instead of interfacial changes. This difference enables the design of sensors in which the transducer is isolated from the sample. This characteristic also presents a challenge and it's that the PnC obtain a speed of sound value that is related to a mixture inside the defect layer and not of a specific component of the mixture. This is not a problem when binary mixtures are characterized, however, when complex mixtures are used as samples, like most biofluids, the identification of specific compounds inside the mixture is practically impossible at this frequency ranges and with the current sensing modality. [124, 153]

Biosensors have been widely used to measure specific analytes in complex mixtures. The detection of biomarkers is mostly based on the enhancement of the surface of a transducer with a biorecognition agent that react to the presence of specific compounds in the sample. QCM biosensors make use of this methodology and enable the resonant sensors to measure with very high sensitivity and resolution multiple biomarkers. QCM biosensors are however far from being implemented in real field applications to their large dependence on a controlled environment. Temperature plays a big role in the acoustic properties of materials and state of the art QCM work at 50MHz or even 100MHz which are very challenging frequencies to work with when temperature fluctuations are present. [124, 153]

This research presented an alternative phononic crystal structure that uses additional defect modes to create a transmission band that can be used as reference. Conventional modalities to cancel the effects of temperature use complex environment control units or reference samples. The current solutions imply higher costs and complicated or bulky equipment. The proposed differential phononic crystal has a fundamental difference and is that it obtains all the relevant transmission information related to the analyte and the reference from the same PnC structure and using a single frequency

sweep. This model can not only be used as a temperature compensation mechanism for phononic crystals but also for other resonant structures that make use of transmission features to develop sensing applications. [151]

In spite of the differential measurement, phononic crystal sensors still need binary mixtures to be able to characterize a sample. This thesis presented and discussed in chapter 10 a phononic crystal biosensor that can detect a target molecule in a complex mixture through the surface modification of a resonant cavity, in this case the defect layer, adding a biorecognition agent to the glass that attaches itself to a target molecule when is present in the sample. This attachment converts itself into a new layer of the crystal and modifies its frequency response. This is the first experimental realization of a multi-layered phononic crystal biosensor. The results are very promising and along with the other results of the thesis show that phononic crystals are a viable alternative to develop point of care testing devices.

13 Conclusions and Future Work

This chapter concludes this research thesis by summarising the main results and linking them to the initial aims and objectives. Whereas some suggestions for the improvement of the methodologies used and the phononic crystals developed have been given in the Discussion chapter, concluding suggestions on the direction of future work will also be given at the end of this chapter.

This thesis aimed to investigate the feasibility of using phononic crystals as liquid sensors for biomedical applications, especially for developing point of care devices. In order to do so, theoretical and experimental investigations using multiple PnC sensor designs were carried out, each one of them aiming at solving previously identified barriers or limitations of current state of the art.

Along with multiple phononic crystal structures, an electronic characterisation system was designed and manufactured for the generation and acquisition of ultrasonic signals that were used to characterise the phononic crystal sensors using different analytes.

The developed phononic crystals were successfully utilised as sensors and present viable solutions to overcome the limitations present in the state of the art. The characteristics of the developed sensors are the multi-layered design, resembling a 1D model, and the successful introduction of relevant transmission features inside the bandgap by using the symmetry reduction technique that allowed the acquisition of the speed of sound of liquid samples under test by tracking changes in their frequency.

The transmission line model was effectively used to simulate and understand the behaviour of phononic crystal sensors. Furthermore, it was also used for designing the novel sensors that were investigated in this work.

A theoretical study using the TLM allowed to obtain essential insights for the design of phononic crystal sensors. The study analysed the effect that geometrical and material parameters have on bandgap engineering and how they could be best used for designing sensors. Overtones were also investigated in this study and it was found that

their use is favourable to develop sensors with high frequencies even when using larger dimensions.

Two alternative models of point of care phononic crystal sensor are presented on this work. The first alternative consists of a main unit that encloses all the electronics and transducers needed for the generation and acquisition of the signals. This main unit is connected to a phononic crystal structure whose only function is to generate adequate boundary conditions for measuring a relevant transmission peak that is generated by the third element of the system; the analyte container that is located in the middle of the phononic crystal and that introduces a disruption in symmetry that allows the generation of the transmission peak that is located inside the bandgap. The analyte container can be understood as a sensor chip that can be either discarded or sterilized after each test. The analyte container used in this work is a glass cuvette and during the experimental realizations it showed great results with transmission spectra that clearly presented a transmission peak well differentiated from the bandgap and whose frequency was governed by the speed of sound of the analyte. The second alternative consists of the same main unit connected to a single sensor chip containing both the phononic crystal and the analyte cavity. The second alternative explores a disposable phononic crystal sensors that is both easy to manufacture and low cost.

The investigations performed to reduce the effect of varying the temperature in phononic crystal sensors resulted in a temperature compensation mechanism that uses multiple transmission modes generated by three symmetric defects introduced in an otherwise periodic phononic crystal structure. The compensation of the effect of temperature is done using one of the transmission modes as reference and measuring the frequency changes with respect to it. When temperature varies, all the transmission relevant peaks suffer a displacement in frequency that is almost equal, however, when only the analyte suffers a modification in its speed of sound due to the presence of a protein or compound of interest, only two of the relevant transmission peaks are displaced in frequency and the reference peak stays in its position. This effect enables cancelling the effect of temperature and other unwanted ambient alterations allowing the use of phononic crystal sensors in field applications where temperature might be variable.

Since the use of phononic crystal sensors strongly depends on having applications where samples are composed of binary mixtures in which the sensors detect variations on the concentration of their components that can be easily tracked using the speed of sound of the sample, their introduction to point of care tests was very complicated and required prior preparation of the samples. In order to overcome this barrier this thesis presents a phononic crystal biosensor that through the functionalization of the resonant cavity that contains the analyte enables the detection of specific molecules inside complex mixtures, thus, permitting the use of phononic crystals in point of care tests. The results show that the use of a biorecognition agent is feasible to modify the properties of the defect layer when the target compound is present in the sample.

The proposed future work is focused on conducting additional experimental investigations with challenging analytes (e.g. lithium, glucose, lactate, cholesterol, or cortisol) in complex mixtures (e.g. blood, saliva, urine or cerebrospinal fluid). It is also encouraged to explore the combination of phononic crystal sensors with other optical and electrochemical sensors. Phononic crystal sensors introduce a fundamentally different sensing principle and it could prove positive to combine its results with the ones of other sensing principles in challenging applications. One of the main advantages of using this technology is that the analyte doesn't need to enter in contact with the transducers, giving them the possibility to be implemented in a wide range of applications. It is also encouraged to develop fully 3D printed phononic crystals which will facilitate its manufacture and implementation in point of care testings.

This research explored the use of transient time response as an additional measure for characterising phononic crystals. The results showed that it is related to the properties of the liquid sample and that it could be used in applications where the wideband characterisation is not needed, therefore, reducing the cost and complexity of the characterisations system. It is recommended for future works that further variables, such as phase, can be explored to evaluate their implementation for the characterisation of the sensors. Higher frequencies should also be evaluated in order to increase the sensitivity of the tests.

Concluding, the novel results presented in this thesis demonstrate that the full capabilities of phononic crystal sensors are still not fully exploited and the range of

applications of these resonant structures may be successfully extended beyond its current limits and applications.

References

- [1] Bronzino, J. D. (2000). *The Biomedical Engineering Handbook* (Vol. 1). Boca Raton: CRC PRESS IEEE PRESS.
- [2] E. Casis and J. Bedini, "Bases para la discusión en la implantación del point of care testing (POCT)," in *Sociedad Española Dirección Gestión de Laboratorios Clínicos (SEDIGLAC)*, Madrid, Spain, 2002.
- [3] V. Gubala, L. F. Harris, A. J. Ricco, M. X. Tan, and D. E. Williams, "Point of care diagnostics: Status and future," *Anal. Chem.*, vol. 84, pp. 487–515, Dec. 2011.
- [4] G. L. Cote, R. M. Lec, and M. V. Pishko, "Emerging biomedical sensing technologies and their applications," *IEEE Sensors J.*, vol. 3, no. 3, pp. 251–266, Jun. 2003.
- [5] M. M. Sigalas and E. N. Economou, "Elastic and acoustic wave band structure," *Journal of Sound and Vibration*, vol. 158, no. 2, pp. 377–382, 1992.
- [6] Lucklum, R., Li, J.: Phononic crystals for liquid sensor applications. *Meas. Sci. Technol.* 20, 124014 (2009)
- [7] Luppá, P. B., Müller, C. Schlichtiger, A. Schlebush, H. Point-of-care testing (POCT): Current techniques and future perspectives. *TrAC Trends in Analytical Chemistry*, Volume 30, Issue 6, p. 887-898, June 2011.
- [8] Kushwaha M.S., Halevi P., Dobrzynski L., and Djafari-Rouhani B. Acoustic band structure of periodic elastic composites. *Physical Review Letters*, 71(13):2022-2025, September 1993.
- [9] J.-F. Robillard, O. Bou Matar, J. O. Vasseur, P. A. Deymier, M. Stippinger, A.-C. Hladky-Hennion, Y. Pennec, and B. Djafari-Rouhani. "Tunable magnetoelastic phononic crystals". In: *Applied Physics Letter* 95 (2009), p. 124104 (cit. on pp. 16, 31, 32, 77).

- [10] Yeh, J.-Y. (2007) \Control analysis of the tunable phononic crystal with electrorheological material," *Physica B: Condensed Matter*, 400(1-2), pp. 137-144.
- [11] ELBOUDOUTI, E. (2009). Acoustic waves in solid and fluid layered materials. *Surface Science Reports*, 64(11), 471-594. <http://dx.doi.org/10.1016/j.surfrep.2009.07.005>
- [12] G. Floquet. Sur les équations différentielles linéaires à coefficients périodiques. *Annales scientifiques de l'École Normale Supérieure*, 1:181-238, 1883.
- [13] F. Bloch. Über die quantenmechanik der elektronen in kristallgittern. *Zeitschrift für Physik*, 52(7-8):555-600, 1929.
- [14] J. O. Vasseur, P. A. Deymier, G. Frantziskonis, F. Hong, B. Djafari-Rouhani, and L. Dobrzynski. Experimental evidence for the existence of absolute acoustic bandgaps in two-dimensional periodic composite media. *Journal of Physics: Condensed Matter*, 10(27):6051-6064, 1998.
- [15] E.N. Economou, M.M. Sigalas, Classical wave propagation in periodic structures: cermet versus network topology. *Phys. Rev. B* 48, 13434 (1993)
- [16] Aravantinos-Zafiris, N., Sigalas, M., Kafesaki, M., & Economou, E. (2014). Phononic crystals and elastodynamics: Some relevant points. *AIP Advances*, 4(12), 124203. <http://dx.doi.org/10.1063/1.4904406>
- [17] R. Lucklum, C. Behling, R. Cernosek, S. Martin, "Determination of complex shear modulus with thickness shear mode resonators", *Journal of Applied Physics*, pp. 346-356, 1997.
- [18] I. Newton, *Principia*, Book II, 1686.
- [19] Brillouin. *Wave Propagation in Periodic Structures*. American Institute for Aeronautics, 1946.
- [20] H. Levine. Reflection and transmission by layered periodic structures. *Quarterly Journal of Mechanics and Applied Mathematics*, 14(1):107-122, 1966.

- [21] C. Rorres. Transmission coefficients and eigenvalues of a finite one-dimensional crystal. *SIAM Journal on Applied Mathematics*, 27(2):303-321, 1974.
- [22] V. Narayanamurti, H. L. Störmer, M. A. Chin, A. C. Gossard, and W. Wiegmann. "Selective Transmission of High-Frequency Phonons by a Superlattice: The "Dielectric" Phonon Filter". In: *Phys. Rev. Lett.* 43.27 (1979), pp. 2012–2016
- [23] Bragg, W.H.; Bragg, W.L. (1913). "The Reflexion of X-rays by Crystals". *Proc R. Soc. Lond. A* 88 (605): 428–38. Bibcode:1913RSPSA..88..428B. doi:10.1098/rspa.1913.0040. (Free access)
- [24] J.D. Achenbach, M. Kitahara, "Harmonic waves in a solid with a periodic distribution of spherical cavities", *J. Acoust. Soc. Am.* 81(3), 595 (1987).
- [25] Yablonovitch E. Inhibited spontaneous emission in solid-state physics and electronics. *Physical Review Letters*, 58(20):2059-2062, May 1987.
- [26] J. Sajeev. Strong localization of photons in certain disordered dielectric superlattices. *Physical Review Letters*, 58(23):2486-2489, 1987.
- [27] Ralf Lucklum & Mikhail Zubtsov & Aleksandr Oseev. Phoxonic crystals—a new platform for chemical and biochemical sensors. *Anal Bioanal Chem* (2013) 405:6497–6509.
- [28] Ma, T., Wang, Y., Zhang, C., & Su, X. (2016). Theoretical research on a two-dimensional phoxonic crystal liquid sensor by utilizing surface optical and acoustic waves. *Sensors And Actuators A: Physical*, 242, 123-131. <http://dx.doi.org/10.1016/j.sna.2016.03.003>
- [29] Martinez-Sala R., Sancho J., Sanchez J.V., Gomez V., Llinares V., and Meseguer J.F. Sound attenuation by sculpture. *Nature*, 378:241, November 1995.
- [30] M. M. Sigalas and E. N. Economou, *Europhys. Lett.* 36,241 (1996).
- [31] Kushwaha M. Stop-bands for periodic metallic rods: Sculptures that can filter noise. *Applied Physics Letters*, 70(24):3218-3220, June 1997.

- [32] Kushwaha M.S. and Djafari-Rouhani B. Sonic stop-bands for periodic arrays of metallic rods: Honeycomb structure. *Journal of Sound and Vibration*, 218(4):697-709, 1998.
- [33] Robertson W.M. and Rudy J.F. Measurement of acoustic stop bands in two dimensional periodic scattering arrays. *Journal of the Acoustic Society of America*, 104(2):694{699, August 1998.
- [34] Arte en Madrid, Eusebio Sempere en la vanguardia, <https://artedemadrid.wordpress.com/2010/03/24/eusebio-sempere-en-la-vanguardia/> (Accessed: 1 sept 2016).
- [35] Montero de Espinosa F. R., Jimenez E., and Torres M. Ultrasonic bandgap in periodic two-dimensional composite. *Physical Review Letters*, 80(6):1208-1211, February 1998.
- [36] Sanchez-Perez J.V., Caballero D., Martinez-Sala R., Rubio C., Sanchez-Dehesa J., Meseguer F., Llinares J., and F. F., Galvez. Sound attenuation by a two dimensional array of rigid cylinders. *Physical Review Letters*, 80(24):5325-5328, June 1998.
- [37] Kushwaha M.S. and Halevi P. Bandgap engineering in periodic composites. *Applied Physics Letters*, 64(9):1085-1087, February 1994.
- [38] Kushwaha M.S., Halevi P., and Martinez G. Theory of acoustic band structure of periodic elastic composites. *Physical Review B*, 49(4):2313-2322, January 1994.
- [39] M.S. Kushwaha, P. Halevi, "Ultrawideband Filter for Noise Control", *Jpn. J. Appl. Phys.* 36, L 1043 (1997).
- [40] Rubio C., Caballero D., Sanchez-Perez J.V., Martinez-Sala R., Sanchez-Dehesa J., Meseguer F., and Cervera F. The existence of full gaps and deaf bands in two dimensional sonic crystals. *Journal of Lightwave Technology*, 17(11):2202-2207, November 1999.
- [41] Goffaux, C. and J. P. Vigneron (2001) \Theoretical study of a tunable phononic bandgap system," *Physical Review B*, 64(7), p. 075118.

- [42] Sigalas M.M. and Economou E.N. Band structure of elastic waves in two dimensional systems. *Solid State Communications*, 186(3):141-143, 1993.
- [43] Kafesaki M., Sigalas M.M., and Economou E.N. Elastic wave bandgaps in 3D periodic polymer matrix composites. *Solid State Communications*, 96(5):285-289, 1995.
- [44] Kee C., Kim J., Park H.Y., and Chang K.J. Essential role of impedance in the formation of acoustic bandgaps. *Journal of Applied Physics*, 87(4):1593-1596, February 2000.
- [45] M. S. Kushwaha. Classic band structure of periodic elastic composites. *International Journal of Modern Physics B*, 10(9):977-1094, 1996.
- [46] Kushwaha M.S. and Djarfari-Rouhani B. Complete acoustic stop bands for cubic arrays of spherical liquid balloons. *Journal of Applied Physics*, 80(6):3191-3195, September 1996.
- [47] Weimin Kuang, Zhilin Hou, Youyan Liu, "The effects of shapes and symmetries of scatterers on the phononic bandgap in 2D phononic crystals", *Physics Letters A* 332 (2004) 481-490
- [48] Zhengyou Liu, Xixiang Zhang, Yiwei Mao, Y. Y. Zhu, Zhiyu Yang, C. T. Chan and Ping Sheng, *Science* 289,1734 (2000). Locally Resonant Sonic Materials
- [49] Z. Liu, C.T. Chan, P. Sheng, "Three-component elastic wave bandgap material", *Phys. Rev. B* 65, 165116 (2002); Z. Liu, C.T. Chan, P. Sheng, "Analytic model of phononic crystals with local resonances", *Phys. Rev. B* 71, 014103 (2005).
- [50] S. Yang, J.H. Page, Z. Liu, M.L. Cowan, C.T. Chan, P. Sheng, "Focusing of Sound in a 3D Phononic Crystal", *Phys. Rev. Lett.* 93, 024301 (2004).
- [51] X. Zhang, Z. Liu, "Negative refraction of acoustic waves in two-dimensional phononic crystals", *Appl. Phys. Lett.* 85, 341 (2004).

- [52] C. Luo, S.G. Johnson, J.D. Joannopoulos, J.B. Pendry, "All-angle negative refraction without negative effective media", *Phys. Rev. B* 65, 201104(R) (2002).
- [53] C. Qiu, X. Zhang, Z. Liu, "Far-field imaging of acoustic waves by a twodimensional sonic crystal", *Phys. Rev. B* 71, 054302 (2005).
- [54] M. Ke, Z. Liu, C. Qiu, W. Wang, J. Shi, "Negative refraction imaging with twodimensional phononic crystals", *Phys. Rev. B* 72, 064306 (2005).
- [55] J. Li, Z. Liu, C. Qiu, "Negative refraction imaging of acoustic waves by a twodimensional three-component phononic crystal", *Phys. Rev. B* 73, 054302 (2006).
- [56] A. Hakansson, F. Cervera, J. Sanchez-Dehesa, "Sound focusing by flat acoustic lenses without negative refraction", *Appl. Phys. Lett.* 86, 054102 (2005).
- [57] R. H. Olsson III and I. El-Kady. "Microfabricated phononic crystal devices and applications". In: *Measurement science and technology* 20 (2009), p. 012002 (cit. on pp. 15, 16, 29–31).
- [58] Ramprasad R. and Shi N. Scalability of phononic crystal heterostructures. *Applied Physics Letters*, 87(11):1{3, 2005.
- [59] El-Kady I., Olsson III R.H., and Flemin J.G. Phononic bandgap crystals for rf communications. *Applied Physics Letters*, 92(23), 2007
- [60] Mohammadi S., Eftekhar A.A., Khelif A., Hunt W.D., and Adibi A. Evidence of large high frequency complete phononic bandgaps in silicon phononic crystal plates. *Applied Physics Letters*, 92, 2008.
- [61] T. Gorishnyy. "Hypersonic phononic crystals". PhD thesis. Department of Materials Science and Engineering at the Massachusetts Institute of Technology, 2007 (cit. on pp. 15, 31).
- [62] M. Torres, F. R. Montero de Espinosa, D. Garcia-Pablos and N. Garcia, *Phy. Rev. Lett.* 82,3054 (1999).

- [63] M. Torres, F.R. Montero de Espinosa and J. L. Aragon, *Phys. Rev. Lett.* 86, 4282(2001).
- [64] Sigalas M.M. Defect states of acoustic waves in a two-dimensional lattice of solid cylinders. *Journal of Applied Physics*, 84(6):3026{3029, September 1998.
- [65] Caballero, D., J. Sánchez-Dehesa, C. Rubio, R. Martínez-Sala, J. V. Sánchez-Pérez, F. Meseguer, and J. Llinares (1999) \Large twodimensional sonic bandgaps," *Physical Review E*, 60(6), pp. R6316-R6319.
- [66] James R., Woodley S.M., Dyer C.M., and Humphrey V.F. Sonic bands, bandgaps, and defect states in layered structures-theory and experiment. *Journal of the Acoustic Society of America*, 97(4):2041-2047, April 1995.
- [67] J.N. Munday, C.B. Bennet, W.M. Robertson, "Bandgaps and defect modes in periodically structures waveguides",/. *Acoust. Soc. Am.* 112(4), 1353 (2002).
- [68] Psarobas, I. E., N. Stefanou, and A. Modinos (2000) \Scattering of elastic waves by periodic arrays of spherical bodies," *Physical Review B*, 62(1), pp. 278-291.
- [69] Psarobas I.E. and Stefanou N. Phononic crystals with planar defects. *Physical Review B*, 62(9):5536{5540, September 2000.
- [70] A. Khelif, A. Choujaa, B. Djafari-Rouhani, M. Wilm, S. Ballandras, V. Loude, "Trapping and guiding of acoustic waves by defect modes in a full-bandgap ultrasonic crystal", *Phys. Rev. B* 68, 214301 (2003).
- [71] A. Khelif, P.A. Deymier, B. Djafari-Rouhani, J.O. Vasseur, L. Dobrzynski, "Twodimensional phononic crystal with tunable narrow pass band: Application to a waveguide with selective frequency",/. *Appl. Phys.* 94, 1308 (2003).
- [72] A. Khelif, A. Choujaa, S. Benchabane, B. Djafari-Rouhani, V. Loude, "Guiding and bending of acoustic waves in highly confined phononic crystal waveguides", *Appl. Phys. Lett.* 84, 4400 (2004);

- [73] Y. Pennec, B. Djafari-Rouhani, J.O. Vasseur, A. Khelif, P.A. Deymier, "Tunable filtering and demultiplexing in phononic crystals with hollow cylinders", *Phys. Rev. E* 69, 046608 (2004).
- [74] Bertoldi, K. and M. C. Boyce (2008) \Mechanically triggered transformations of phononic bandgaps in periodic elastomeric structures," *Physical Review B*, 77(5), p. 052105.
- [75] Yang, W.-P., L.-Y. Wu, and L.-W. Chen (2008) \Refractive and focusing behaviours of tunable sonic crystals with dielectric elastomer cylindrical actuators," *Journal of Physics D: Applied Physics*, 41(13), p. 135408.
- [76] Yang, W.-P. and L.-W. Chen (2008) \The tunable acoustic bandgaps of two-dimensional phononic crystals with a dielectric elastomer cylindrical actuator," *Smart Materials and Structures*, 17(1), p. 015011.
- [77] X. Li and Z. Liu, "Bending and branching of acoustic waves in twodimensional phononic crystals with linear defects," *Phys. Lett, A* 338, pp. 413-419, March 2005.
- [78] X. Li and Z. Liu, "Coupling of cavity modes and guiding modes in twodimensional phononic crystals," *Solid State Commun.*, 133, pp. 397- 402, Febr. 2005.
- [79] V. Laude, L. Robert, W. Daniau, A. Khelif, and S. Ballandras, "Surface acoustic wave trapping in a periodic array of mechanical resonators," *Appl. Phys. Lett.*, 89, pp. 083515, Aug. 2006.
- [80] Sigalas M.M. and Economou E.N. Elastic waves in plates with periodically placed inclusions. *Journal of Applied Physics*, 75(6):2845-2850, March 1994.
- [81] Sun, J.-H. and T.-T. Wu (2005) \Analyses of mode coupling in joined parallel phononic crystal waveguides," *Physical Review B*, 71(17), p. 174303.
- [82] Sigalas, M. M. (1998) \Defect states of acoustic waves in a two-dimensional lattice of solid cylinders," *Journal of Applied Physics*, 84(6), p. 3026.

- [83] Kafesaki M., Sigalas M.M., and Garcia N. Frequency modulation in the transmissivity of wave guides in elastic-wave bandgap materials. *Physical Review Letters*, 85(19):4044-4047, November 2000.
- [84] Bria, D. and B. Djafari-Rouhani (2002) \Omnidirectional elastic bandgap in finite lamellar structures Omnidirectional elastic bandgap in finite lamellar structures," *Physical Review E*, 66(5), p. 056609.
- [85] A. Khelif, A. Choujaa, S. Benchabane, B. Djafari-Rouhani, V. Loude, "Experimental study of guiding and filtering of acoustic waves in a two dimensional ultrasonic crystal", *Z. Kristallogr.* 220, 836 (2005).
- [86] Yao, Y., Z. Hou, and Y. Liu (2006) \The propagating properties of the hetero-structure phononic waveguide," *Journal of Physics D: Applied Physics*, 39(24), p. 5164.
- [87] Lin, K.-H., C.-F. Chang, C.-C. Pan, J.-I. Chyi, S. Keller, U. Mishra, S. P. DenBaars, and C.-K. Sun (2006) \Characterizing the nanoacoustic superlattice in a phonon cavity using a piezoelectric single quantum well," *Applied Physics Letters*, 89(14), p. 143103.
- [88] Yao, Y.-W., Z.-L. Hou, and Y.-Y. Liu (2007) \Transmission Frequency Properties of Elastic Waves along a Hetero-Phononic Crystal Waveguide," *Chinese Physics Letters* Chinese Physics Letters, 24(2), p. 468.
- [89] Tanaka, Y., T. Yano, and S. ichiro Tamura (2007) \Surface guided waves in two-dimensional phononic crystals," *Wave Motion*, 44(6), pp. 501- 512.
- [90] Industrial embedded systems, Acoustic wave sensors, <http://industrial.embedded-computing.com/article-id/?3803=> (Accessed: 1 sept 2016).
- [91] Arnau A (2008) *Piezoelectric Transducers and Applications* (2- ed.). Berlin: Springer, ISBN: 978-3-540-77507-22.
- [92] M. Ke, M. Zubtsov, R. Lucklum, Sub-wavelength phononic crystal liquid sensor, *J. Appl. Phys.* 110 (2011) 026101. [92]

- [93] R. Lucklum. Phononic crystal sensor. 2008 IEEE Freq. Contr. Symp., Honolulu, Proc.: 85-90.
- [94] R. Lucklum, D. Soares, & K. Kanazawa, "Models for Resonant Sensors", in A. Arnau, *Piezoelectric Transducers and Applications*, Springer, pp. 64-96, 2008.
- [95] Lucklum, R., Li, J.: Transmission Properties of 1D and 2D Phononic Crystal Sensors. 10.1109/ULTSYM.2009.0278
- [96] M. Zubtsov, R. Lucklum. Tailoring 2D phononic crystal sensor properties by lattice symmetry reduction, Proc. Eurosensors XXIV, September 5-8, 2010, Linz, Austria
- [97] R. Lucklum, J. Li, M. Zubtsov. 1D and 2D Phononic Crystal Sensors, Proc. Eurosensors XXIV, September 5-8, 2010, Linz, Austria
- [98] R. Lucklum, P. Hauptmann. Resonant sensors: new principles and perspectives for (bio) chemical applications. *Int J Adv Eng Sci Appl Math* (Jan-June 2010) 2(1-2):8-16
- [99] Lucklum, Ralf. Hauer, I. Transmission properties of a 1D resonant cavity. Frequency Control Symposium, 2009 Joint with the 22nd European Frequency and Time forum. IEEE International. 248 - 253
- [100] R. Lucklum, M. Zubtsov, M. Ke, Liquid sensor utilizing a regular phononic crystal with normal incidence of sound, in: Proc. Freq. Contr. Symp., Europ. Freq. Time Forum, 2011, pp. 1-4.
- [101] R. Lucklum, M. Zubtsov, M. Ke, A. Oseev, U. Hempel and B. Henning "Determining liquid properties by extraordinary acoustic transmission through phononic crystals", Proc. 2011 IEEE Sensors, pp.1554 -1557
- [102] R. Lucklum, M. Zubtsov, M. Ke, B. Henning, U. Hempel, 2D Phononic Crystal Sensor with Normal Incidence of Sound. Proc. Eurosensors XXV, September 4-7, 2011, Athens, Greece

- [103] M. Zubtsov, R. Lucklum, M. Ke, A. Oseev, R. Grundmann, B. Henning, U. Hempel. 2D phononic crystal sensor with normal incidence of sound. *Sensors and Actuators A: Physical* Volume 186, October 2012, Pages 118–124
- [104] R. Lucklum. Phononic crystal sensors. *European Frequency and Time Forum (EFTF)*, 2012. 196 – 199
- [105] R. Lucklum. Phononic crystal sensors - Insides behind the scene. *Ultrasonics Symposium (IUS)*, 2012 IEEE International. 1126 - 1128
- [106] R. Lucklum, M. Ke, M. Zubtsov, Two-dimensional phononic crystal sensor based on a cavity mode, *Sensors and Actuators B* 171– 172 (2012), 271– 277.
- [107] A. Oseev, M. Zubtsov, R. Lucklum, Gasoline properties determination with phononic crystal cavity sensor, *Sens. Actuators B: Chem.* (2012), <http://dx.doi.org/10.1016/j.snb.2013.03.072>.
- [108] A. Oseev, M. Zubtsov, R. Lucklum, Octane Number Determination of Gasoline with a Phononic Crystal Sensor. *Procedia Engineering* 47 (2012) 1382 – 1385
- [109] Jyun-Hong Lu, Dong-Po Cai, Cheng-Yi Hsieh, Fu-Li Hsiao, Chii-Chang Chen. Liquid sensor composed of one-dimensional sonic Helmholtz resonator array. *Appl. Phys. A* (2015) 120:509–517
- [110] Aysevil Salman, Olgun Adem Kaya, Ahmet Cicek. Determination of concentration of ethanol in water by a linear waveguide in a 2Dimensional phononic crystal slab. *Sensors and Actuators A* 208 (2014) 50– 55
- [111] Yan Pennec, Mikhail Zubtsov, Ralf Lucklum. Phononic crystal wave mechanics in periodically modulated tubular structures. *ICSV22, Florence (Italy) 12-16 July 2015*
- [112] Ralf Lucklum, Mikhail Zubtsov, Yan Pennec. Tubular Bell – New Class of (Bio) Chemical Microsensors. *Procedia Engineering*, Volume 120, 2015, Pages 520–523. *Eurosensors 2015*

- [113] B. Figeys, R. Jansen, S. Severi, B. Nauwelaers, H.A.C. Tilmans, and X. Rottenberg. Study of broadband propagation characteristic of quasi-fractal phononic crystal for enhanced sensing applications.
- [114] Arafa H. Aly, Ahmed Mehane, Ehab Abdel-Rahman, “study of physical parameters on the properties of phononic bandgaps”. *International Journal of Modern Physics B*. Vol. 27, No. 11 (2013) 1350047 (15 pages)
- [115] C. Xu, F. Cai, S. Xie, J. Li, H. Zheng Thermal tuning of acoustic transmission enhancement through a phononic crystal slab. 2013 symposium on Piezoelectricity, Acoustic Waves and Device Applications. Oct. 25-27, Changsha, Hunan, China.
- [116] Liufeng Geng, Shuhong Xie, Feiyan Cai, Fei Li, Long Meng, Chen Wang, Hairong Zheng. “High sensitivity liquid sensor based on slotted phononic crystal”. 10.11 09IUL TSYM.201S.0110. 201S IEEE International Ultrasonics Symposium Proceedings
- [117] R. Lucklum, M. Zubtsov, A. Oseev, M.P. Schmidt, S. Hirsch, and F. Hagemann, Eds, *Towards a SAW based phononic crystal sensor platform*, 2013.
- [118] Aleksandr Oseev, Marc-Peter Schmidt, Ralf Lucklum, Mikhail Zubtsov, Soeren Hirsch. Phononic crystal based liquid sensor governed by localized defect resonances 10.1109/ULTSYM.2015.0053
- [119] Lucklum, R. Phononic crystals and metamaterials—Promising new sensor platforms. *Procedia Eng.* **2014**, 87, 40–45. doi:10.1016/j.proeng.2014.11.261.
- [120] Damiano Nardi, Marco Travaglini, Margaret M. Murnane, Henry C. Kapteyn, Gabriele Ferrini, Claudio Giannetti, and Francesco Banfi. “Impulsively Excited Surface Phononic Crystals: A Route Toward Novel Sensing Schemes”. *IEEE SENSORS JOURNAL*, VOL. 15, NO. 9, SEPTEMBER 2015
- [121] Richardson, S.K.M., Bhethanabotla, V.R. ; Sankaranarayanan, S.K.R.S. .Design of SH-SAW Phononic devices for Highly sensitive and Ultra-low Power Sensing Applications. *SENSORS*, 2014 IEEE. 2-5 Nov. 2014. 213 – 216. Valencia

- [122] Luca Luschi, Francesco Pieri. Design of MEMS mass sensors based of flexural phononic crystals. 2015 XVIII AISEM Annual Conference.
- [123] Samira Amoudache, Yan Pennec, Bahram Djafari Rouhani, Antoine Khater, Ralf Lucklum, and Rachid Tigrine. Simultaneous sensing of light and sound velocities of fluids in a two-dimensional phoXonic crystal with defects. *JOURNAL OF APPLIED PHYSICS* 115, 134503 (2014)
- [124] Montagut Y, Narbon J G, Jimenez Y, March C, Montoya A, Arnau A, Serra P A (2011) QCM Technology in Biosensors. *Biosensors - Emerging Materials and Applications*, pp. 153-178. DOI: 10.5772/17991
- [125] Z. Hou and B. M. Assouar, "Transmission property of the one-dimensional phononic crystal thin plate by the eigenmode matching theory" *J. Phys. D: Appl. Phys.* 41 095103, (2008)
- [126] Qiu C, Liu Z, Mei J, Ke M (2005) The layer multiple-scattering method for calculating transmission coefficients of 2D phononic crystals. *Solid State Communications*, 134, pp. 765-770.
- [127] Tanaka Y, Tomoyasu Y, Tamura I (2000) Band structures of acoustic waves in phononic lattices: Two-dimensional composites with large acoustic mismatch. *Phys. Rev. B* 62, pp. 7387-7392.
- [128] J. O. Vasseur, P. A. Deymier, B. Chenni, B. Djafari-Rouhani, L. Dobrzynski and D. Prevost, *Phys. Rev. Lett.* 86, 3012 (2001).
- [129] Zhengyou Liu, C. T. Chan, Ping Sheng, A. L. Goertzen and J. H. Page, *Phys. Rev. B* 62, 2446 (2000).
- [130] M. Kafesaki and E. N. Economou, *Phy. Rev. B* 60, 11993 (1999). [54] D. Garcla-Pablos, M. Sigalas, F. R. Montero de Espinosa, M. Torres, M. Kafesaki and N. Garcia, *Phys. Rev. Lett.* 84, 4349 (2000).

- [131] Goffaux C. and Sanchez-Dehesa J. Two-dimensional phononic crystals studied using a variational method: Application to lattices of locally resonant materials. *Physical Review B*, 67(14):1-10, 2003.
- [132] Liu Z., Zhang X., Mao Y., Zhu Y.Y., Yang Z., Chan C.T., and Sheng P. Locally resonant sonic materials. *Science Magazine*, 289:1734{1736, September 2000.
- [133] Garcia-Pablos D., Sigalas M.M., Montero de Espinosa F.R., Torres M., Kafesaki M., and Garcia N. Theory and experiments on elastic bandgap. *Physical Review Letters*, 84(19):4349{4352, May 2000.
- [134] Tanaka, Y., Y. Tomoyasu, and S. Ichiro Tamura (2000) \Band structure of acoustic waves in phononic lattices: Two-dimensional composites with large acoustic mismatch," *Physical Review B*, 62(11), pp. 7387-7392.7
- [135] Vasseur J. O., Deymier P.A., Khelif A., Lambin Ph., Djafari-Rouhani B., Akjouj A., Dobryznski L., Fettouhi N., and Zemmouri J. Phononic crystal with low filling fraction and absolute acoustic bandgap in the audible frequency range: A theoretical and experimental study. *Physical Review Letters*, 65(5):1-6, 2002.
- [136] Jensen J.S. and Sigmund O. Phononic bandgap structures as optimal designs. *Proceedings of the IUTAM Symposium on Asymptotics, Singularities, and Homogenisation in Problems of Mechanics*, pages 73{83, 2003.
- [137] Sigalas M.M. and Garcia N. Importance of coupling between longitudinal and transverse components for the creation of acoustic bandgaps: The aluminum in mercury case. *Applied Physics Letters*, 76(16):2307{2309, April 2000.
- [138] Miyashita T. Numerical studies on bandgap structures and resonant-mode waveguides of typical sonic crystals made of rigid cylinders in fluid by means of elastic ftdt method. In *Proceedings of 2005 ASME-IMECE: ASME 2005 Mechanical Engineering Congress and Exposition*, Orlando Fl, USA, November 5-11, 2005.
- [139] Pain, H. J. *The Physics of Vibrations and Waves*. John Wiley & Sons (2005)
- [140] R. Millner, "Wissensspeicher Ultraschalltechnik", Fachbuchverl, (1987).

- [141] Pennec Y, Vasseur J O, Djafari-Rouhani B, Dobrzyński L, Deymier P A (2010) Two-dimensional phononic crystals: Examples and applications. *Surface Science Reports* 65, pp. 229–291, DOI:10.1016/j.surfrep.2010.08.002
- [142] Lucklum R, Villa S, Zubtsov M (2014) Cavity resonance biomedical sensor, IMECE2014-38222: ASME 2014 International Mechanical Engineering Congress and Exposition, 2014, Montreal, Quebec, Canada. ISBN: 978-0-7918-4962-0
- [143] Lucklum R, Villa S, Zubtsov M, Grundmann R (2014) Phononic crystal sensor for medical applications. *IEEE SENSORS 2014*, November 2-5, 2014, Valencia, Spain, pp. 903 - 906. DOI: 10.1109
- [144] Villa S, Torres R, Lucklum R (2015) Electronic characterisation system for measuring frequency changes in phononic crystals. *Electronics Letters*, Volume 51, Issue 7, pp. 545-546. DOI: 10.1049/el.2014.4151.
- [145] Kuhnkies R, Schaaffs W (1963) Untersuchungen an adiabatisch und isotherm aufgenommenen Schallkennlinien binärer Mischungen, *Acustica* 13, 407.
- [146] World Health Organization, “Diagnostics and Laboratory Technology”, Contributions to Millennium Development Goals, http://www.who.int/diagnostics_laboratory/3by5/en/, (2014)
- [147] Lucklum, R.; Zubtsov, M.; Pennec, Y.; Villa-Arango, S. Disposable phononic crystal liquid sensor. *IEEE Int. Ultrason. Symp. IUS 2016*, 3–6, doi:10.1109/ULTSYM.2016.7728591.
- [148] Aly, A.H.; Mehaney, A. Phononic crystals with one-dimensional defect as sensor materials. *Indian J. Phys.* **2017**, 1–8, doi:10.1007/s12648-017-0989-z.
- [149] Bilaniuk, N.; Wong, G.S. K. Erratum: Speed of sound in pure water as a function of temperature. *J. Acoust. Soc. Am.* **1996**, 99, 3257–3257, doi:10.1121/1.415224.
- [150] Bilaniuk, N.; Wong, G.S. K. Speed of sound in pure water as a function of temperature. *J. Acoust. Soc. Am.* **1993**, 93, 1609–1612, doi:10.1121/1.406819.

- [151] Kaya, O.A.; Cicek, A.; Salman, A.; Ulug, B. Acoustic Mach–Zehnder interferometer utilizing self-collimated beams in a two-dimensional phononic crystal. *Sens. Actuators B Chem.* **2014**, *203*, 197–203, doi:10.1016/j.snb.2014.06.097.[150]
- [152] Futrell, K. *The Future Outlook for Laboratory Point-of-Care Testing*; Orchard Software: Carmel, IN, USA 2015, 8–18. Available online: http://bbvreview.com/images/resources/Other/Other_white_paper_lab_poc_testing.pdf (accessed on 5 October 2018)
- [153] Montagut, Y., Garcia, J. V., Jimenez, Y., March, C., Montoya, A., Arnau, A., 2011. Validation of a Phase-Mass Characterization Concept and Interface for Acoustic Biosensors. *Sensors*. *11*, 4702–4720. doi:10.3390/s110504702
- [154] Nagel, T., Ehrentreich-Förster, E. Singh, M., Schmitt, K., Brandenburg, A., Berka, A., Bier, F. F., 2008. Direct detection of tuberculosis infection in blood serum using three optical label-free approaches. *Sensors Actuators, B Chem.* *129*, 934–940. <https://0-doi-org.wam.city.ac.uk/10.1016/j.snb.2007.10.009>
- [155] Mirmohseni, A.; Abdollahi, H.; Rostamizadeh, K. Analysis of transient response of single quartz crystal nanobalance for determination of volatile organic compounds. *Sensor. Actuat. B-Chem.* **2007**, *121*, 365–371, doi: <https://doi.org/10.1016/j.snb.2006.03.054>.
- [156] Constantinou, L.; Triantis, I.F.; Hickey M.; Kyriacou, P.A. On the Merits of Tetrapolar Impedance Spectroscopy for Monitoring Lithium Concentration Variations in Human Blood Plasma. *IEEE Trans. Biomed. Eng.* **2017**, *64*, 601–609, doi:10.1109/TBME.2016.2570125.
- [157] Qassem, M.; Constantinou, L.; Triantis, I.; Hickey, M.; Palazidou, E.; Kyriacou, P.A. A Novel Method for Low-Volume Measurement of Lithium in Human Blood to use in Personalized Monitoring of Lithium Treatment. *IEEE Trans. Biomed. Eng.* **2018**, doi:10.1109/TBME.2018.2836148.

- [158] May, J.; Hickey, M.; Triantis, I.; Palazidou, E.; Kyriacou, P.A. Spectrophotometric analysis of lithium carbonate used for bipolar disorder. *Biomed. Opt. Express* **2015**, *6*, 1067–1073, doi: <https://doi.org/10.1364/BOE.6.001067>.